Spring 4-30-2012

A Comparative Analysis of Feature Extraction Techniques for EEG Signals from Alzheimer patients

Ramya Priya Mudhiganti

A Comparative Analysis of Feature Extraction Techniques for EEG Signals from Alzheimer patients

by

Ramya Priya Mudhiganti

A thesis submitted in partial fulfillment
of the requirements for the degree of
Master of Science in Electrical Engineering
Department of Electrical Engineering

Hassan El-Kishky, Ph.D., P.E., Committee Chair

College of Engineering and Computer Science

The University of Texas at Tyler
May 2012

The University of Texas at Tyler
Tyler, Texas

This is to certify that the Master's thesis of

Ramya Priya Mudhiganti

has been approved for the thesis requirements on
March 28th 2012
for the Master of Science Degree in Electrical Engineering

Approvals:

Thesis Chair: Hassan El-Kishky, Ph.D., P.E.

Member: Mukul V. Shirvaikar, Ph. D.

Member: Hector R. Ochoa, Ph.D.

Chair and Graduate Coordinator: Mukul V. Shirvaikar, Ph. D.

James K. Nelson, Jr., Ph.D., P.E.,
Dean, College of Engineering and Computer Science,
Brazzel Professor of Engineering

Acknowledgements

It is a pleasure to thank those who made this thesis possible. I would like to thank my family members: my father Narayana Reddy Mudhiganti, mother Radha Kumari Mudhiganti, sister Sowmya Reddy Mudhiganti and my brother-in-law Srikanth Reddy Sandhi for their constant love, support and encouragement to complete my Master's Degree. A special thanks goes to my Advisor Dr. Hassan El-Kishky for his supervision and motivation throughout my thesis. He has made available his support in a number of ways without which this would not be accomplished.

I would like to show my gratitude to the committee members, Dr. Hector Ochoa and Dr. Mukul Shirvaikar for spending their valuable time in reviewing my work. I owe my deepest gratitude to Dr. Mukul Shirvaikar through whom I got admitted into this Master's Degree program and for his support and guidance to me throughout my Master's degree.

I also thank the entire EE department and The University of Texas at Tyler for supporting me in many ways.

Last but not the least I would like to thank my friends for their support through the duration of this thesis.

Table of Contents

List of Figures

List of Tables

Abstract

A COMPARATIVE ANALYSIS OF FEATURE EXTRACTION TECHNIQUES FOR EEG SIGNALS FROM ALZHEIMER PATIENTS

Ramya Priya Mudhiganti
Thesis chair: Hassan El-Kishky, Ph.D.

The University of Texas at Tyler

May 2012

This research deals with the study of Alzheimer Disease (AD). Electroencephalogram (EEG) signal is a clinical tool for the diagnosis and detection of AD. EEG signals are analyzed for the diagnosis of AD applying several linear and non-linear methods of signal processing. This work studies and implements several measures of EEG signal complexity and then compares the complexity features measured or extracted from EEG signals. Time domain analysis of EEG signals is performed using several signal processing techniques such as higher order moments, entropies and fractal dimension calculation using fractal analysis. Frequency domain analysis of EEG signals is performed using signal processing techniques such as Welch Power spectrum and Discrete Fourier Transform (DFT). EEG signal analysis using Wavelet Transform was also performed. Higher order moments, entropies, fractal dimension estimation using fractal analysis and Welch Power Spectrum are also implemented along with moving windows. This work also deals with the artifact removal or de-noising of EEG signals using a band pass filter. EEG signal data recorded from AD subjects and their respective age-matched control subjects are used to test the performance of the methods in

diagnosing AD. In addition, this work outlines the drawbacks of the methods used and compares the methods for the best feature extraction techniques.

Chapter One

Introduction

Alzheimer disease (AD) is a brain disorder which may lead to complete memory loss. AD cannot be cured and it may gradually lead to death [1]. Approximately five percent of the United States population suffers from AD and it has become one of the primary causes of death in United States of America. Intensive research has been going on in this area trying to improve the diagnosis and treatment of AD by detecting the disease in its early stages and developing ways to diagnose the disease using advanced medical technology [1].

AD has four different stages of intensity: preclinical, mild, moderate and severe. The symptoms of this disease include memory loss such as not remembering people names and regular events, unable to do simple tasks like speaking or writing. People suffering from AD are mostly around the age of 65 except in few cases in which it may affect people less than the age of 65 [1] .The brain may show the changes in its structure few years before the symptoms of AD appear.

1.1 EEG and ERP

Electroencephalogram (EEG) signals are measurements of the electrical activity of the human brain [2]. Research shows that EEG signals can be very helpful in the detection, diagnosis and treatment of the AD. EEG signals recorded for the analysis and detection of AD are the coherence values with a selected frequency band. Coherence of EEG signals is the coupling between two sub-regions on human scalp per frequency band. The application of signal processing techniques on the EEG signals for feature

extraction represents one of the main techniques used to diagnose AD. Detailed and diligent analyses of the EEG recordings can help in understanding the causes for the brain disorder leading to AD. EEG signals are non-linear and non-stationary and their spectrum varies with time. EEG signal amplitudes are normally in the range of 10 to 100 micro volts and they are divided into different wave groups based on the frequency range [3]. The different wave groups are shown in the Table 1.1. EEG signals are recorded by placing electrodes on the human scalp as shown in Figure 1.1 [2].

Table 1.1: Frequency range of the wave groups of an EEG signal

Wave group	**Starting frequency**	**End Frequency**
Delta	0.5 Hz	3.5 Hz
Theta	3.5 Hz	7.5 Hz
Alpha	7.5 Hz	12.5 Hz
Bheta	12.5 Hz	And above

Event related Potential (ERP) is a method of measuring electrical brain activity in EEG signal processing. ERP is a neural signal that reflects coordinated neural network activity. Moreover, ERP represents the ongoing EEG changes during the simulation [3]. ERPs have amplitudes smaller than the ones from the EEG signals and their visualization is improved by repeated trials of EEG recordings [3]. ERPs are used to study the abnormal and normal nature of EEG signals.

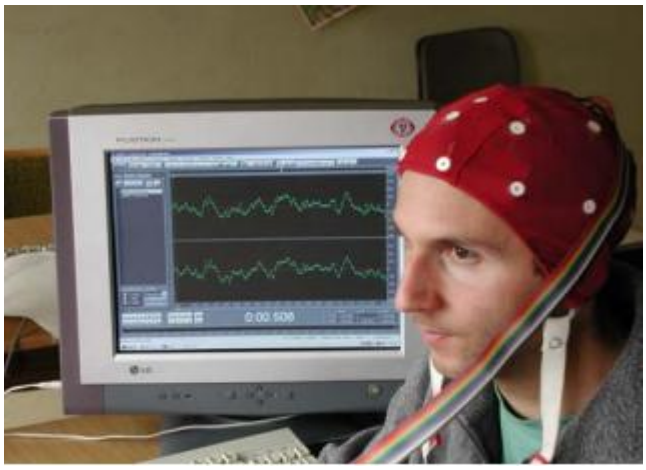

Figure 1.1: Electrodes placed on the human scalp for EEG recordings

1.2 Research Objectives

The main objective of this work is to analyze the EEG signals from a set of AD patients and normal persons. Moreover this research aims at comparing the complexity of these signals by applying several signal processing techniques to extract discriminating features from these signals. In this study, 18 AD subjects and 16 control subjects (normal persons) are considered for EEG signal processing to diagnose AD. The EEG recordings of the coherence features of these subjects are analyzed and the results are discussed. Features of the EEG signals are extracted in the time domain and frequency domain. These features are studied and compared between AD subjects and control subjects. The best feature extraction techniques are determined and proposed for further study of this research.

1.1 Thesis Outline

The thesis outline is as follows; Chapter 2 discusses the literature review used in this research. Chapter 3 discusses the time domain analysis of EEG signals which includes the extraction of statistical features like higher order moments, entropies and fractal values. Chapter 4 discusses the frequency domain analysis of EEG signals, which includes the

application of the Welch Power Spectrum and the Discrete Fourier Transform. Chapter 5 discusses artifacts removal of EEG signals and the de-noised signals analysis. Chapter 6 gives the conclusions and the discussion of the future work of this thesis.

Chapter Two

Literature Review

Previous studies on EEG signal analysis used several signal processing techniques such as Shannon entropy, Higuchi fractal Dimension (HFD), Rescaled Range Analysis and Box counting method for fractal dimension estimation, Fast Fourier Transform (FFT), Short Time Fourier Transform (STFT), Auto Regressive Moving Average Modeling (ARMAX) and adaptive filtering for artifact removal.

Shannon entropy and HFD methods of analyzing the complexity of EEG signals were studied by Fernets [4]. The main reason for choosing the methods by Ferenets is their computational efficiency and reliable results when applied to short signal segments. Shannon entropy is a measure of order in the signal, and is sensitive to the amplitude distribution. Order of a signal is the measure of randomness of the signal. Entropies reveal different properties of signals and their main drawback is difficulty in interpreting results [4].

A statistical method named Rescaled Range Analysis developed by Hurst was used by Islam to analyze long records of data [5]. The two factors used in this analysis are Range and the standard deviation of data set. Hurst found that the ratio works well with large data records [5].

The fractal dimension of signals in the time domain is calculated using the box-counting method [6]. Fractal dimension is applicable to data sets that may or may not be self-similar over all ranges of time. It has been shown that fractal dimension analysis does not differentiate between fractal and non-fractal data sets and gives a measure of the

appropriateness of describing the data set using fractal analysis. Author Raghavendra in this paper [6] has concluded that the fractal dimension finds applications in distinguishing signals having similar mean and variance but of different nature [6].

The fractal dimension of EMG signal was calculated using the R/S method. By using this non-linear method any random signal can be analyzed. Hurst found that for large values of H, the signal is strongly non-gaussian which means that the signal is highly irregular [7].

The raw EEG signal is a time domain signal and the energy distribution of the signal is scattered. EEG signals were analyzed to extract the features either in the time or the frequency domain. Analysis of EEG signals in frequency is better detecting any brain disorder [8]. Hence, the Fast Fourier Transform (FFT) based spectral analysis has been used to determine spectrum and spectral components of EEG signals by Suleiman in his article [8]. He applied FFT and Short-Time Frequency Transform (STFT) and his results showed that the Short Time Fourier Transform (STFT) method was able to differentiate between signals for different mental tasks. The STFT gave a better time-frequency representation of EEG signals compared to other methods [8]. In the paper by Deivanayag [9] has discussed the FFT algorithm in extracting the spectral components of an EEG signal. A 1024 point FFT is used to extract the spectral components of EEG signal data sets to extract frequency features.

In the paper by Shaker, he applied the Discrete Wavelet Transform (DWT) and FFT for the spectral analysis of the signals [10]. The results showed that the Wavelet Transform outperformed FFT as a classifier of EEG frequencies. The undesired

frequencies of the input EEG signal data sets were rejected well using Wavelet Transform with more efficiency [10].

During EEG signal recording, noise is added to the signal due to the interferences from the subject and equipment. Among the artifacts added to the EEG signal, ocular artifacts are the ones that need to be removed first [11]. Shooshtari applied two methods of artifact removal [11]: Auto Regressive Moving Average (ARMAX) modeling and Adaptive filtering. The ARMAX model considers the recorded EEG signal a linear combination of brain activity and ocular artifacts and yields better results for higher model order until a certain ceiling after which performance of this modeling was not effective. The reason for this is that an ARMAX model for lower orders, a negative spike appeared at the presence of EOG artifact in the EEG signal. However, this spike was not seen when higher order models are considered. ARMAX modeling cannot detect artifacts in the early samples of the EEG signal recording which is a drawback that can be remedied by adaptive filtering. This method is simple and no complex calculations are needed to implement it.

A band pass filter with a pass band of 0.5 to 40 Hz and filter order 4 is designed and used for the processing of EEG signals [9]. The upper cut-off frequency is 40 Hz and the lower cut-off frequency is 0.5 Hz. FIR filters are chosen rather than IIR filters as they give constant group delay throughout the frequency spectrum and complete stability at all frequencies regardless of the size of the filter. This filter was designed in MATLAB. The data filtered in this way was analyzed using FFT for extraction of frequency components. The data filtered showed a very clear frequeny response [9].

The methods chosen in this study for analysis of EEG signals are: Higher order moments, entropies, fractal analysis, Wavelet transform, Welch Power spectrum and Discrete Fourier Transform. Artifact removal of EEG signals is performed using a linear band pass filter.

Chapter Three

Time Domain Analysis of EEG Signals

3.1 Introduction

Data sets of EEG signals composed of 18 Alzheimer Disease (AD) subjects and 16 control (normal persons) subjects are analyzed in the time domain employing several non-linear signal processing techniques. These techniques include the estimation of higher order moments, Shannon entropy, energy entropy and the fractal dimension analysis methods. Generally these methods determine the non-linear behavior of the processed these signals.

3.2 Higher Order Moments

Higher order moments such as skewness and kurtosis are statistical quantities that measure the complexity of the EEG signals and measure signal element distribution [12].

3.2.1 Skewness

Skewness is a measure of the lack of symmetry or the asymmetry of an EEG signal data set. Positive skewness indicates that an EEG signal data set is distributed more to the left of the mean point and negative skewness indicates that the data set is distributed more to the right of the mean point.

Skewness of a signal data set $\boldsymbol{x}(n)$ is given by [13],

$$\gamma_1 = \frac{E[(\boldsymbol{x}(n)-\mu)^3]}{\sigma^3} \tag{3.1}$$

Where μ is the mean of the data set, σ is the standard deviation of the data set and E is the expected value estimator of the signal $\boldsymbol{x}(n)$.

The Skewness of the EEG signals for AD subjects and control subjects are calculated using the MATLAB signal processing toolbox. The analysis is also made with and without using moving windows. The results for the AD and control subjects are compared. The bar graph in Figure 3.1 shows the comparison of the skewness for the EEG signals without moving windows.

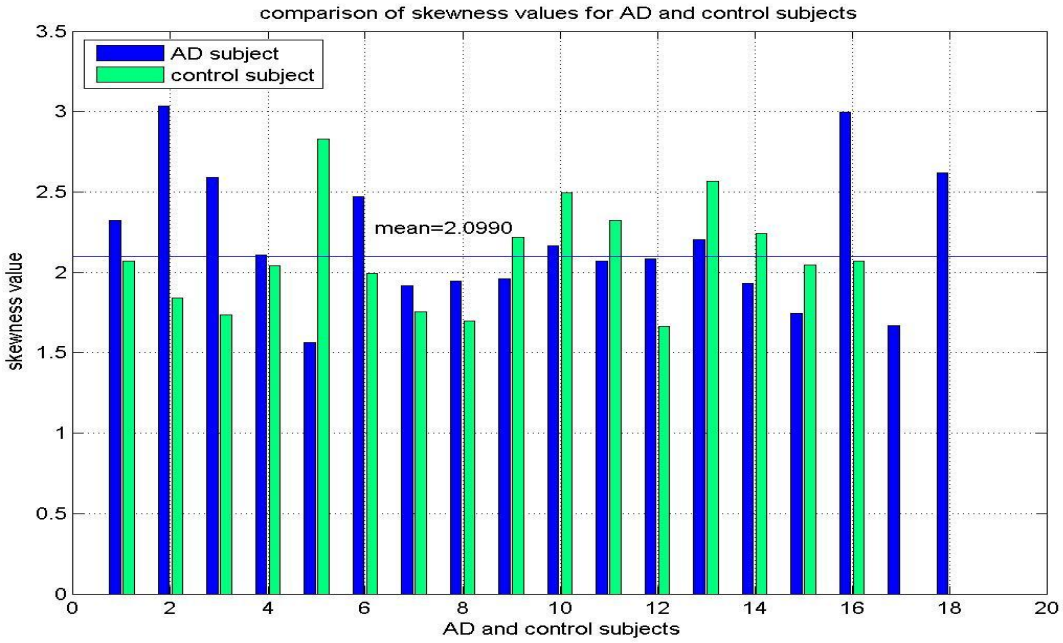

Figure 3.1: Skewness values for AD subjects and control subjects

From Figure 3.1, it is observed that the skewness values are very high for AD subject 2, AD subject 3 and AD subject 16 than their respective age-matched control subjects. The average value of the skewness values for control subjects is 2.0990 and 2.1882 for AD subjects. AD subjects 1, 2, 3, 5, 10, 13 and 16 have a skewness value greater than the average skewness value of control subjects. Analysis rate of skewness for AD subjects and control subjects is 25% with a false alarm of 6.25%. Analysis rate is the number of subjects the method used to analyze EEG signals can differentiate between

AD and control subjects. False alarm is the number of control subjects considered as normal patients but could be AD patient.

3.2.1.1 Skewness with Moving Window Analysis

For the moving window analysis, each EEG signal data set is segmented into an integer number of windows or segments with a percentage of overlap between windows or segments. For a 5%, 15% and 25% overlap the parameter is calculated for a particular data set by averaging the values from each individual segment. The Skewness using moving window analysis is applied to the EEG signal data sets. The bar graphs from Figures 3.2 and 3.3 show the skewness values of EEG signal data sets with the moving window analysis having different overlap percentages.

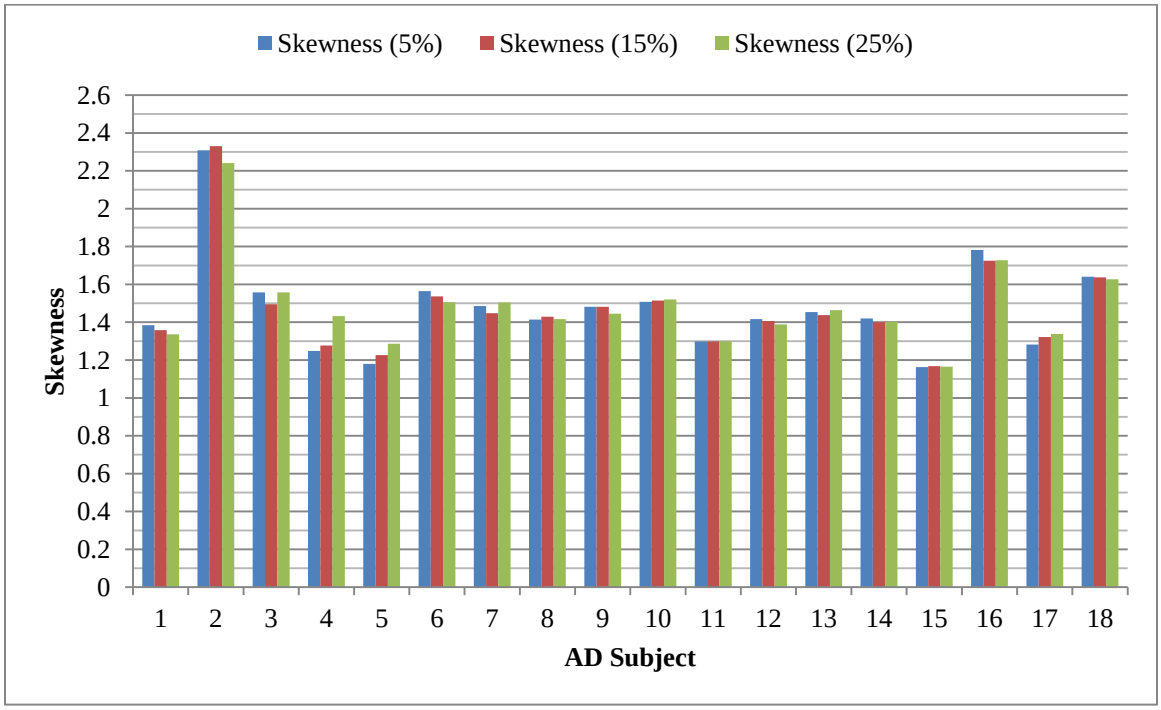

Figure 3.2: Skewness values for AD subjects with moving window analysis

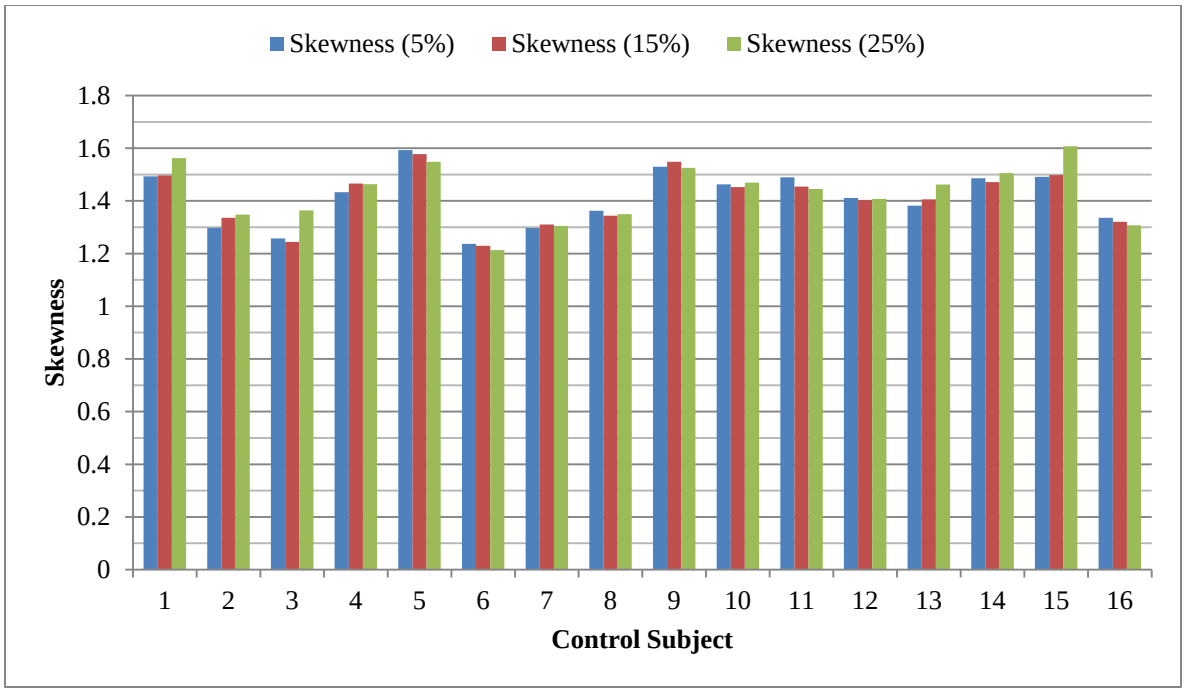

Figure 3.3: Skewness values for control subjects with moving window analysis

Skewness values for AD subjects and control subjects with the moving window analysis are lesser compared to the skewness values of EEG signal data sets of AD subjects and control subjects without moving window analysis. Mean skewness for AD subjects is 1.476, 1.4707 and 1.4733 with 5%, 15% and 25% overlap respectively. Mean skewness for control subjects is 1.41, 1.4087 and 1.4241 with 5%, 15% and 25% overlap respectively. Analysis rate for skewness with moving windows is also 25% with a false alarm of 6.25%.

3.2.2 Kurtosis

Kurtosis is a statistical quantity which measures the complexity of an EEG data set. It also determines if the EEG signal has a peak or rather flat at the mean point of the signal [13]. Higher values of kurtosis indicate that the signal has a sharp peak at the mean point of an EEG signal data set and low values of kurtosis indicate that that the signal has

a flat nature at the mean point of the signal. The Kurtosis for a signal $\boldsymbol{x}(n)$ is given by [13],

$$\gamma_2 = \frac{E[(\boldsymbol{x}(n)-\mu)^4]}{[E[(\boldsymbol{x}(n)-\mu)^2]]^2} \tag{3.2}$$

Where μ is the standard deviation and E is the expected value estimator of the signal $\boldsymbol{x}(n)$.

The Kurtosis for EEG signals from AD subjects and control subjects are calculated. The values for the AD subjects and control subjects are compared and shown in the Figure 3.4.

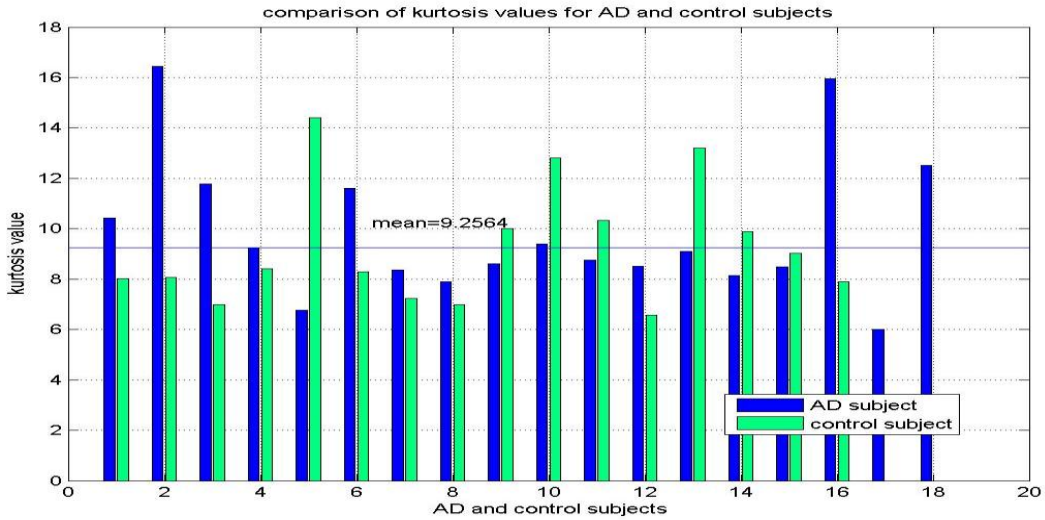

Figure 3.4: Kurtosis values for AD subjects and control subjects

From the Figure 3.4, it is observed that the kurtosis for AD subject 2 and 16 are very high compared to the kurtosis values of the respective control subjects, and the kurtosis for AD subject 5 is very low compared to the kurtosis value of the respective age-matched control subject. AD subjects 1, 2, 3, 6, 10 and 16 have the kurtosis values higher than the mean kurtosis from the control subjects which is 9.2564 and 9.8855 for AD subjects.

3.2.2.1 Kurtosis with Moving Window Analysis

The Kurtosis using moving window analysis is applied to the EEG signal data sets. Figures 3.5 and 3.6 show the kurtosis for EEG signal data sets with different overlap percentages.

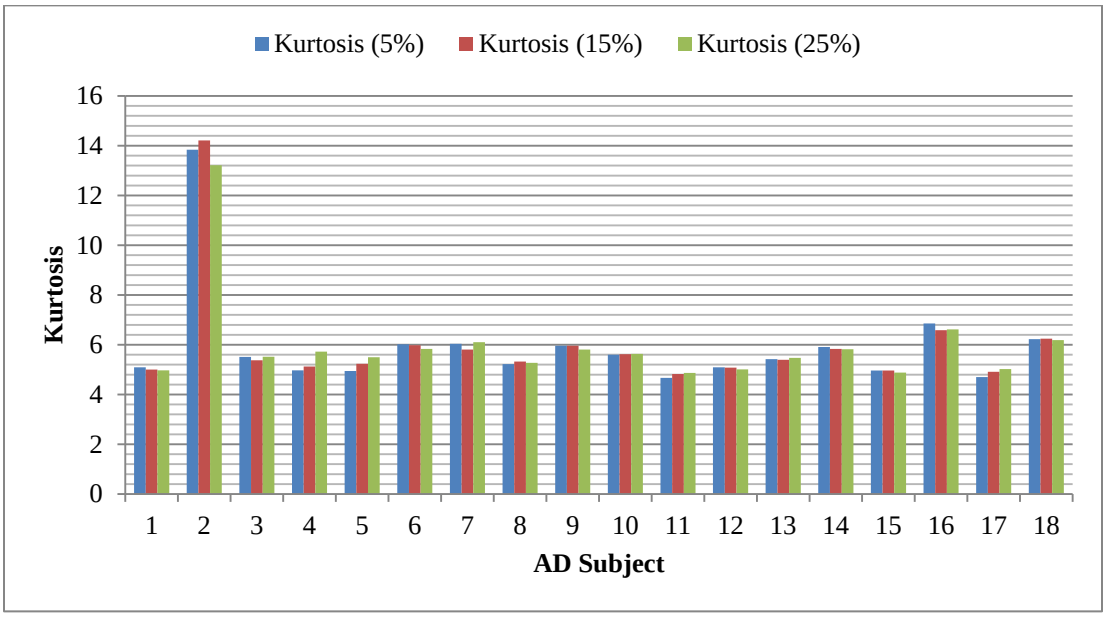

Figure 3.5: Kurtosis values for AD subjects with moving window analysis

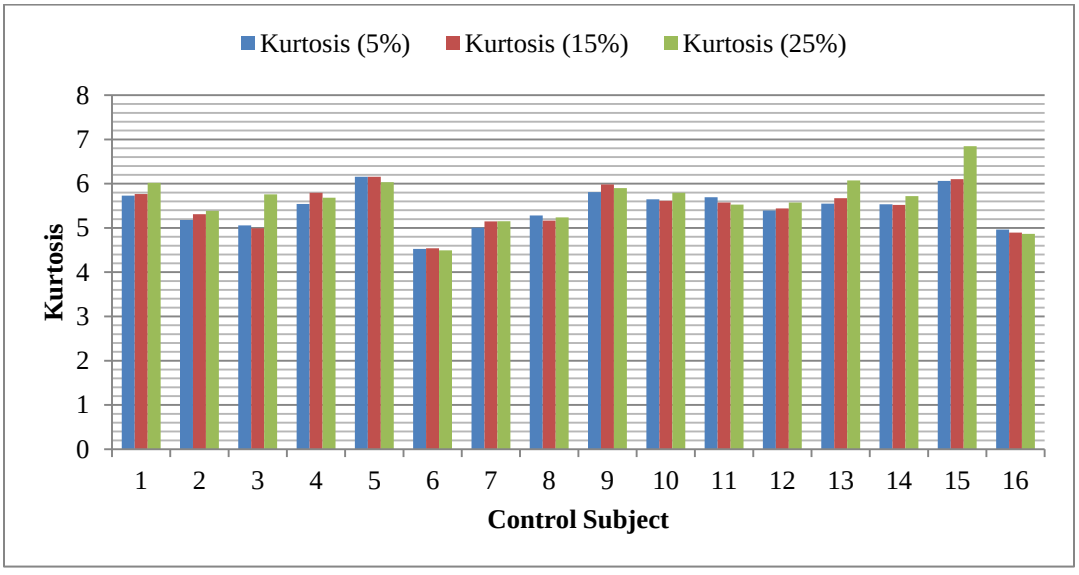

Figure 3.6: Kurtosis values for control subjects with moving window analysis

From Figures 3.5 and 3.6, it is observed that the kurtosis of the EEG signal data sets for AD subjects and control subjects with the moving window analysis are lower than the kurtosis values calculated without the moving window analysis. Kurtosis for AD subjects is 5.9463, 5.9527 and 5.9446 with 5%, 15% and 25% overlap respectively. Kurtosis for control subjects is 5.4458, 5.4706 and 5.5965 with 5%, 15% and 25% overlap respectively.

3.3 Entropies

Entropy is the measure of randomness or uncertainty associated with a random variable [14]. Shannon entropy and energy entropy are non-linear methods employed for the feature extraction of EEG signals data sets for AD subjects and control subjects. Shannon entropy is a statistical quantity which measures the uncertainty of an EEG signal and the expected value of the information contained in an EEG signal data set [14]. In other words, it is the measure of the order in an EEG signal [4]. Signal order is the degree of randomness of the signal. Energy entropy is a statistical quantity which measures the distribution of the energy of an EEG signal. Both shannon and energy entropy of EEG signal data sets for AD subjects and control subjects are calculated. Figures 3.7 and 3.8 show the comparison of the entropies values for AD subjects and control subjects.

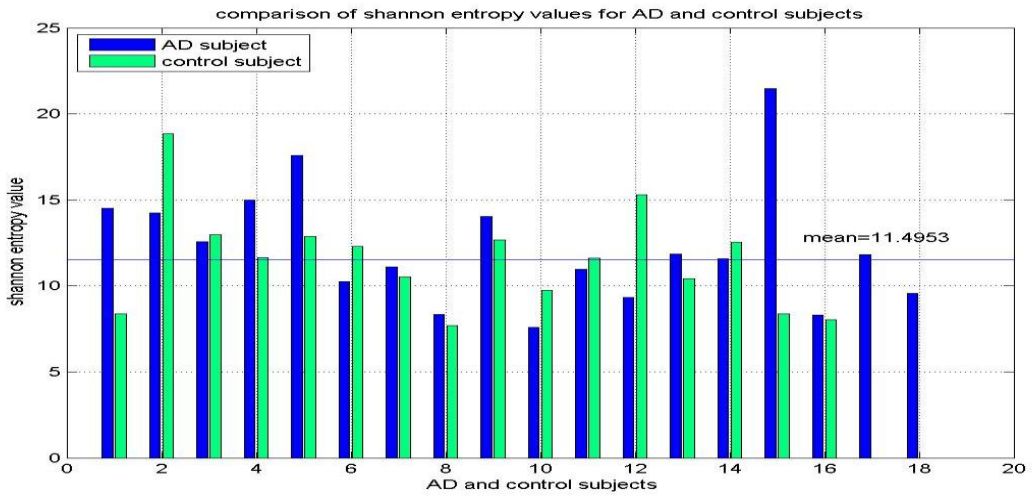

Figure 3.7: Shannon entropy values for AD subjects and control subjects

From Figure 3.7, it is observed that the shannon entropy value of AD subject 15 is very high compared to the shannon entropy value of the respective control subject. AD subjects 1, 2, 3, 4, 5, 9, 13 and 15 have a higher shannon entropy values compared to the mean shannon entropy value of the control subjects which is 11.4953 and 12.2306 for AD subjects.

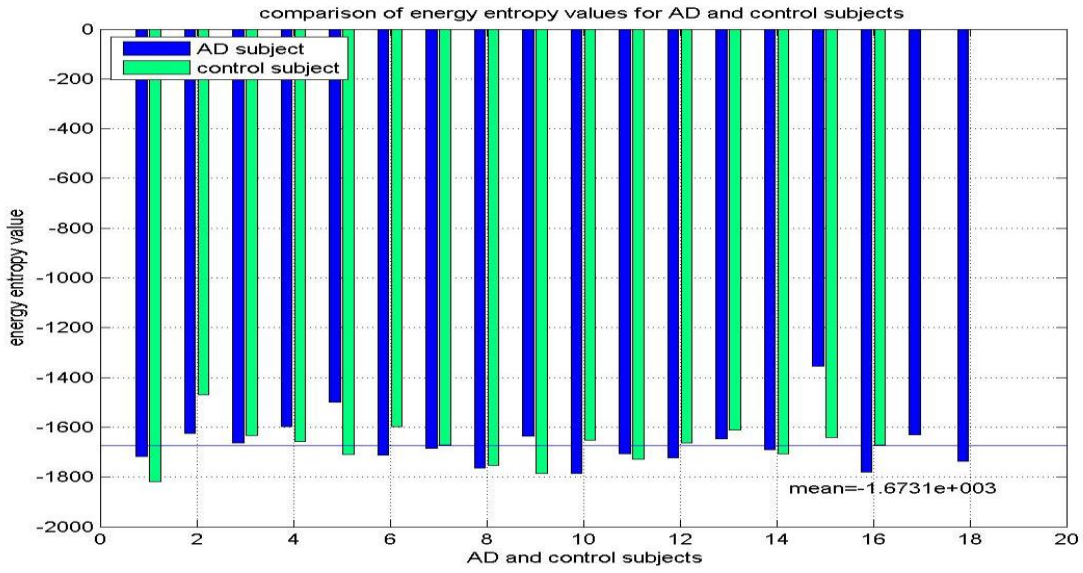

Figure 3.8: Energy entropy values for AD subjects and control subjects

From Figure 3.8, it is observed that the energy entropy values are not much different for AD subjects and control subjects. AD subjects 1, 6, 7, 8, 10, 11, 12, 14 and 16 have energy entropy values greater than the mean energy entropy value of control subjects which is -1673.1 and -1664.3 for AD subjects.

3.3.1 Entropies with Moving Window Analysis

Shannon entropy and energy entropy of EEG signals data sets are also calculated using a moving window analysis and values of the entropies are shown in Figures 3.9-3.12.

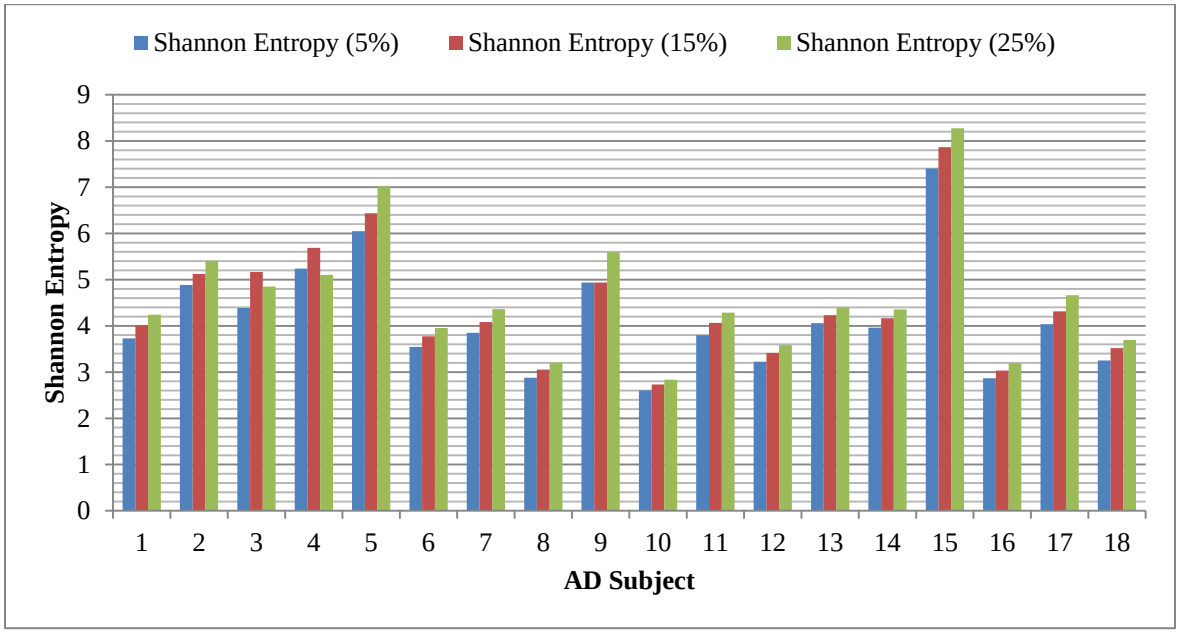

Figure 3.9: Shannon entropy values for AD subjects with moving window analysis

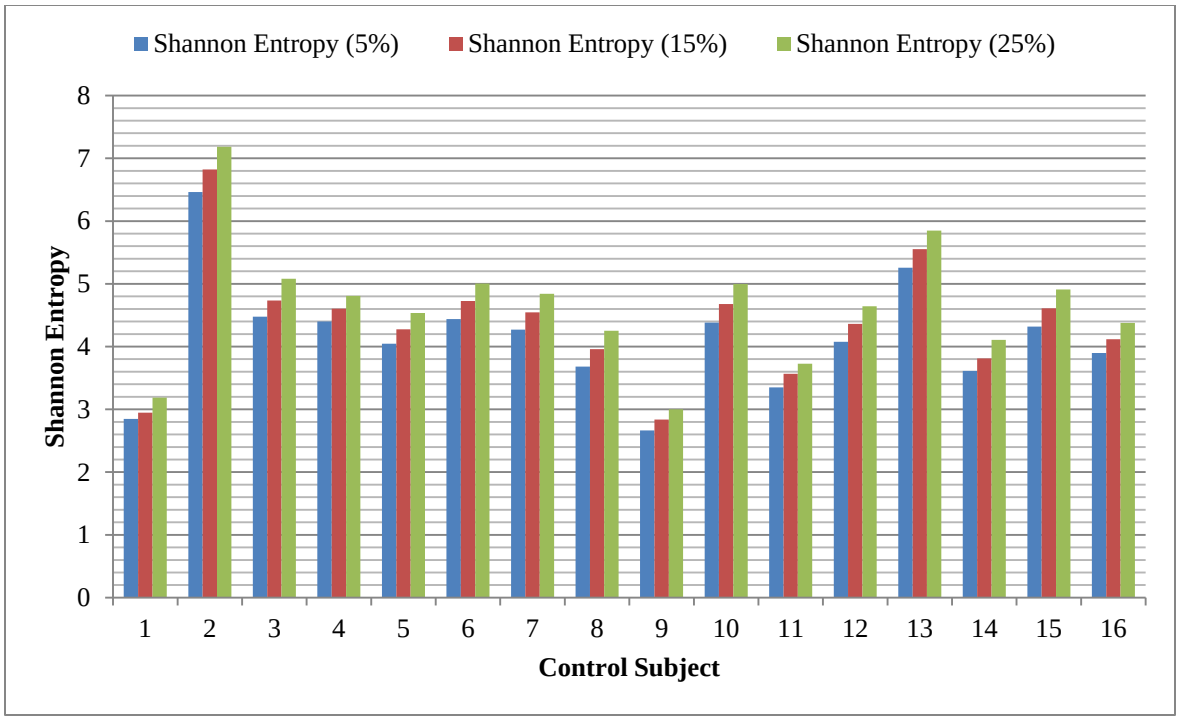

Figure 3.10: Shannon entropy values for control subjects with moving window analysis

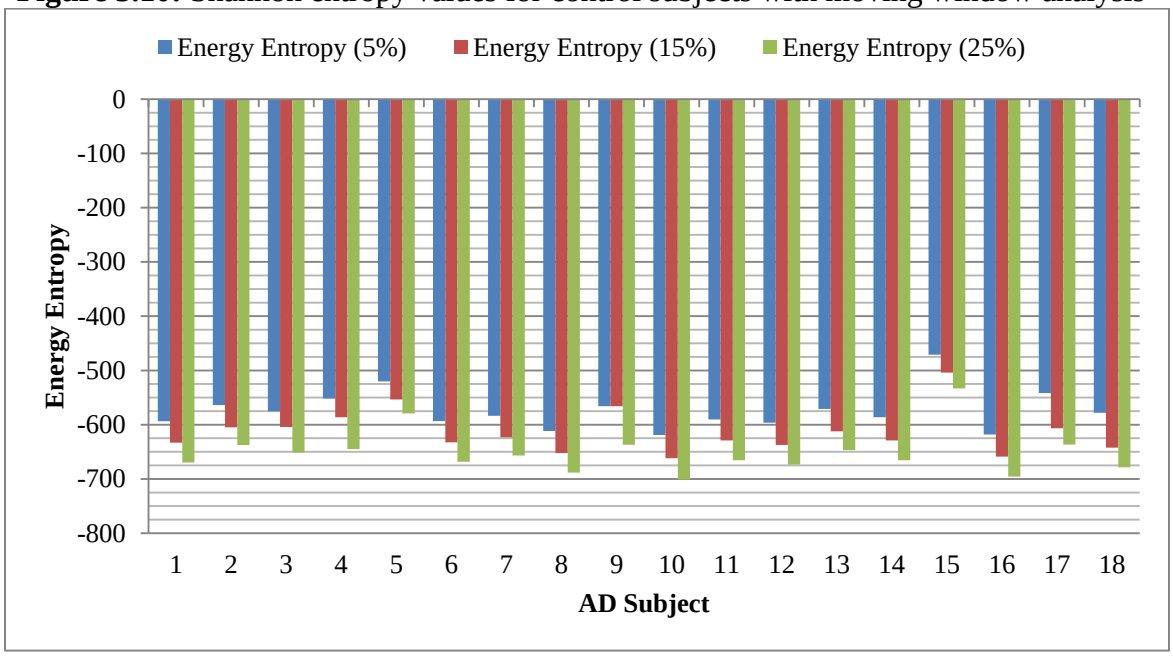

Figure 3.11: Energy entropy values for AD subjects with moving window analysis

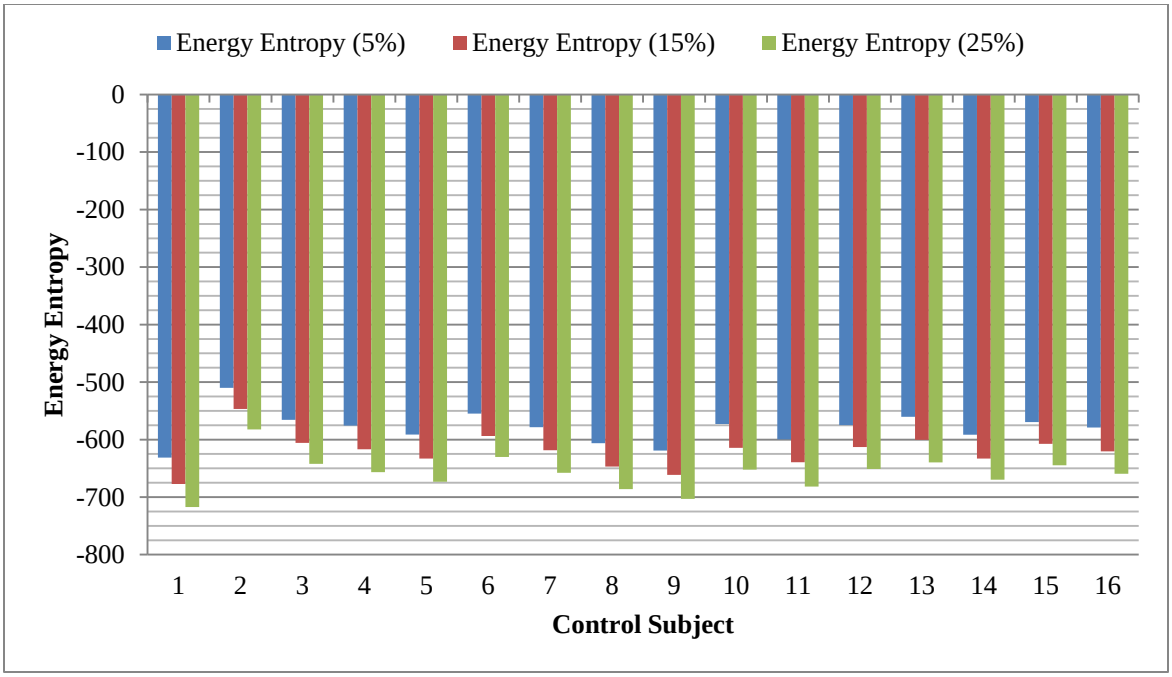

Figure 3.12: Energy entropy values for control subjects with moving window analysis

From the Figures 3.9-3.12, it is observed that the entropies values are lesser with the moving window analysis compared to the entropies values of EEG signal data sets without moving window analysis. Mean shannon entropy for AD subjects is 4.1501, 4.3886 and 4.6676 and energy entropy is -573.9325, -611.2375 and -651.5833 with 5%, 15% and 25% overlap respectively. Mean shannon entropy for control subjects is 4.1363, 4.3568 and 4.6247 and energy entropy is -579.9821, -615.9793 and -654.8878 with 5%, 15% and 25% overlap respectively.

3.4 Fractal Analysis

Fractal is a term which applies to fluctuations or irregularities in time for a time series data [5]. When magnifying a fractal signal, the fractal value increases. For a non-fractal signal or signal with very low complexity, the relationship between the fractal size and the magnification factor is a constant when plotted in a log-log scale. For a fractal

signal, the relationship is linear which indicates that as the magnification increases, the fractal value also increases. Fractal Dimension is a non-linear statistical parameter used for the measurement of the complexity of EEG signal data sets of AD subjects and control subjects [5]. The self-similarity of an EEG signal is a statistical quantity measured by the Hurst component of the rescaled range analysis. It is a non-linear fractal analysis method employed to estimate the fractal dimension from the Hurst component of the rescaled range analysis [15]. The algorithm behind the estimation of the fractal dimension of a signal in this tool is given below [5, 7]:

The factors range, R and standard deviation, S are defined by,

$$R(\tau) = \max_{1\le t\le \tau} \boldsymbol{X}(\mathrm{t},\tau) - \min_{1\le t\le \tau} \boldsymbol{X}(t,\tau) \tag{3.3}$$

$$S(\tau) = \{1/\tau \sum_{t=1}^{\tau} [\zeta(t) - (\zeta)_{\tau}]^2\}^{1/2} \tag{3.4}$$

$$(\zeta)_{\tau} = 1/\tau \sum_{t=1}^{\tau} \zeta(t) \tag{3.5}$$

$$\boldsymbol{X}(t,\tau) = \sum_{u=1}^{t} [\zeta(u) - (\zeta)_{\tau}] \tag{3.6}$$

Where $\boldsymbol{X}(t,\tau)$ is the time series, τ is the time span and t is the integer-valued time.

3.4.1 Hurst Component

The Hurst component (H) is determined for time series data sets which exhibit self-similarity attribute by calculating the rescaled range over sub-regions of the data. Self-similarity is the similarity of the statistical properties for an entire data set and for the sub-regions of a data set. The Hurst component and the fractal dimension are related by the following expression.

$$D = 2\text{-}H \tag{3.7}$$

3.4.2 Fractal Analysis Results

The fractal dimensions for the EEG data sets are calculated using the Benoit 1.3 computational package tool both with and without applying moving window analysis. Figures 3.17- 3.19 show the fractal dimensions of the processed EEG signal data sets of AD subjects and control subjects.

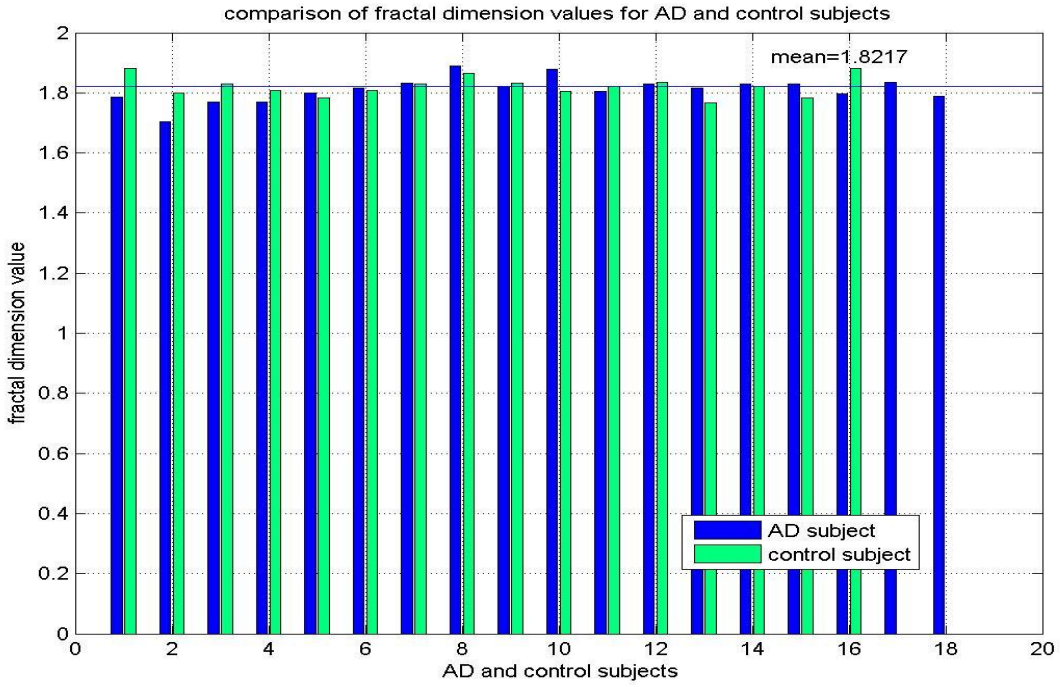

Figure 3.13: Fractal dimension values for AD subjects and control subjects

From Figure 3.13, it is observed that AD subjects 8 and 10 have a fractal dimension value greater than the mean fractal dimension of control subjects which is 1.8217 and 1.8110 for AD subjects.

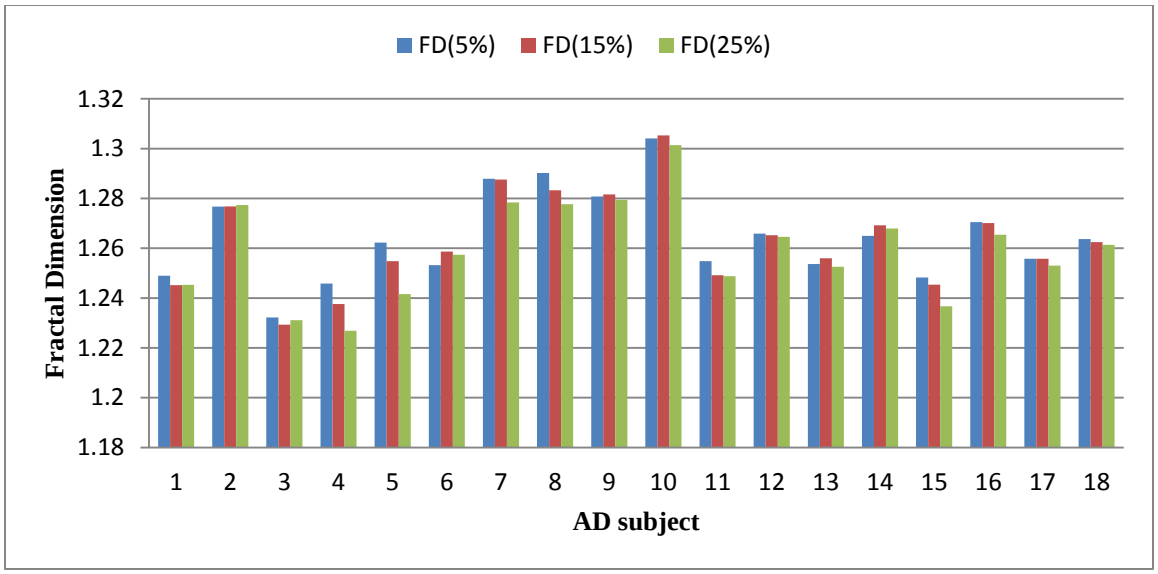

Figure 3.14: Fractal dimension values for AD subjects with moving window analysis

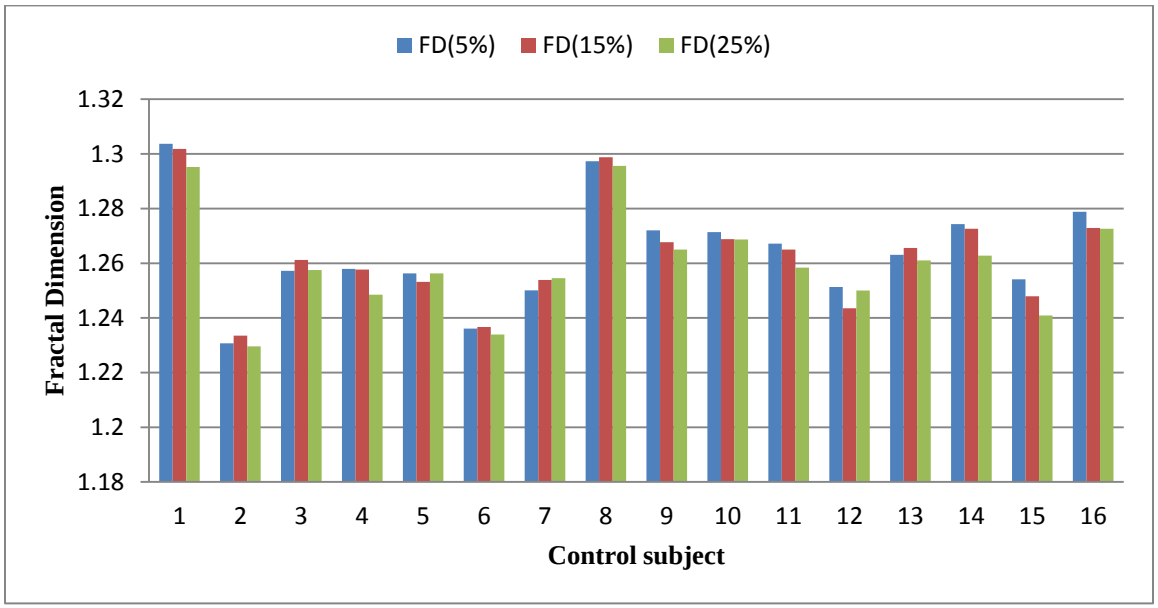

Figure 3.15: Fractal dimension values for control subjects with moving window analysis

From Figures 3.14 and 3.15, it is observed that the fractal dimension using moving window analysis give effective results compared to the fractal dimension without moving window analysis. Mean fractal dimension for AD subjects is 1.2644, 1.2630 and

1.2593 with 5%, 15% and 25% overlap respectively. Mean fractal dimension for control subjects is 1.2638, 1.2626 and 1.2594 with 5%, 15% and 25% overlap respectively.

3.5 Summary

In this chapter, the time-domain analysis of EEG signals using signal processing techniques namely Higher order moments calculation which include skewness and kurtosis calculation, Shannon entropy and energy entropy calculation and fractal dimension analysis were discussed. These techniques were also applied using a moving window analysis are also discussed. The results of the techniques discussed are the non-linear features extracted from EEG signal data sets for AD subjects and control subjects. The features are compared for the best feature extraction technique of the time domain analysis of EEG signals. The techniques are tabulated in table 3.1 with their analysis, false alarm and inconclusive rates. Recognition % is the percentage of number of subjects the feature extraction technique could differentiate between an AD and the respective control subject. False alarm rate is the number of control subjects misinterpreted as an AD subject and inconclusive rate is the number of subjects which the technique could not give any differentiation.

Table 3.1: Recognition and false alarm rates of time domain analysis methods

Time Domain Analysis method	**Recognition rate**	**False Alarm rate**	**Inconclusive rate**
Skewness	25 %	6.25 %	68.75 %
Kurtosis	43.75 %	18.7 %	37.55 %
Shannon Entropy	31.25 %	12.5 %	56.25 %
Energy Entropy	31.25 %	18.75 %	50 %
Fractal Dimension	25 %	12.5 %	62.5 %
Skewness with Moving Windows	25 %	6.25 %	68.75 %
Kurtosis with Moving Windows	18.75 %	12.5 %	31.25 %
Shannon entropy with Moving Windows	25 %	6.25 %	68.75 %
Energy entropy with Moving Windows	18.75 %	6.25 %	75 %

Chapter Four

Frequency and Frequency-Time Domain Analysis of EEG Signals

4.1 Introduction

EEG signal data sets of 18 AD subjects and 16 control subjects are analyzed by applying signal processing techniques such as the Wavelet Analysis, the Welch Power Spectrum and the Discrete Fourier Transform. These signal processing techniques are linear methods applied to extract the linear features of the EEG signals.

4.2 Wavelet Analysis

The Wavelet Transform is a signal processing tool which can be used for processing and analysis of EEG signals. As EEG signals are non-stationary i.e. their frequency components vary with time, the Wavelet Transform is applied.

4.2.1 EEG Signal De-noising Using Wavelets

Wavelets are used for the de-noising or removing random noise from EEG signals. EEG signal de-noising is performed using the Discrete Wavelet Transform (DWT). The DWT is preferred to Continuous wavelet Transform (CWT) as CWT gives lot of redundant information of the EEG signals [16]. The process of de-noising includes EEG signal decomposition, wavelet detail coefficients thresholding and signal reconstruction.
The Wavelet toolbox in MATLAB is used to implement the wavelet analysis of the EEG signals.

EEG signal decomposition is performed in the wavelet toolbox by using the daubechies wavelet function ‘db5’ at the level 3 decomposition. EEG signal is

decomposed into different frequency components at each level of decomposition. They are the approximation coefficients at level 3, A3 and detail coefficients at the levels from 1 to 3 D1, D2 and D3.

There are different thresholding methods available like the default thresholding, the soft thresholding and the hard thresholding. After de-noising using the default threshold, the signal is smooth, but it may lose some useful signal components. After hard threshold de-noising, the restored signal is almost the same than the original signal hence it is not preferred. The Soft threshold de-noising eliminates noise effectively and has a very good retention of the useful signal components. First level detail coefficients are usually considered as noise. Hence D1 detail coefficients are thresholded using the soft thresholding.

The Signal to noise ratio is calculated for the original data and the de-noised data. The signal is decomposed at level '3' by using the wavelet 'db5'.The first level detail coefficients, D1 is usually considered as noise for the signal decomposed. The noise is separated from the signal and SNR is calculated using the following formula.

$$SNR = 10 * log10\left(\frac{\sum signal^2}{\sum noise^2}\right) \quad (4.1)$$

The de-noised EEG signal data sets for AD subjects and control subjects are analyzed with the signal processing techniques discussed in chapter one and the results are compared before and after EEG signal de-noising using wavelet analysis. The parameters, skewness, kurtosis, Shannon entropy, energy entropy and fractal dimension discussed in chapter one are applied for the de-noised EEG signals and the results showing the bar graphs are shown in chapter 5.

4.3 Welch Power Spectrum

Welch Power Spectrum is used to estimate the power spectral density of EEG signals data sets for the extraction of features used in the classification of EEG signals. The Welch Power Spectrum is performed by analyzing EEG signals, and plotting the Power Spectral Densities (PSDs) in the MATLAB. The frequency components are studied and analyzed.

In Welch Power Spectrum analysis, an EEG signal data set is divided into an integer number of segments with default overlapping percentage between the segments of 50%. For each segment, a modified periodogram is computed and the PSD estimates are averaged. By averaging the PSD estimates of the modified periodograms of the segments, the variance of the overall PSD estimate decreases. This is the advantage of Welch Power Spectrum method for the extraction of spectral components of EEG signal data sets.

The Welch Power Spectrum of EEG signal data sets for AD subjects and control subjects is implemented in MATLAB. The plots of the PSD estimates using the Welch Power Spectrum method are shown in the Appendix A. A sample Welch Power Spectrum plot is shown in Figure 4.6.

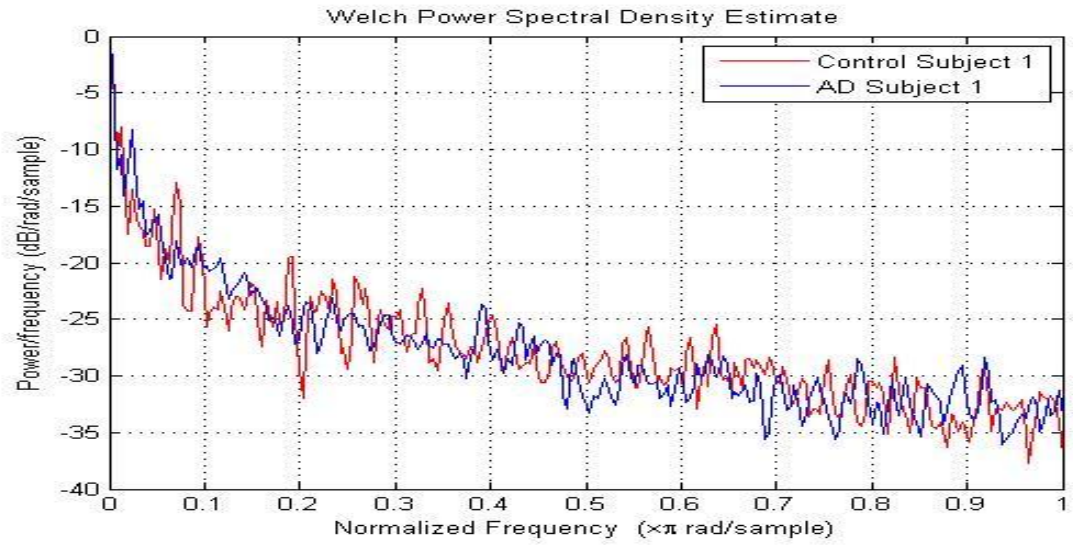

Figure 4.1: Welch PSD estimate for AD subject 1 and control subject 1

4.3.1 Welch Power Spectrum with Moving Window Analysis

Welch Power Spectrum for EEG signal data sets is implemented using moving window analysis in which the data sets are segmented and the overlapping percentages between the segments are 5%, 15% and 25%. The plots for the Welch PSD estimates of the data are shown in Appendix B. A sample plot of Welch Power Spectrum with moving windows is shown in Figure 4.7.

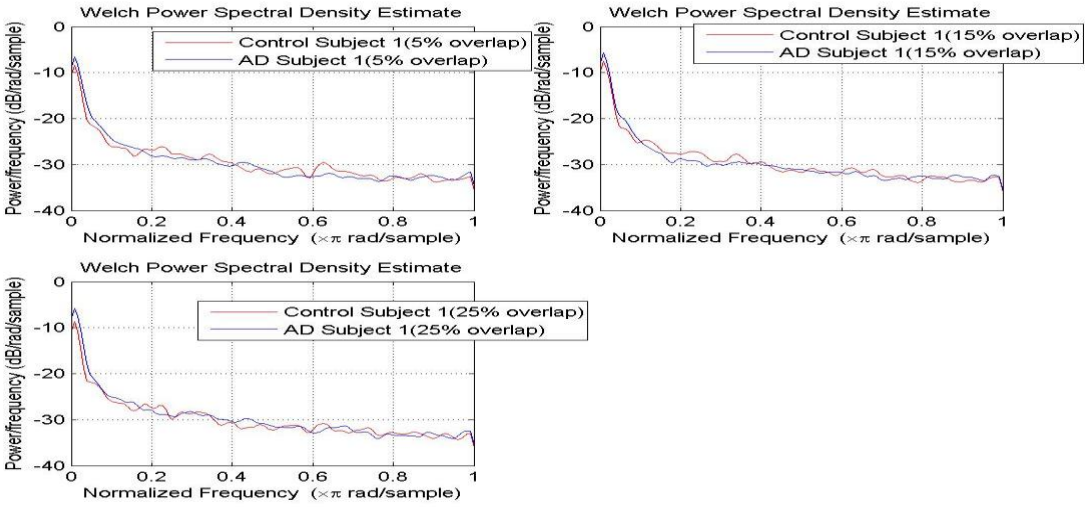

Figure 4.2: Welch PSD estimate for AD subject 1 and control subject 1 with moving window analysis

4.4 Discrete Fourier Transform

Discrete Fourier Transform (DFT) is the signal processing technique used for the frequency domain analysis of EEG signals to extract the spectral frequency components from EEG signals.

The DFT is implemented in MATLAB using the Fast Fourier Transform (FFT) algorithm. The plots of the DFT of the EEG signal data sets for AD subjects and control subjects are shown in Appendix C. A sample DFT plot is shown in the Figure 4.8.

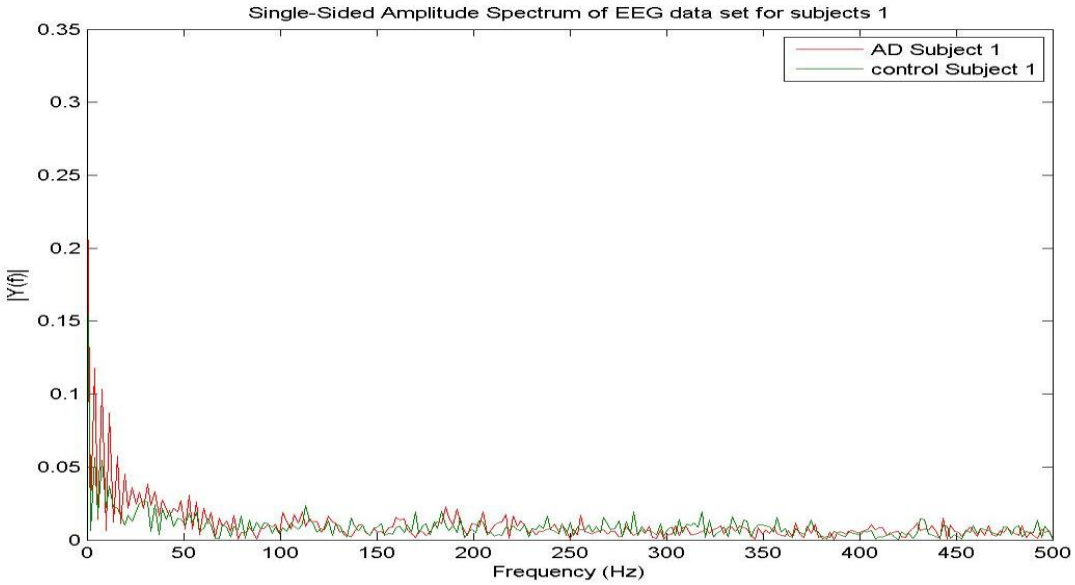

Figure 4.3: The DFT for AD subject 1 and control subject 1

4.5 Comparison of Spectral Analysis Methods

The DFT and the Welch Power Spectrum methods for spectral analysis give the frequency variations of EEG signals with the time which is defined as the frequency resolution. Due to the frequency variations, change occurs in the time domain of an EEG signal. These techniques give the frequency components but not the times at which these

frequency components exist. However, this is possible using wavelet analysis which provides both the frequency resolution and the time resolution.

4.6 Summary

Frequency domain analysis for EEG signal data sets of AD subjects and control subjects employing the signal processing techniques of spectral analysis Wavelet analysis, Welch Power Spectrum and Discrete Fourier Transform were discussed in this chapter. The methods are compared for the best feature extraction technique in the frequency domain analysis which gives the frequency components of EEG signals. Frequency domain analysis methods used for analysis of EEG signals are tabulated with their analysis and false alarm rates in the Table 4.1.

Table 4.1: Recognition and false alarm rates of frequency domain analysis methods

Frequency Domain Analysis method	**Recognition rate**	**False Alarm rate**	**Inconclusive rate**
Wavelet Transform	9.36 %	6.25 %	84.39 %
Welch Power Spectrum	50 %	12.5 %	37.5 %
Discrete Fourier transform	37.5 %	18.75 %	43.75 %
Welch Power Spectrum with moving windows	37.5 %	6.25 %	56.25 %

Chapter Five

Artifact Removal of EEG Signals

5.1 Introduction

EEG signals are de-noised for the extraction of features which are easy to classify compared to the classification of features extracted from raw EEG signals. The influence of artifacts present in an EEG signal will make the task of analyzing it more difficult.

5.2 Artifacts

During EEG signals recording, some unwanted waveforms or artifacts are added to the signals [17]. There are three types of artifacts in EEG signals namely Electrooculogram (EOG), Electrocardiogram (ECG) and Electromyogram (EMG) signal artifacts. The most severe artifacts are due to eye blinks and eyeball movements during EEG signal recording [17]. During eye movement, the electric field around the eye changes, which produces an electric signal called EOG [11]. These are low frequency signals and are very sensitive to interferences. EMG signals are electrical currents generated during muscle contraction [18]. ECG signals are electrical currents generated in heart muscle during a heartbeat [19]. EOG signal artifacts are seen more below 4 Hz frequency, ECG signal artifacts around 1.2 Hz and EMG signal artifacts above 30 Hz [17].

5.3 Artifact Removal

Artifacts need to be removed from EEG signals. Frequencies above 40 Hz do not contain any brain activity and hence they are eliminated. A band pass filter is designed using the MATLAB signal processing toolbox, with a pass band frequencies in the range

of [0.1 Hz, 40 Hz]. EEG signals are band pass filtered and digitized with a sampling rate of 1 KHz. The de-noised EEG signal obtained using a band pass filter is shown in the Figure 5.1

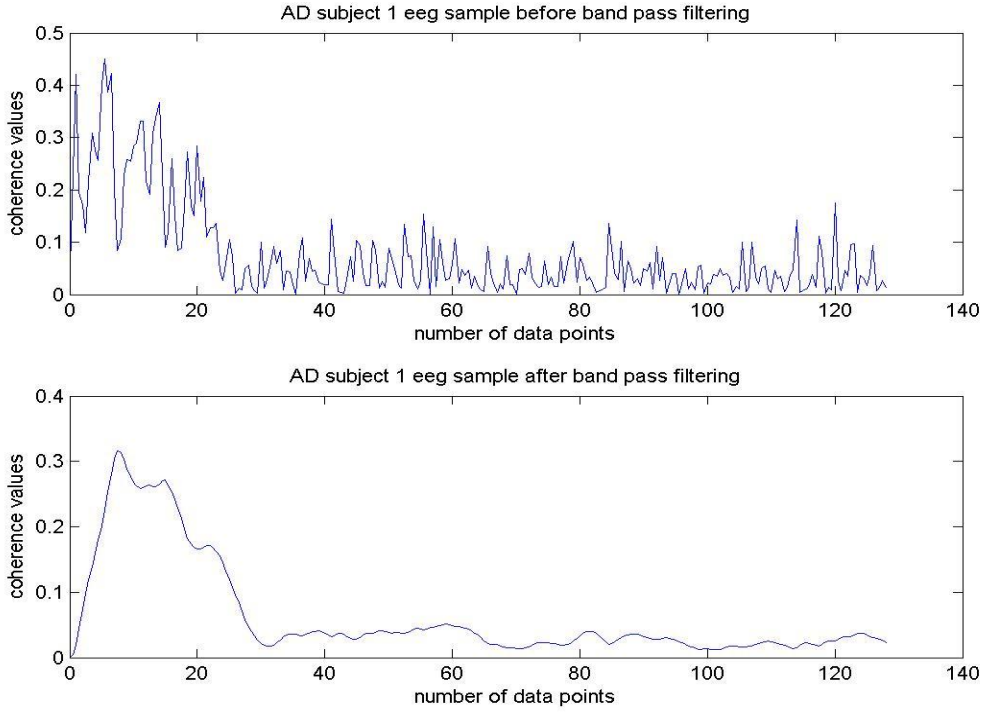

Figure 5.1: EEG signal sample before and after artifact removal

EEG signal data sets for 18 AD subjects and 16 control subjects are de-noised with the band pass filter and the de-noised data is analyzed using the signal processing techniques discussed in chapters three and four. The results analysis after artifact removal for the EEG signals are shown in the Figures 5.2-5.21.

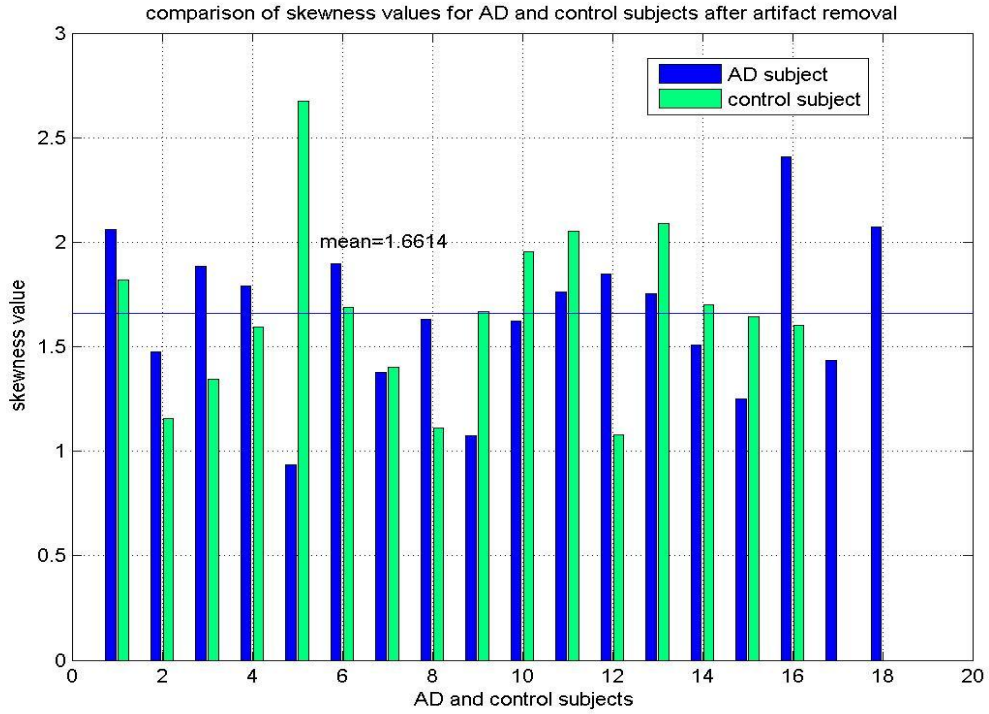

Figure 5.2: Skewness for AD subjects and control subjects after artifact removal

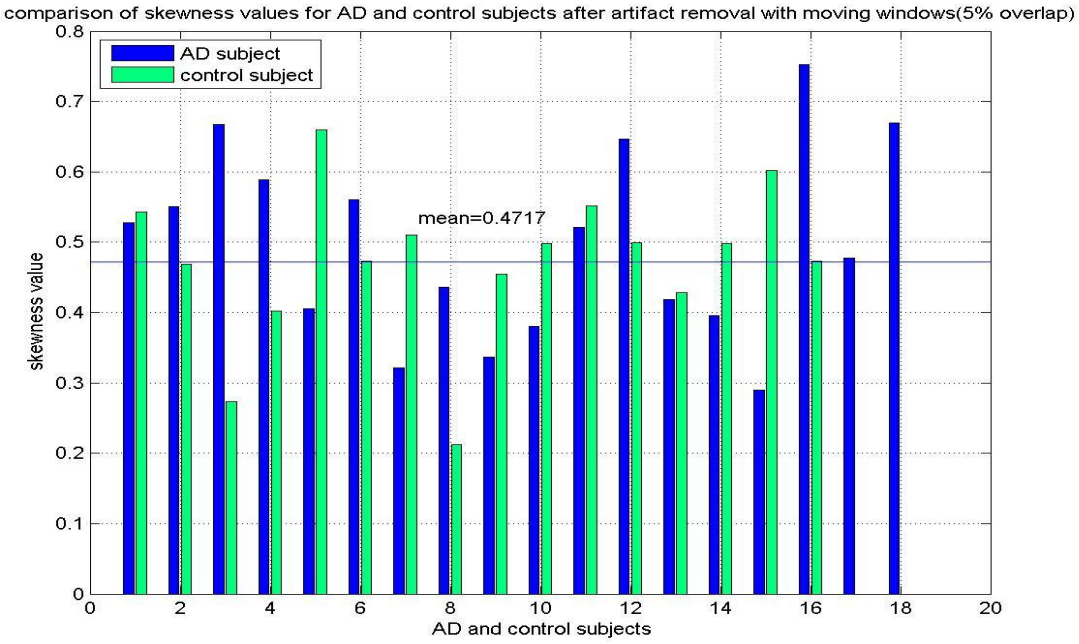

Figure 5.3: Skewness for AD subjects and control subjects with 5% overlap after artifact removal

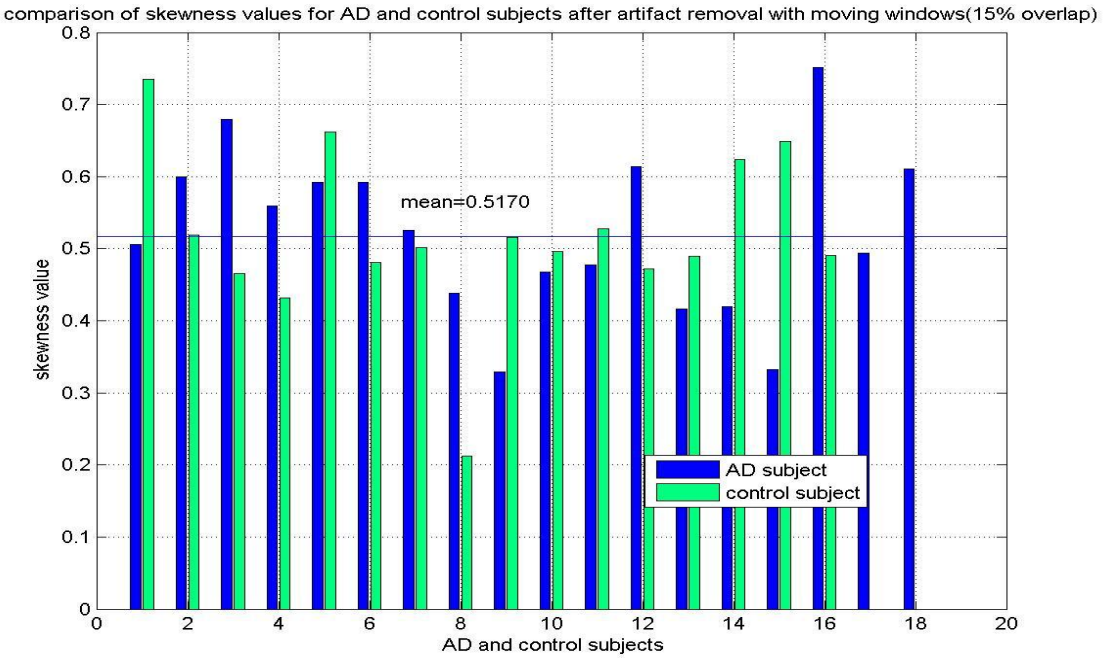

Figure 5.4: Skewness for AD subjects and control subjects with 15% overlap after artifact removal

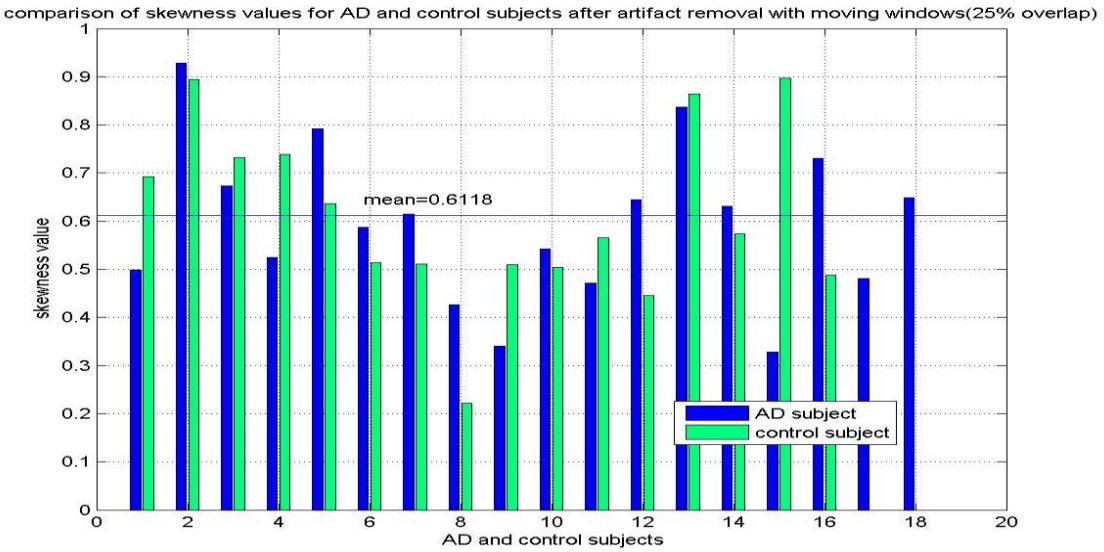

Figure 5.5: Skewness for AD subjects and control subjects with 25% overlap after artifact removal

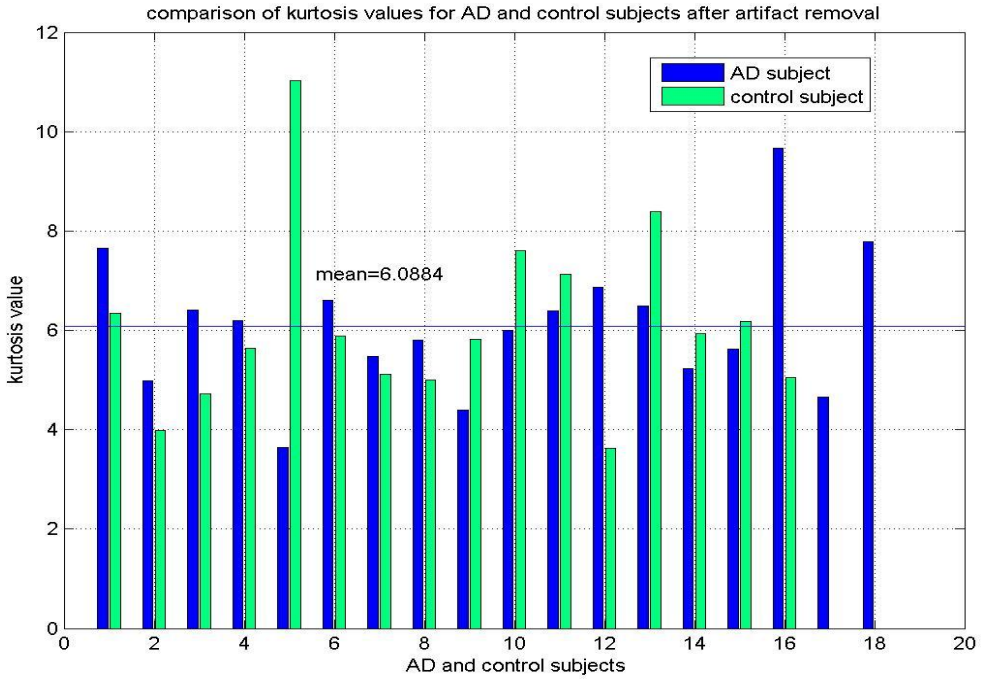

Figure 5.6: Kurtosis for AD subjects and control subjects after artifact removal

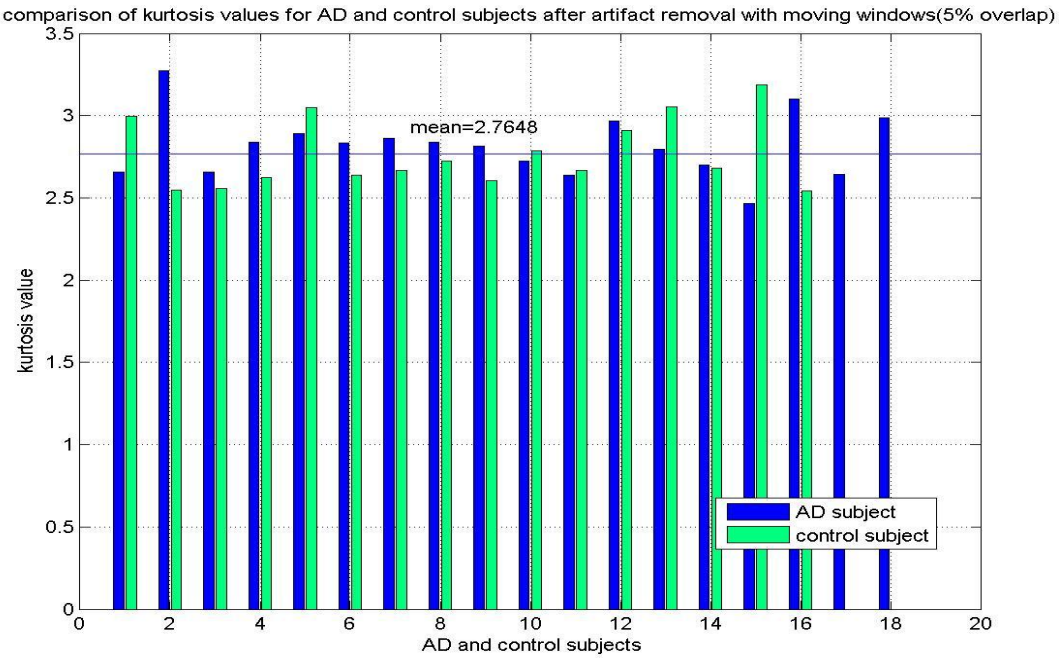

Figure 5.7: Kurtosis for AD subjects and control subjects with 5% overlap after artifact removal

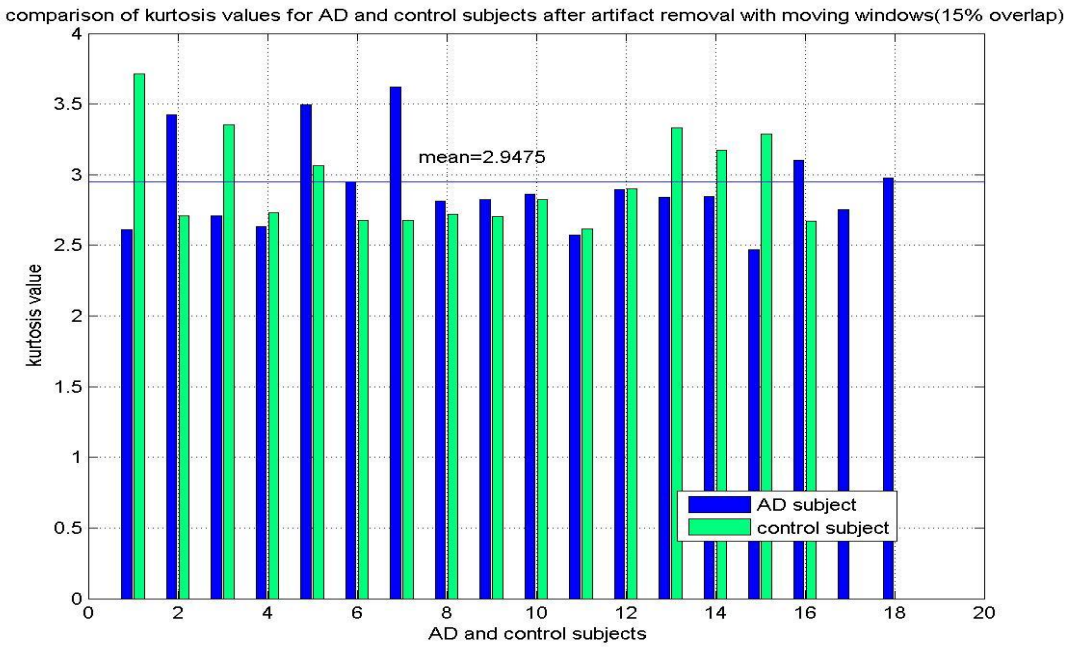

Figure 5.8: Kurtosis for AD subjects and control subjects with 15% overlap after artifact removal

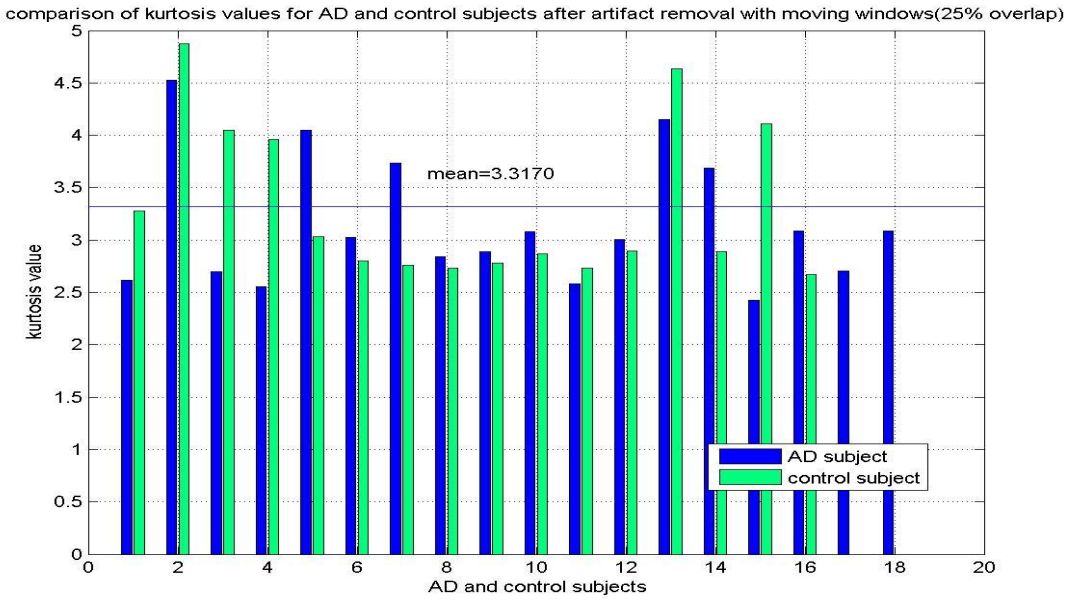

Figure 5.9: Kurtosis for AD subjects and control subjects with 25% overlap after artifact removal

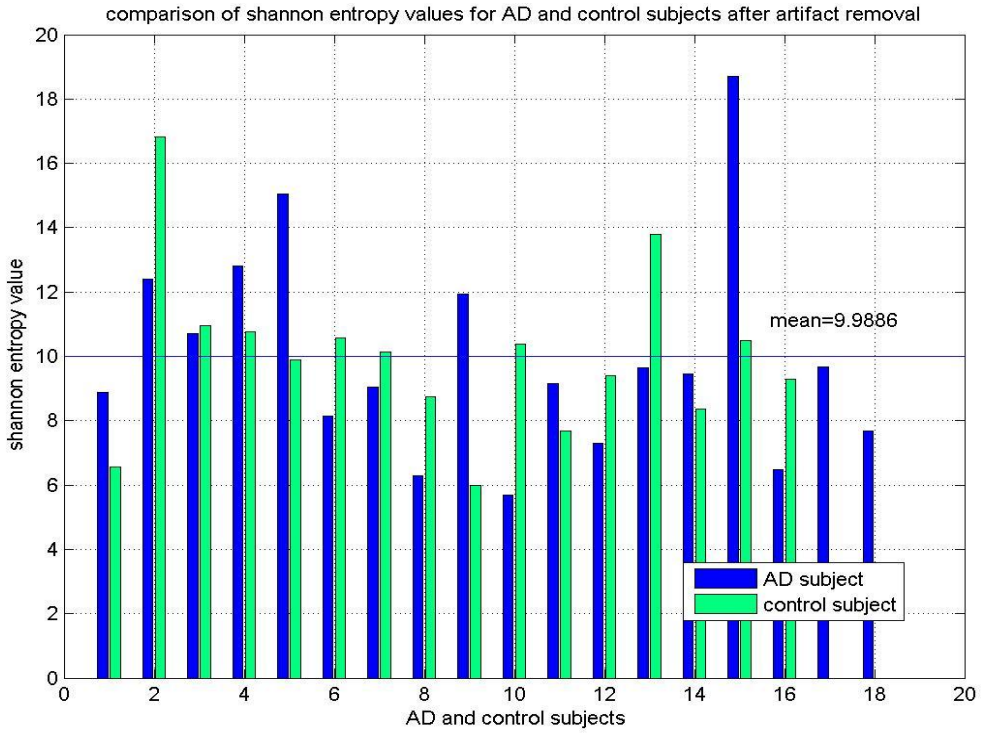

Figure 5.10: Shannon entropy for AD subjects and control subjects after artifact removal

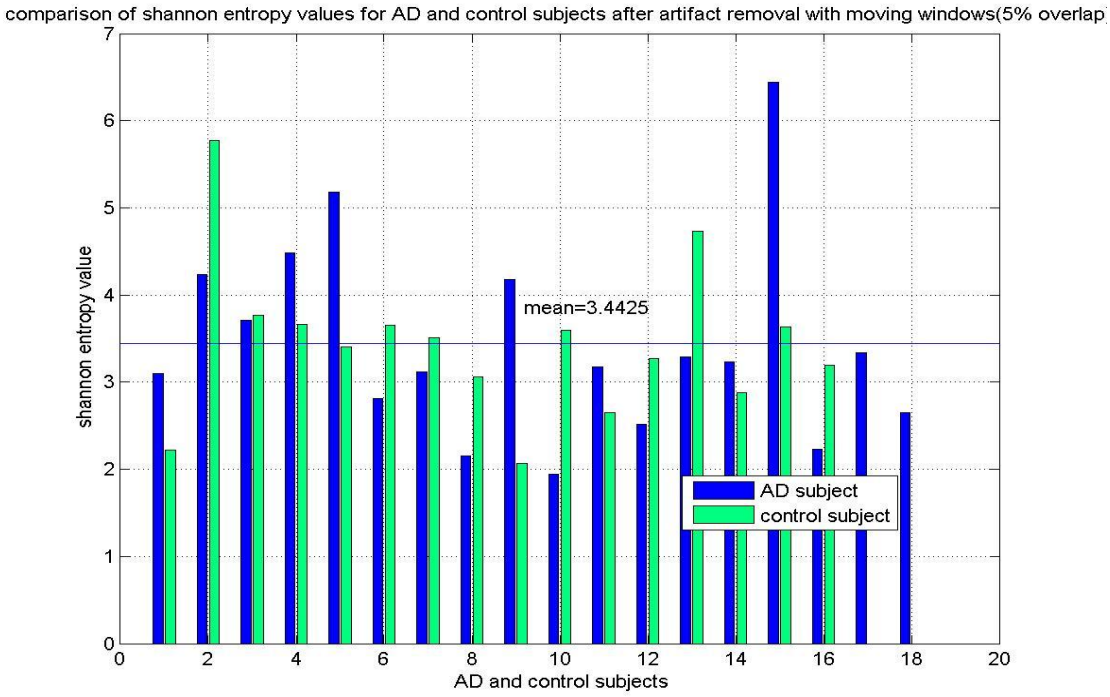

Figure 5.11: Shannon entropy for AD subjects and control subjects with 5% overlap after artifact removal

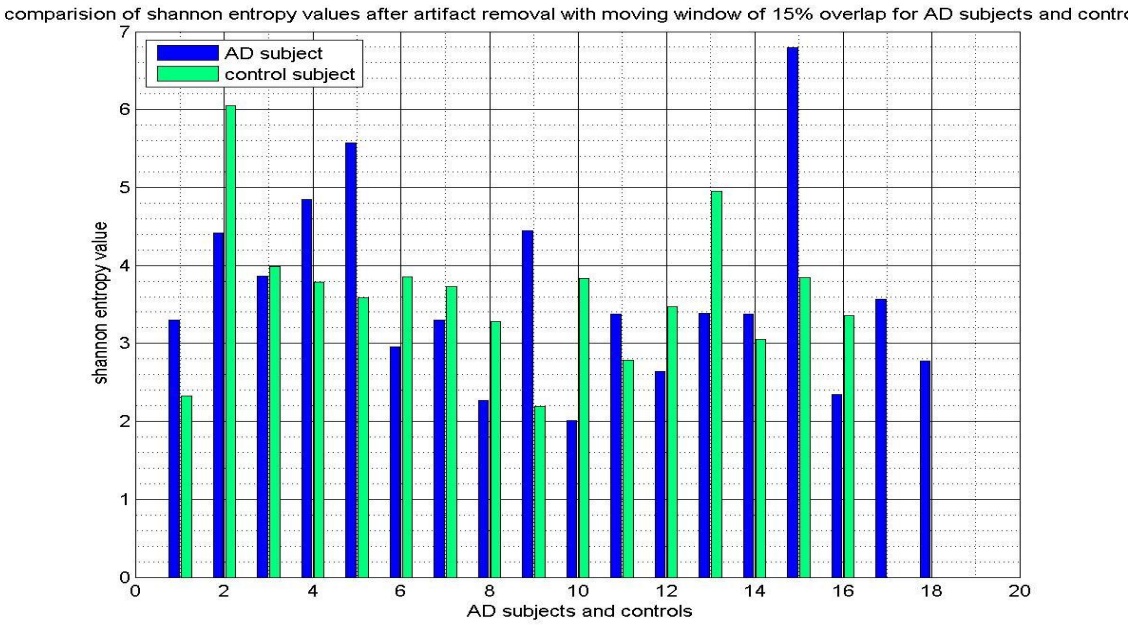

Figure 5.12: Shannon entropy for AD subjects and control subjects with 15% overlap after artifact removal

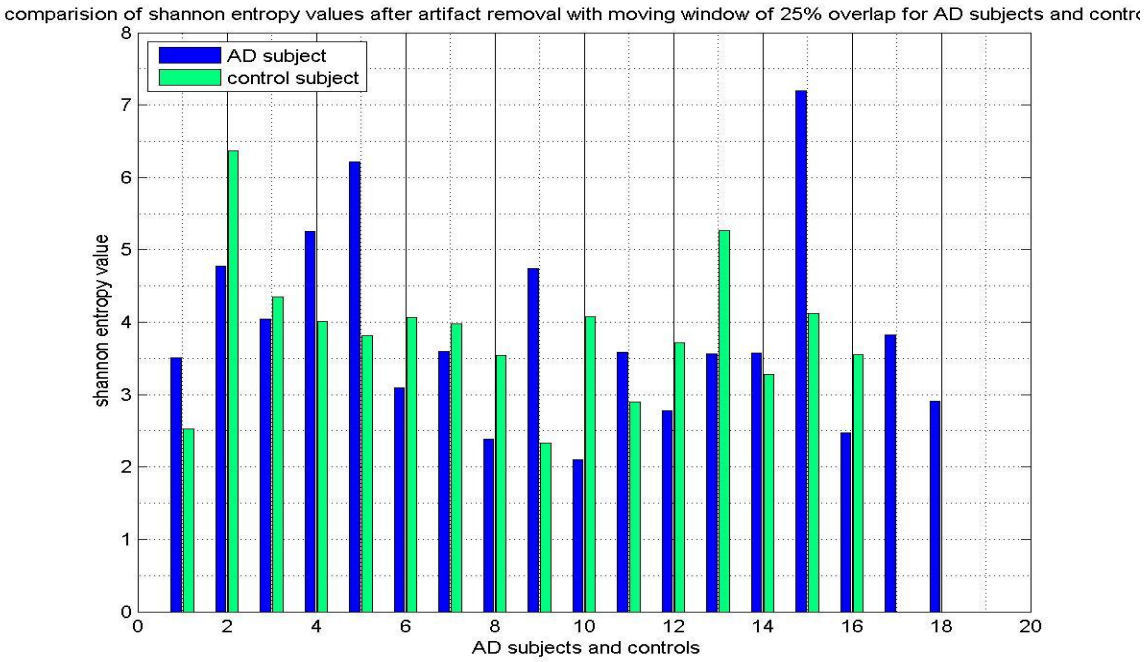

Figure 5.13: Shannon entropy for AD subjects and control subjects with 25% overlap after aircraft removal

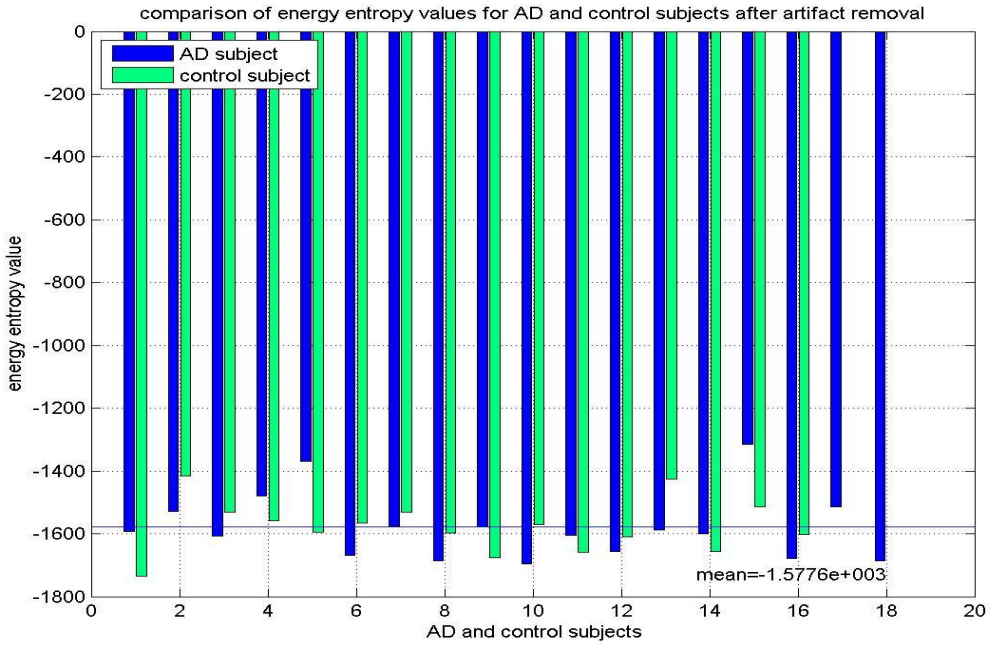

Figure 5.14: Energy entropy for AD subjects and control subjects after artifact removal

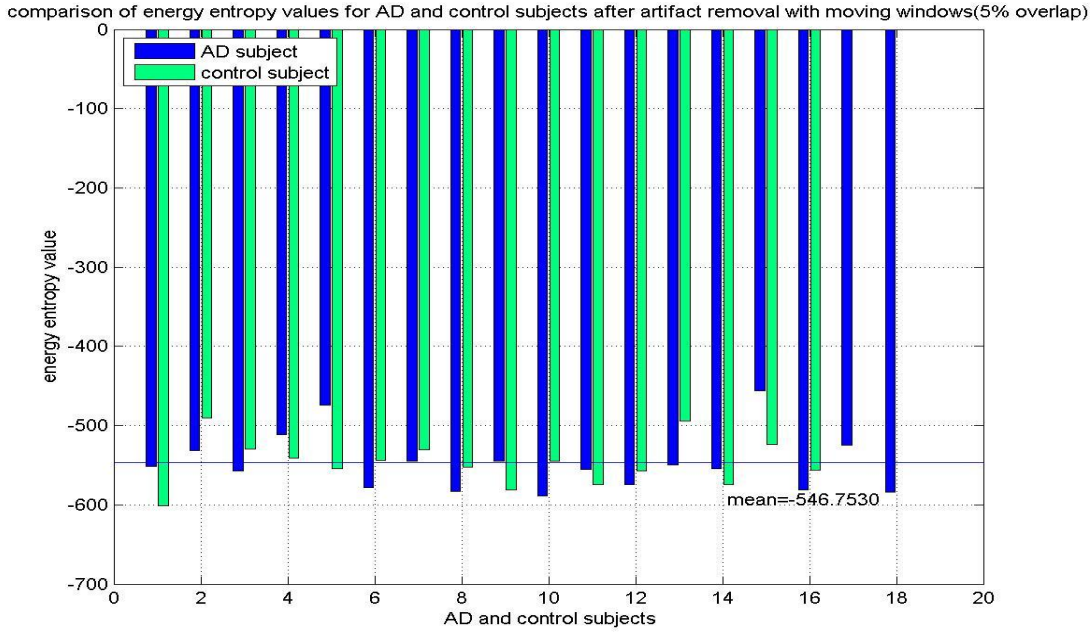

Figure 5.15: Energy entropy for AD subjects and control subjects with 5% overlp after artifact removal

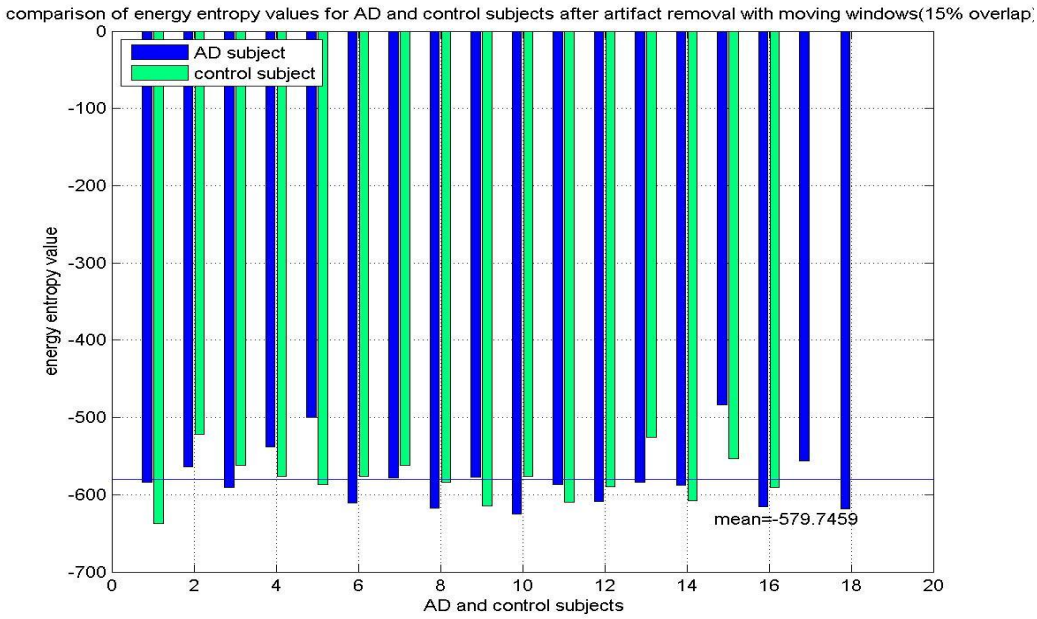

Figure 5.16: Energy entropy for AD subjects and control subjects with 15% overlap after artifact removal

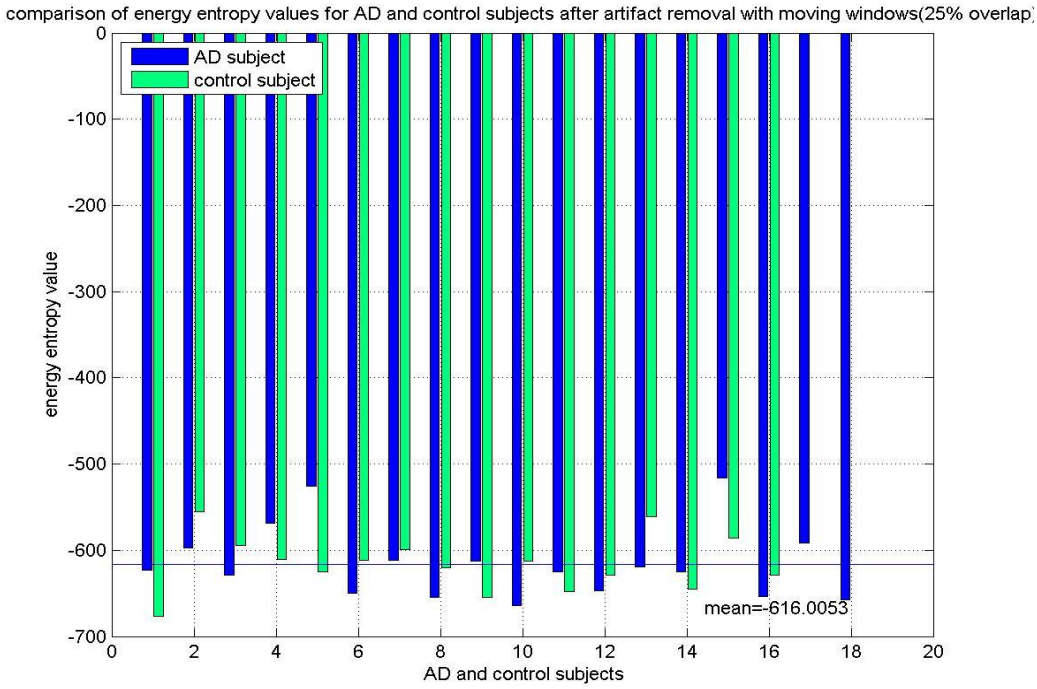

Figure 5.17: Energy entropy for AD subjects and control subjects with 25% overlap after artifact removal

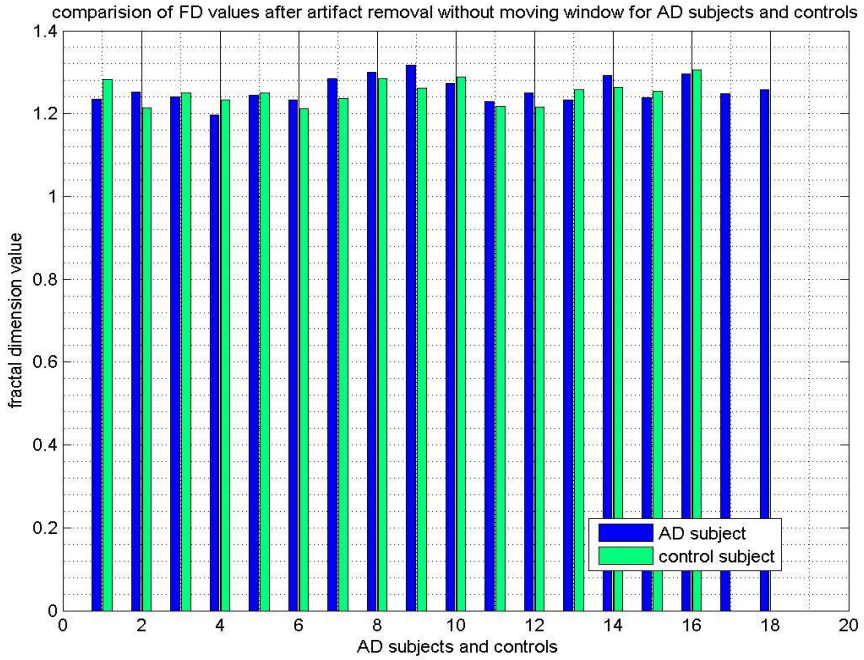

Figure 5.18: Fractal dimensions for AD subjects and control subjects after artifact removal

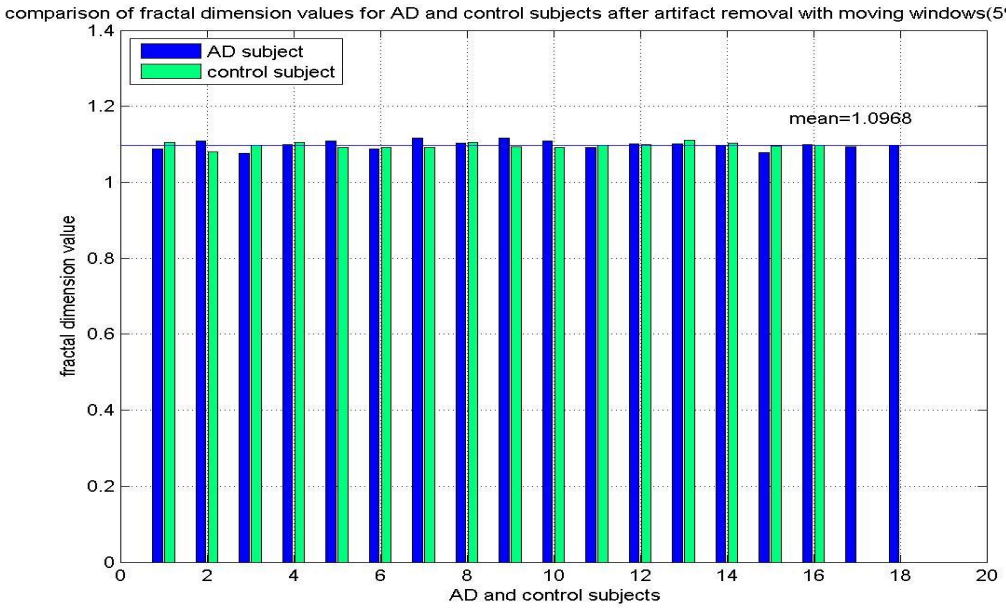

Figure 5.19: Fractal dimensions for AD subjects and control subjects with 5% overlap after artifact removal

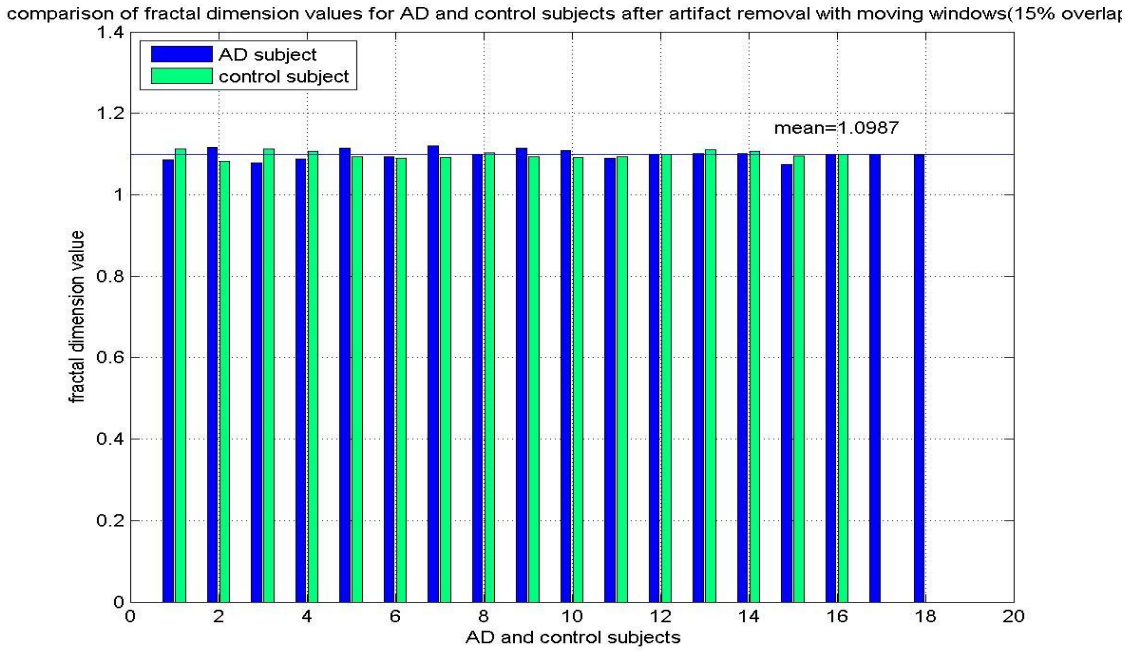

Figure 5.20: Fractal dimensions for AD subjects and control subjects with 15% overlap after artifact removal

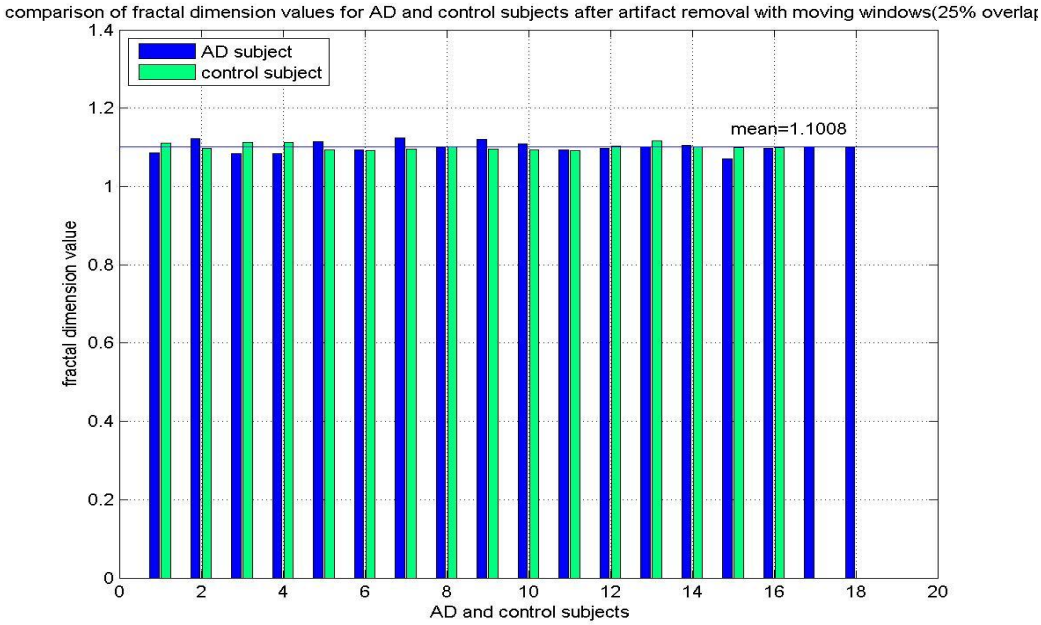

Figure 5.21: Fractal dimensions for AD subjects and control subjects with 25% overlap after artifact removal

Mean values of skewness, kurtosis, Shannon entropy, energy entropy and fractal dimension for AD and control subjects after artifact removal are shown in the table 5.1.

Table 5.1: Mean parameter values for AD and control subjects after artifact removal

EEG signal Feature	**AD subjects mean**	**Control subjects mean**
Skewness	1.6548	1.6614
Skewness with 5% overlap	0.4972	0.4717
Skewness with 15% overlap	0.5225	0.517
Skewness with 25% overlap	0.5945	0.6118
kurtosis	6.1046	6.0884
Kurtosis with 5% overlap	2.8163	2.7648
Kurtosis with 15% overlap	2.9113	2.9475
Kurtosis with 25% overlap	3.1520	3.3170
Shannon entropy	9.9468	9.9886
Shannon entropy with 5% overlap	3.4333	3.4425
Shannon entropy with 15% overlap	3.6246	3.6294
Shannon entropy with 25% overlap	3.8671	3.8684
Energy entropy	-1579.1	-1577.6
Energy entropy with 5% overlap	-546.9193	-546.753
Energy entropy with 15% overlap	-579.2165	-579.7459
Energy entropy with 25% overlap	-615.1397	-616.0053
Fractal dimension	1.2567	1.2518
Fractal dimension with 5% overlap	1.0983	1.0968
Fractal dimension with 15% overlap	1.0989	1.0987
Fractal dimension with 25% overlap	1.1002	1.1008

Also results for the time domain analysis methods applied for de-noised EEG signals through Wavelet Transform are shown in the Figures 5.22-5.26.

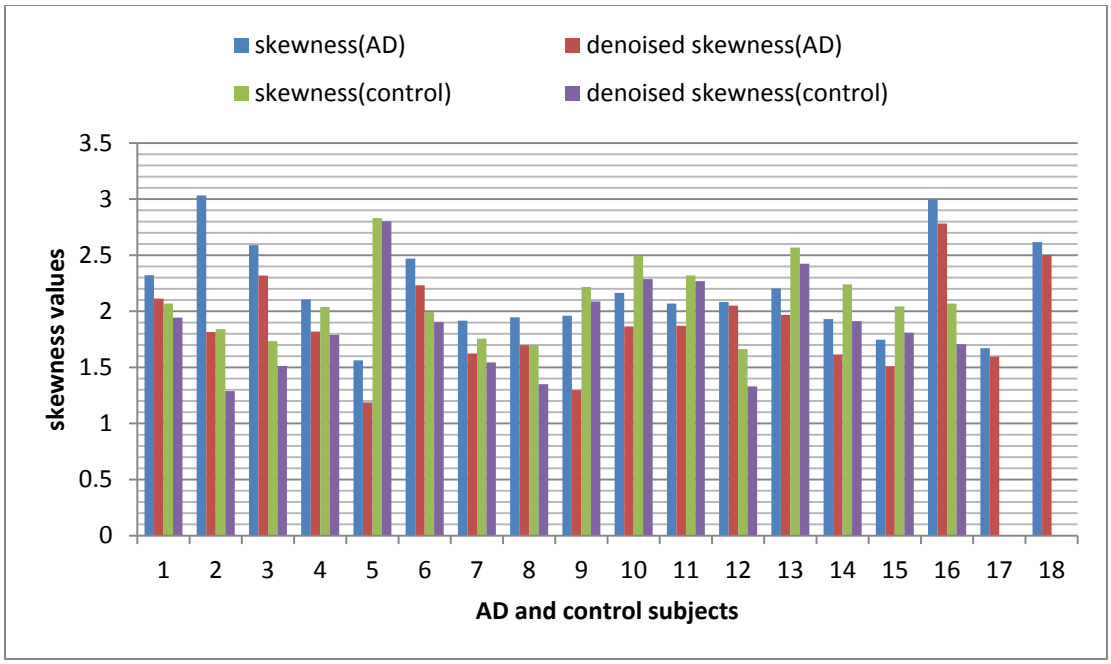

Figure 5.22: Comparison of de-noised and original skewness values for AD subjects and control subjects after wavelet analysis

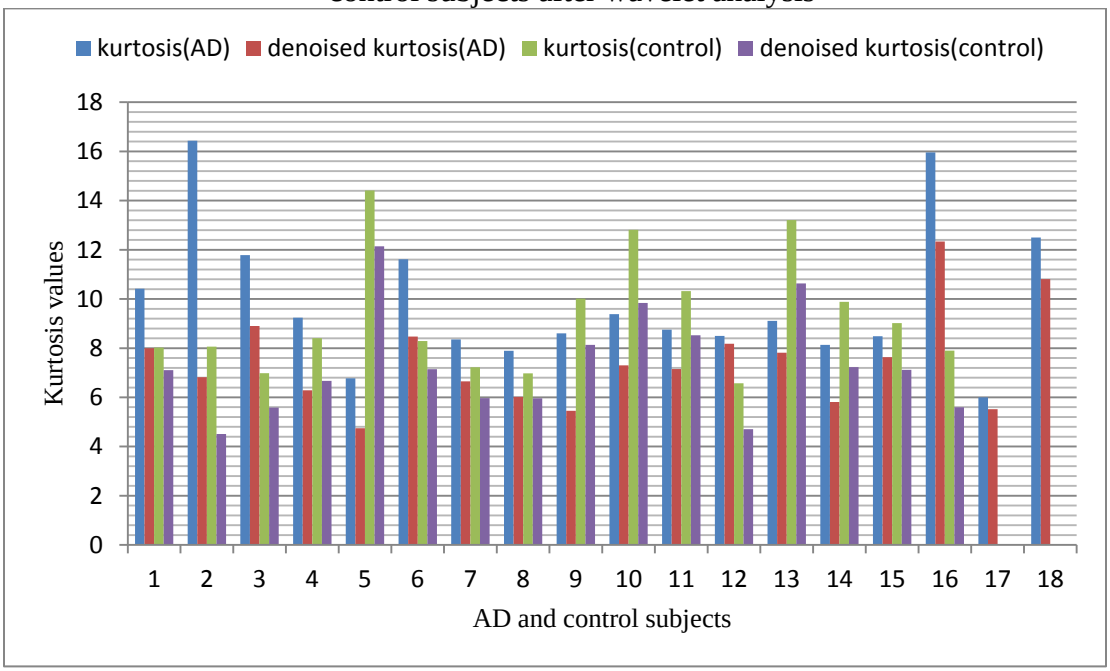

Figure 5.23: Comparison of de-noised and original kurtosis values for AD subjects and control subjects after wavelet analysis

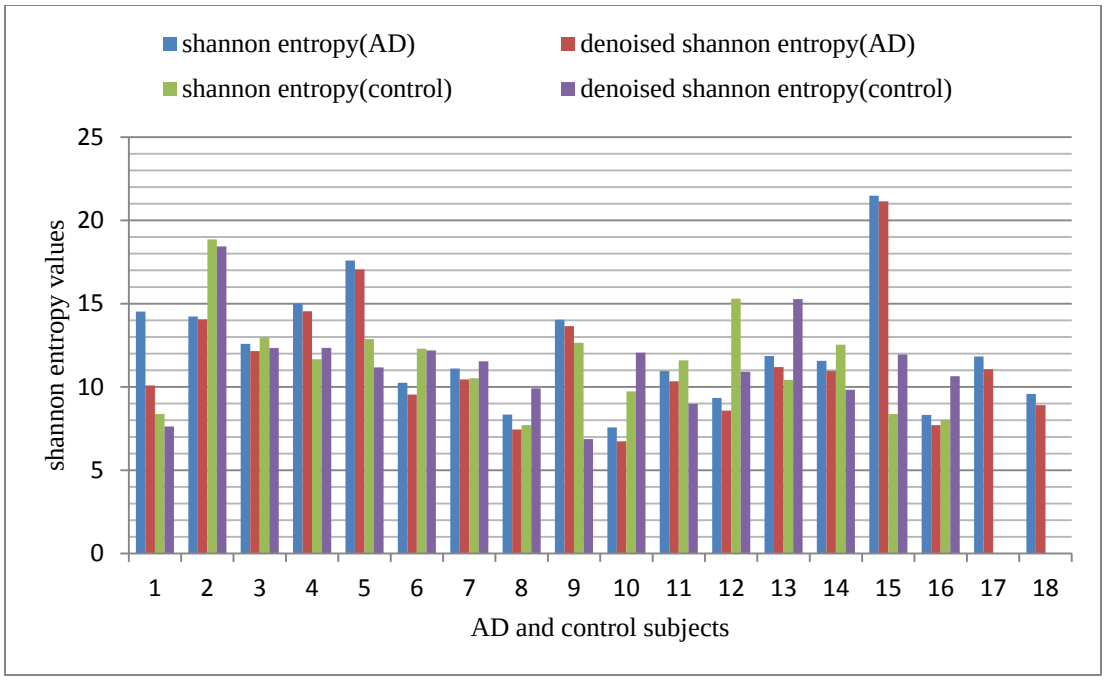

Figure 5.24: Comparison of de-noised and original Shannon entropy values for AD subjects and control subjects after wavelet analysis

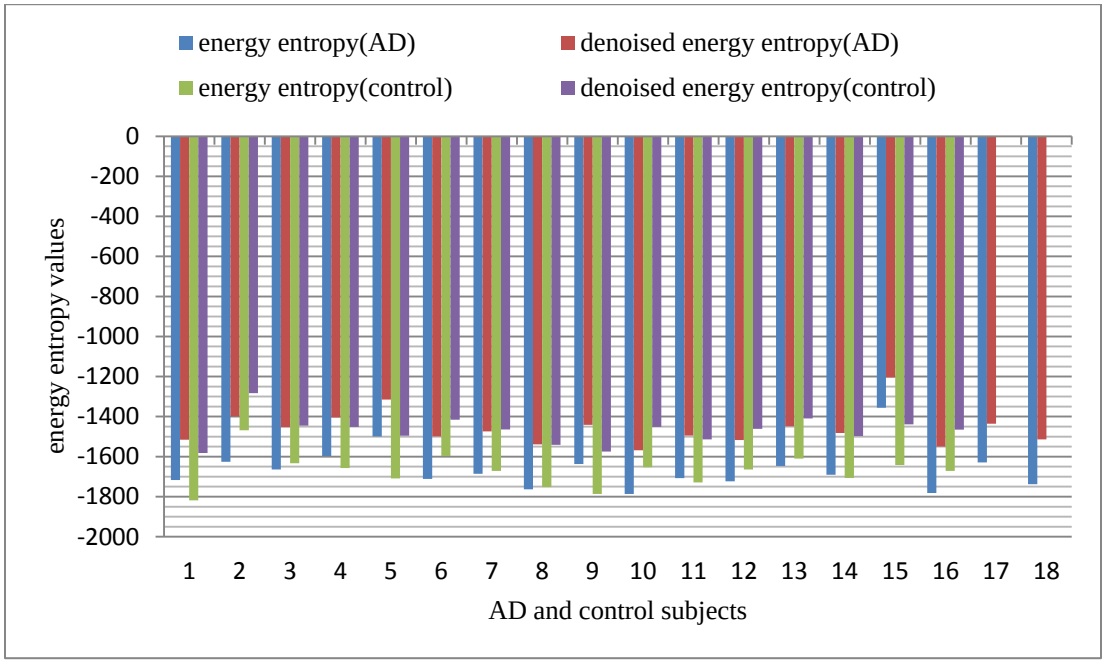

Figure 5.25: Comparison of de-noised and original energy entropy values for AD subjects and control subjects after wavelet analysis

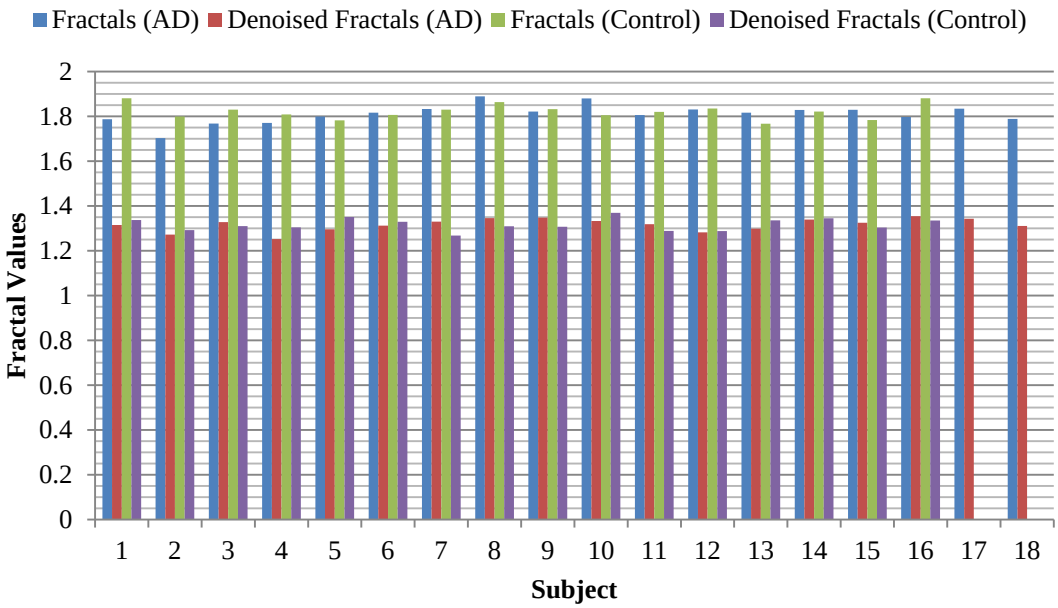

Figure 5.26: Comparison of de-noised and original fractal dimension values for AD subjects and control subjects after wavelet analysis

5.4 Welch Power Spectrum of Artifacts Removed EEG Signals

EEG signal data sets for AD subjects and control subjects are analyzed using Welch Power Spectrum to extract the frequency components of EEG signals. The Welch Power Spectrum plots are shown in the Appendix D. A sample Welch Power Spectrum plot after artifact removal with and without moving windows are shown in Figures 5.22 and 5.23.

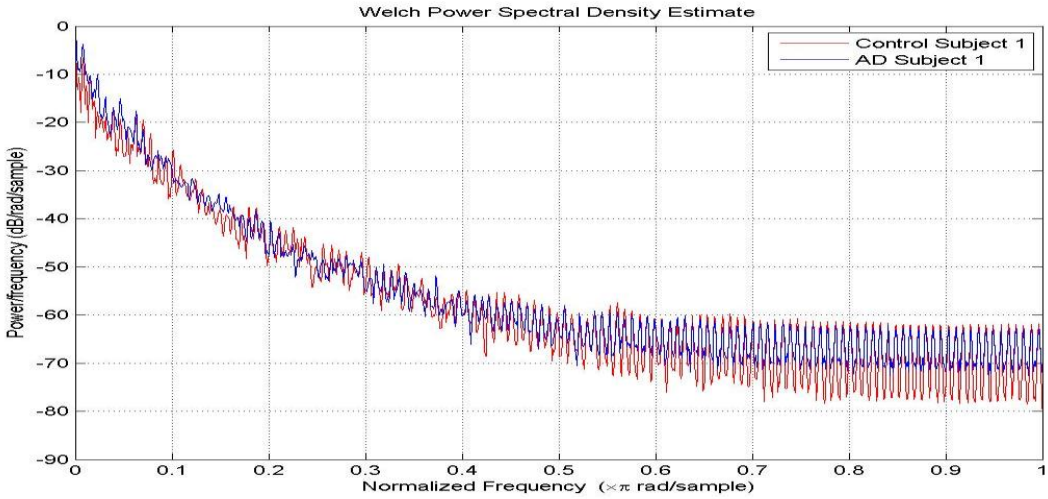

Figure 5.27: Welch Power spectrum of AD subject 1 and control subject 1 after artifact removal

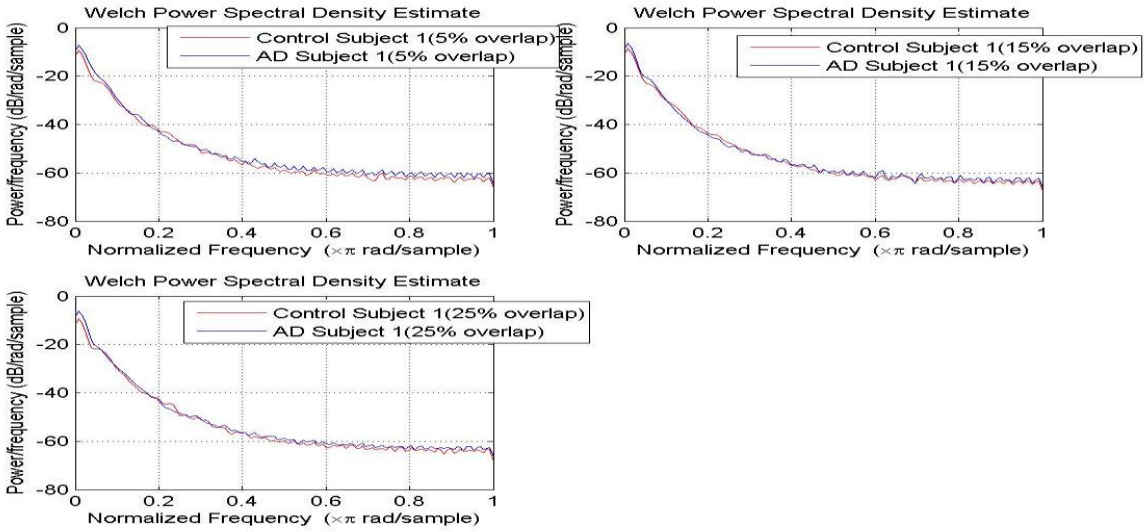

Figure 5.28: Welch Power spectrum of AD subject 1 and control subject 1 with moving window analysis after artifact removal

5.5 Discrete Fourier Transform of Artifacts Removed EEG Signals

EEG signal data sets for AD subjects and control subjects are analyzed using DFT to extract the frequency components. Frequencies above 40 Hz are removed from EEG signals and hence power is almost zero for higher frequencies. This can be observed from the figures in Appendix E. A sample DFT plot after artifact removal is shown in Figure 5.24.

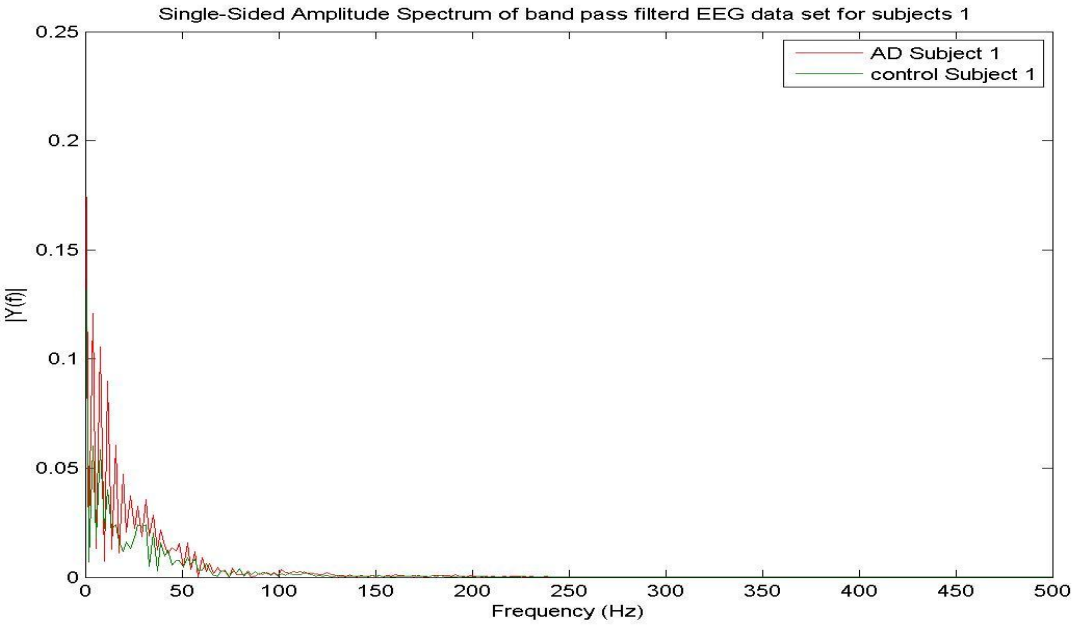

Figure 5.29: The DFT of AD subject 1 and control subject 1 after artifact removal

From the Figures 5.26-5.75, it is observed that the DFTs of the artifacts removed EEG signals have almost zero power at higher frequencies. The power is very low above 50 Hz frequency and it is zero after 150 Hz frequency. This indicates that the noise (high frequency components) is removed and the analysis of the de-noised EEG signals showed effective calculations.

5.5 Summary

Artifact removal of EEG signal data sets for AD subjects and control subjects using the band pass filter with a pass band of frequency range [0.1 Hz, 40 Hz] at a sampling frequency of 1 KHz was discussed in this chapter. Analysis of the de-noised data using the signal processing techniques in time domain and frequency domain discussed in chapter three and chapter four were also discussed in this chapter. The artifacts removed EEG signals analysis and the results are also discussed in this chapter.

Recognition, false alarm and inconclusive rates of the time and frequency domain analysis methods for extracting features from artifacts removed EEG signals are shown in Tables 5.2 and 5.3.

Table 5.2: Recognition and false alarm rates of time domain analysis methods for artifacts removed EEG signals

Time Domain Analysis method	**Recognition rate**	**False Alarm rate**	**Inconclusive rate**
Skewness	37.5 %	12.5 %	50 %
Kurtosis	37.5 %	25 %	37.5 %
Shannon Entropy	43.75 %	18.75 %	37.5 %
Energy Entropy	25 %	18.75 %	56.25 %
Fractal Dimension	18.75 %	6.25 %	75 %
Skewness with Moving Windows	50 %	18.75 %	31.25 %
Kurtosis with Moving Windows	37.5 %	18.75 %	43.75 %
Shannon entropy with Moving Windows	56.25 %	25 %	18.75 %
Energy entropy with Moving Windows	25 %	18.75 %	56.25 %

Table 5.3: Recognition and false alarm rates of frequency domain analysis methods for artifacts removed EEG signals

Frequency Domain Analysis method	**Recognition rate**	**False Alarm rate**	**Inconclusive rate**
Welch Power Spectrum	50 %	18.75 %	31.25 %
Discrete Fourier transform	43.75 %	18.75 %	37.5 %
Welch Power Spectrum with moving windows	50 %	25 %	25 %

Chapter Six

Conclusion and Future Work

6.1 Conclusions

Analysis of EEG signals for the diagnosis and detection of AD was studied in this work. Time domain and frequency domain analyses of EEG signals for 18 AD subjects and 16 control subjects were performed to extract their non-linear and linear features. The non-linear features extracted in the time domain analysis using the non-linear methods of signal processing namely higher order moments, entropies and fractal analysis with and without moving window analysis determined the complexity of EEG signals. The frequency domain analysis of EEG signals using linear methods of signal processing namely Wavelet Transform, Welch Power Spectrum and DFT determined the frequency components of EEG signals. Spectral analysis techniques were applied to analyze EEG signals and power spectra of EEG signal data sets were extracted and plotted. EEG signals are de-noised using band pass filter designed and all the signal processing techniques used before de-noising are used to extract the features of EEG signals after artifact removal. The results obtained after artifact removal were effective as the noises in EEG signals were removed and hence unwanted information was not extracted while extracting the features.

In summary, all the signal processing techniques used in this study are compared to determine the best feature extraction technique. Among the time domain analysis methods, fractal analysis is found to be effective as the fractal dimension values showed significant differences between AD subjects and their respective control subjects. Among the frequency domain analysis methods, Wavelet Transform method is preferred as it

gave both the frequency resolution and time resolution whereas the DFT and Welch Power Spectrum gave only the frequency resolution. Analysis and false alarm rates are estimated for the feature extraction techniques in time and frequency domain.

6.2 Future Work

This study has taken time domain and frequency domain analysis techniques of signal processing to extract features from EEG signals for the diagnosis and detection of AD. Based on the results obtained, the best feature extraction technique among the techniques applied in this study is determined and the features obtained with this technique are used for the classification of EEG signals. The best features obtained in this work using the methods discussed are useful in the future research study of EEG signals by classifying them. Classification of EEG signals is the next step in the diagnosis of AD. The features are given to a classifier chosen and a quantitative index is obtained based on which the level of AD is determined.

REFERENCES

[1] Tang-Kai Yin; Nan-Tsing Chiu; , "Fuzzy Patterns and Classification of Functional Brain Images for the Diagnosis of Alzheimer's Disease," *Fuzzy Systems, 2005. FUZZ '05. The 14th IEEE International Conference on Fuzzy Systems, pp.161-166, 25-25 May 2005.*

[2] M. Tepla, "Fundamentals of EEG Measurement," *MEASUREMENT SCIENCE REVIEW, Vol. 2, Section 2, 2002.*

[3] D. K. Ravis, S. Shenbaga Dev, "Automated Seizure Detection and Spectral Analysis of EEG Seizure Time Series," *European Journal of Scientific Research ISSN 1450-216X Vol.68 No.1 (2012), pp. 72-82, 2012.*

[4] Ferenets, R.; Tarmo Lipping; Anier, A.; Jantti, V.; Melto, S.; Hovilehto, S.; , "Comparison of entropy and complexity measures for the assessment of depth of sedation," *Biomedical Engineering, IEEE Transactions on* , vol.53, no.6, pp.1067-1077, June 2006.

[5] Nahina Islam, Nafiz I.B. Hamid, Adnan Mahmud, Sk.M. Rahman, Arafat H. Khan, "Detection of Some Major Heart Diseases Using Fractal Analysis," *International Journal of Biometrics and Bioinformatics, Vol. 4, Issue 2, pp. 63-70, 2010.*

[6] B. S. Raghavendra, D. Narayana Dutt, "Computing Fractal Dimension of Signals using Multiresolution Box-counting Method," *International Journal of Information and Mathematical Sciences, pp. 50-75, 2010.*

[7] Bodruzzaman, M.; Cadzow, J.; Shiavi, R.; Kilroy, A.; Dawant, B.; Wilkes, M.; , "Hurst's rescaled-range (R/S) analysis and fractal dimension of electromyographic (EMG) signal," *Southeastcon '91., IEEE Proceedings of, pp. 1121-1123 vol.2, 7-10 Apr 1991.*

[8] Abdul-Bary Raouf Suleiman, Toka Abdul-Hameed Fatehi, "Features Extraction Techniques of EEG Signal For BCI Applications." *International Arab Conference on Information Technology, pp. 1-5, 2011.*

[9] S. Deivanayagi, M. Manivannan, Peter Fernandez, "Spectral Analysis Of EEG Signals During Hypnosis," *International Journal of Systemics, Cybernetics and Informatics, pp. 75-80, 2007.*

[10] Maan M. Shaker, "EEG Waves Classifier using Wavelet Transform and Fourier Transform," *International Journal of Biological and Life Sciences, pp. 85-90, 2005.*

[11] Parisa Shooshtari, Gelareh Mohamadi, Behnam Molaee Ardekani, Mohammad Bagher Shamsollahi, "Removing Ocular Artifacts from EEG Signals using Adaptive Filtering and ARMAX Modeling," *World Academy of Science, Engineering and Technology, pp. 457-460, 2005.*

[12] Mohamed Bedeeuzzaman, V.; Farooq, O.; Uzzaman Khan, Y.; , "Automatic Seizure Detection Using Higher Order Moments," *Recent Trends in Information, Telecommunication and Computing (ITC), 2010 International Conference on , vol., no., pp.159-163, 12-13 March 2010.*

[13] Brijil Chambayil, Rajesh Singla, R. Jha, "EEG Eye Blink Classification Using Neural Network," *Proceedings of the World Congress on Engineering, Vol I, pp. 1-4, June 30 - July 2 2010.*

[14] Çağlar Tuncay, "Shannon entropies of the distributions of various electroencephalograms from epileptic Humans." *Medical Physics, pp. 1-8, Nov 2009.*

[15] T. López 1,2,a, C. L. Martínez-González3, J. Manjarrez1, N. Plascencia1 and A. S. Balankin1,b, "Fractal Analysis of EEG Signals in the Brain of Epileptic Rats, with and without Biocompatible Implanted Neuroreservoirs," *Applied Mechanics and Materials Vol. 15, pp. 127-136, 2009.*

[16] E. Hoˇsˇt´alkov´a, A.Proch´azka, "Wavelet Signal and Image Denoising." *International Journal of Electronic Engineering Research, vol. 2, pp. 303-324, 2010.*

[17] G.Geetha, Dr.S.N.Geethalakshmi, "Scrutinizing different techniques for artifact removal from EEG signals," *International Journal of Engineering Science and Technology (IJEST), vol.3 No. 2, pp-1167-1172, 2011.*

[18] Md. R. Ahsan, Muhammad I. Ibrahimy, Othman O. Khalifa, "EMG Signal Classification for Human Computer Interaction: A Review," *European Journal of Scientific Research ISSN 1450-216X Vol.33 No.3, pp.480-501, 2009.*

[19] Gavendra Singh, Varun Gupta, Dilbag Singh, "Coherence Analysis between ECG Signal and EEG Signal," *International Journal of Electronics and Communication Technology, pp. 25-28, December 2010.*

Appendices

Appendix A

The Welch Power Spectrum Plots for AD Subjects and Control Subjects

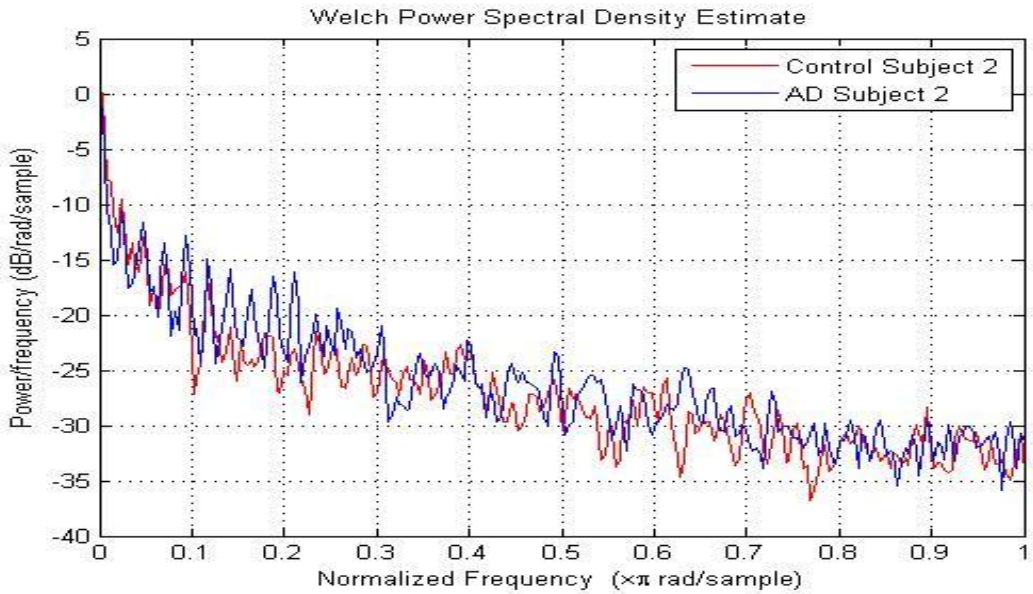

Figure A-1: Welch PSD estimate for AD subject 2 and control subject 2

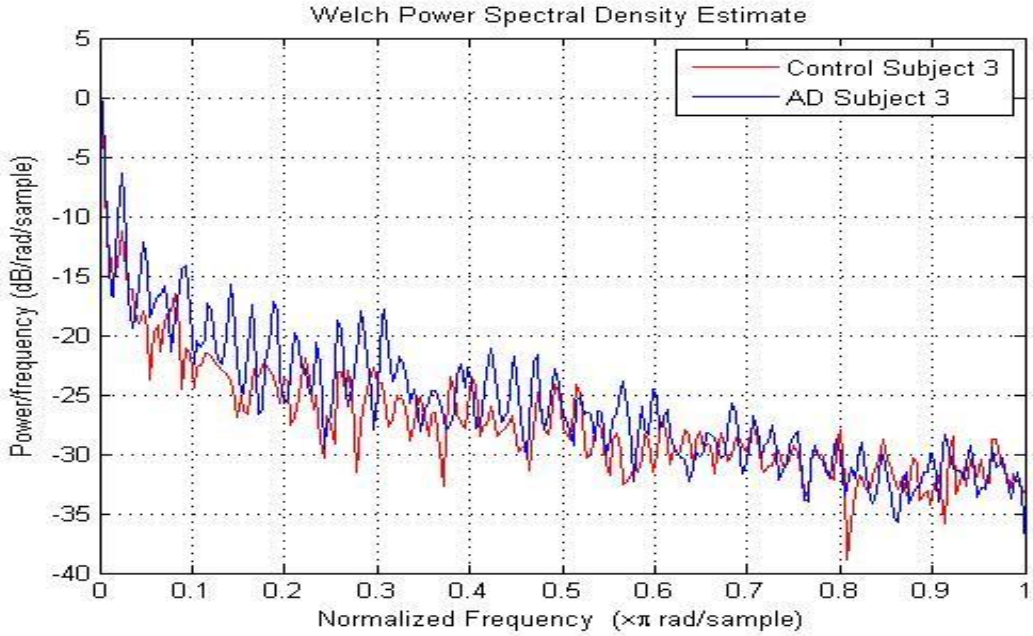

Figure A-2: Welch PSD estimate for AD subject 3 and control subject 3

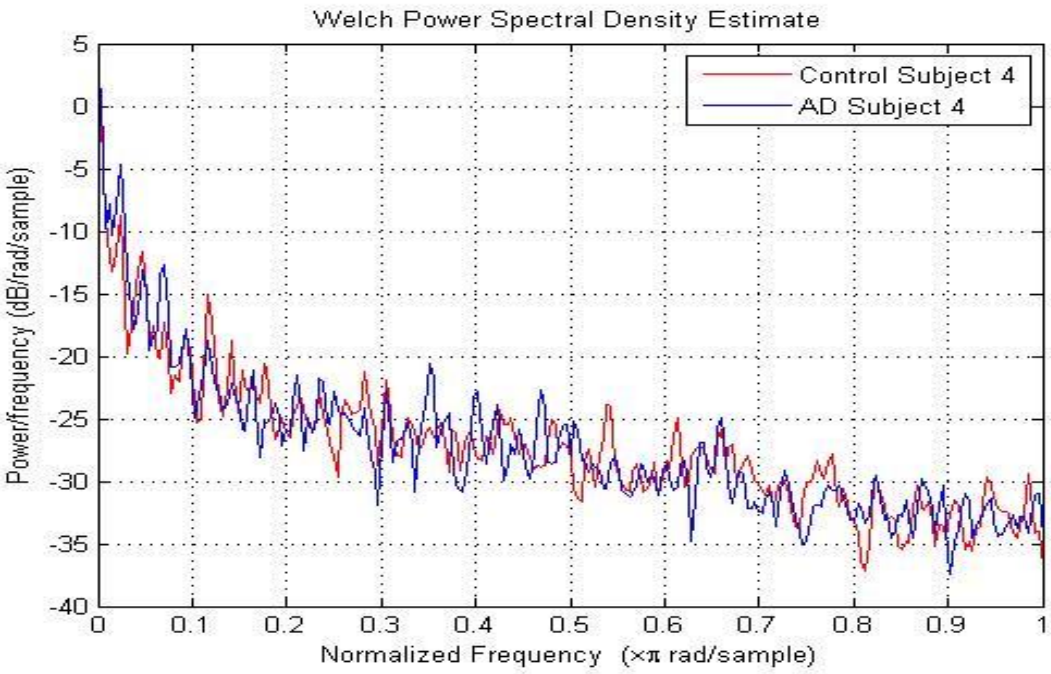

Figure A-3: Welch PSD estimate for AD subject 4 and control subject 4

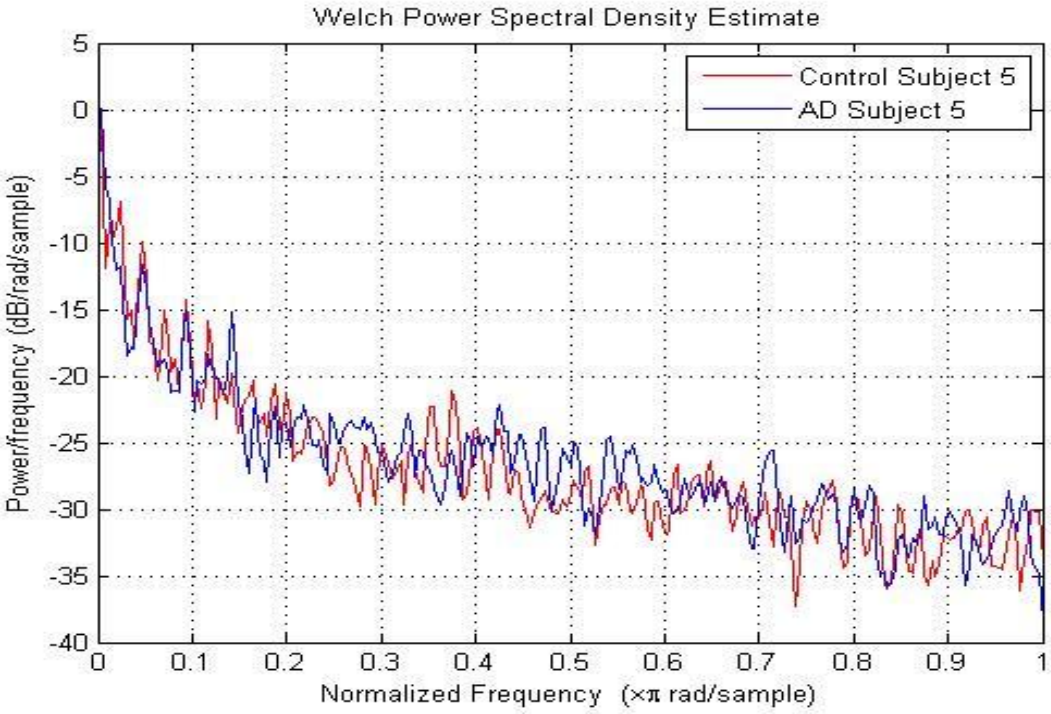

Figure A-4: Welch PSD estimate for AD subject 5 and control subject 5

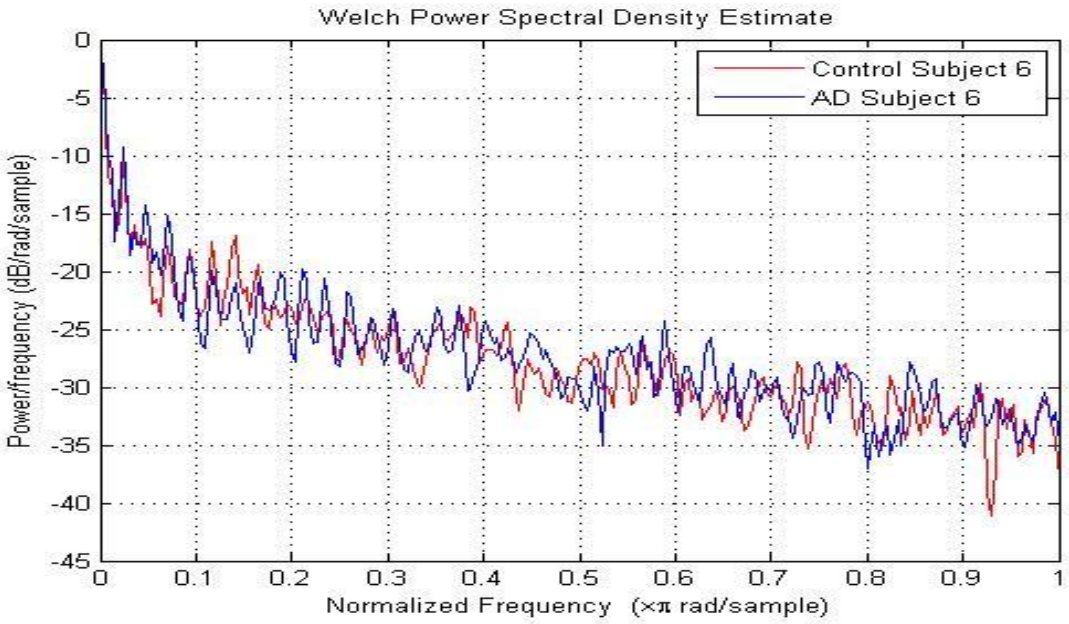

Figure A-5: Welch PSD estimate for AD subject 6 and control subject 6

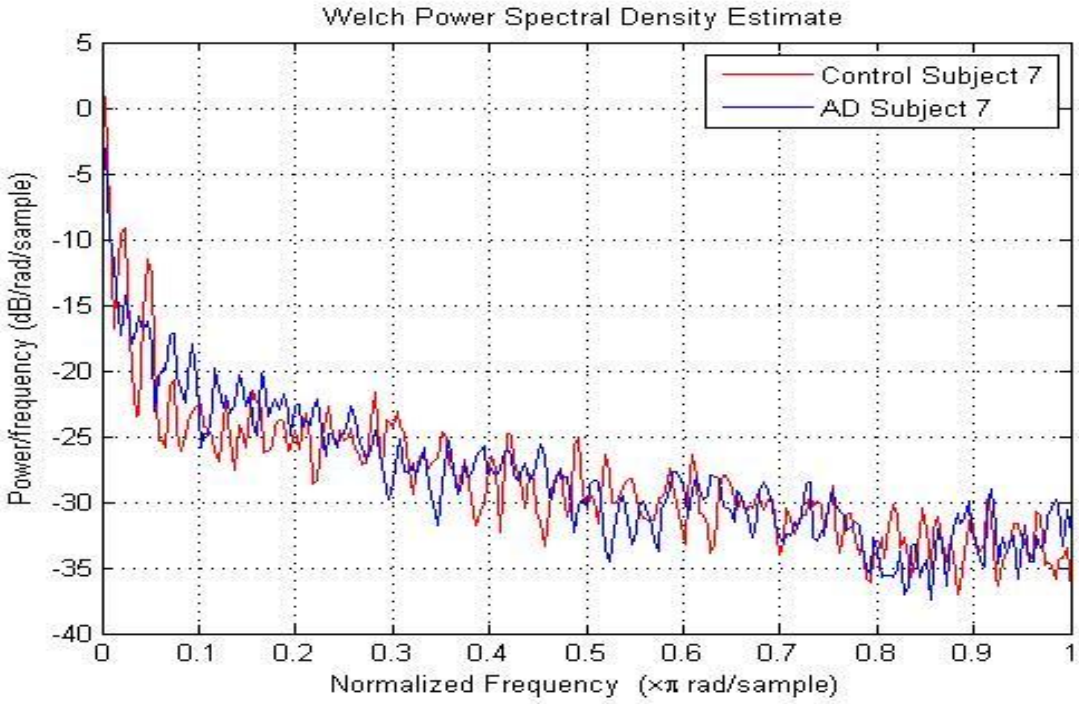

Figure A-6: Welch PSD estimate for AD subject 7 and control subject 7

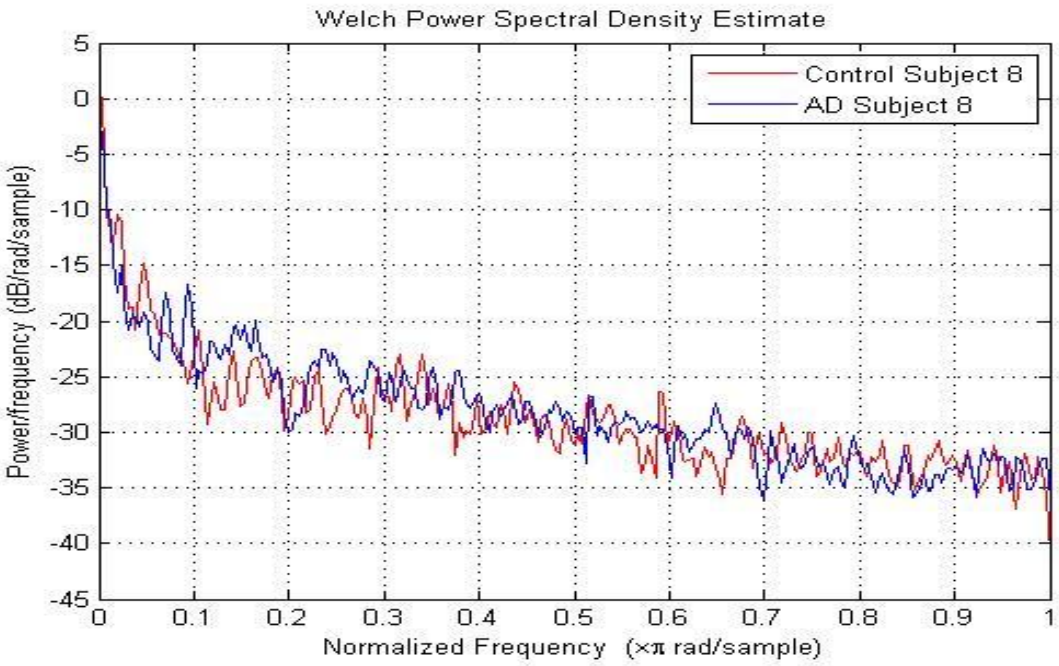

Figure A-7: Welch PSD estimate for AD subject 8 and control subject 8

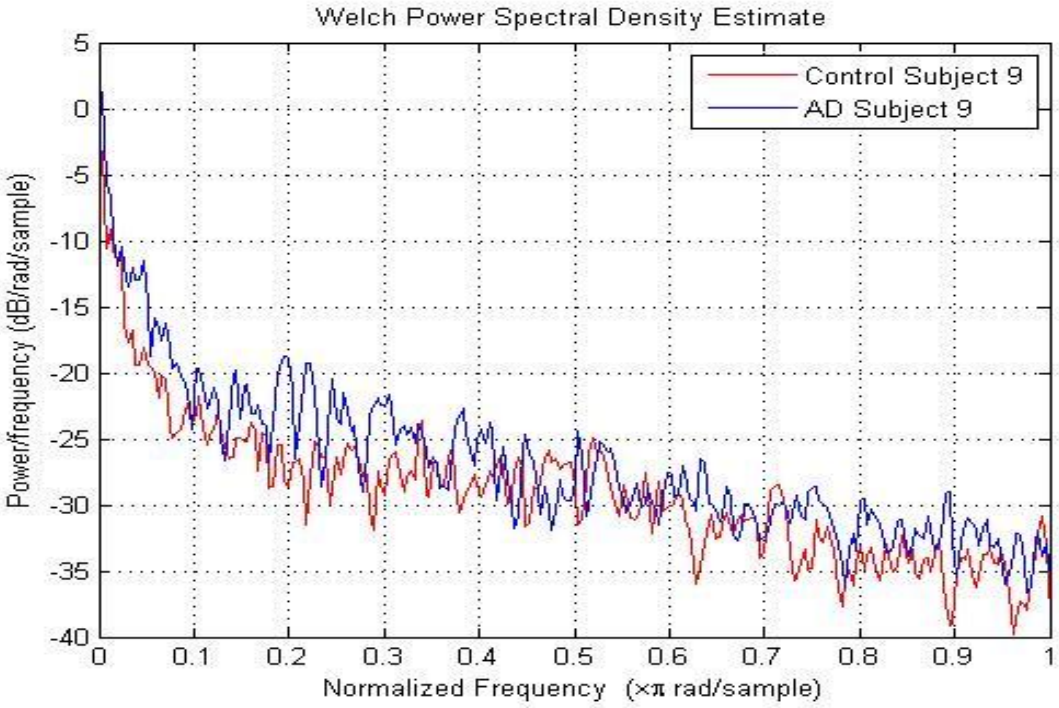

Figure A-8: Welch PSD estimate for AD subject 9 and control subject 9

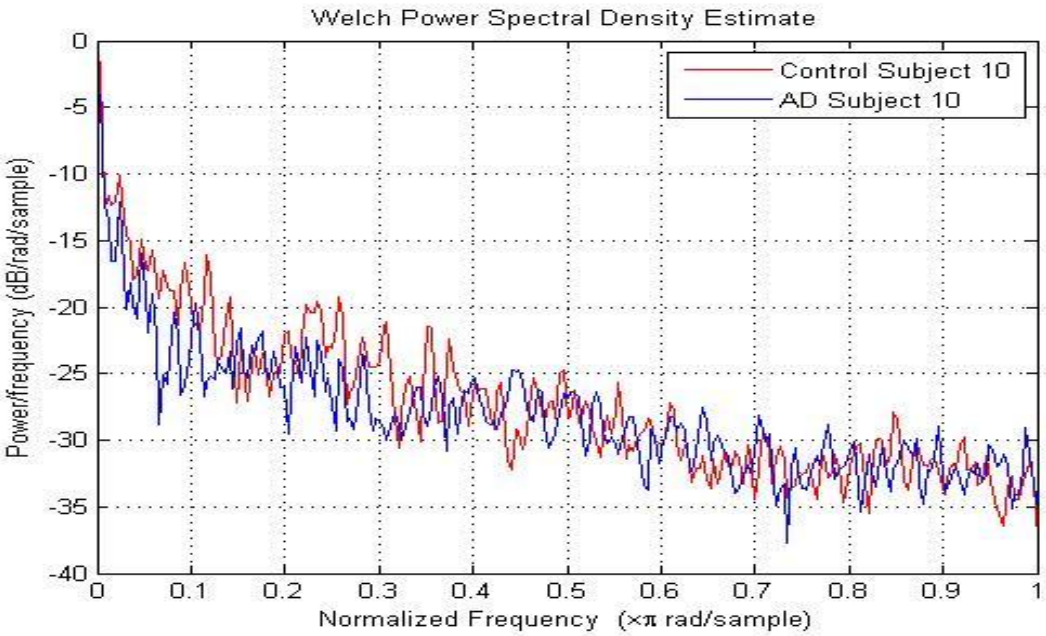

Figure A-9: Welch PSD estimate for AD subject 10 and control subject 10

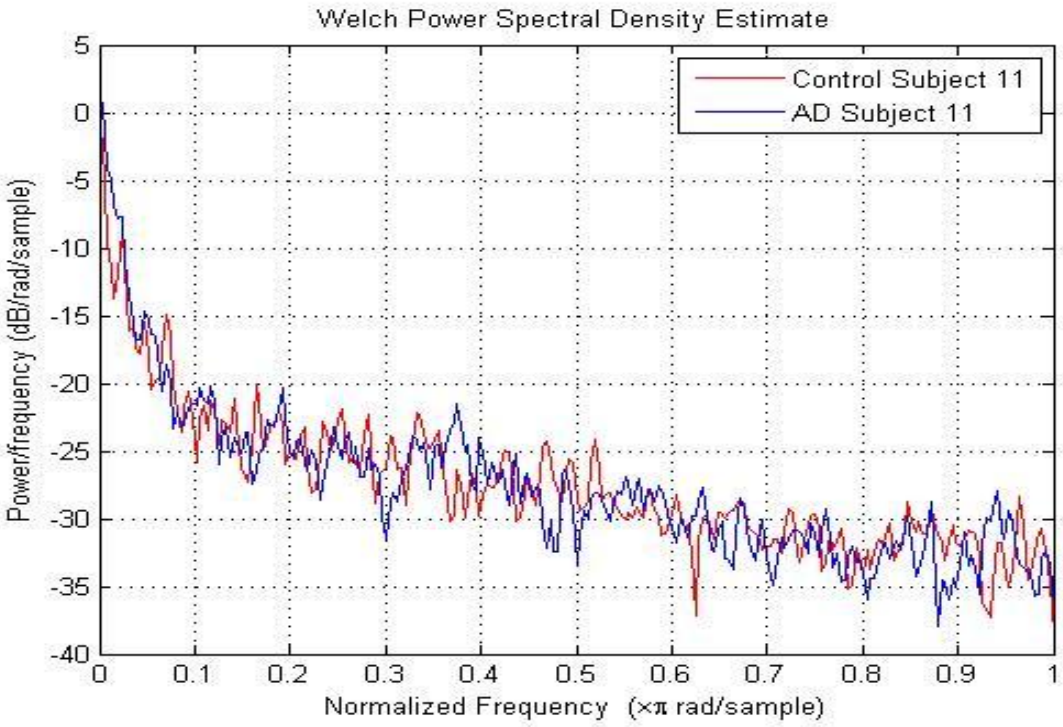

Figure A-10: Welch PSD estimate for AD subject 11 and control subject 11

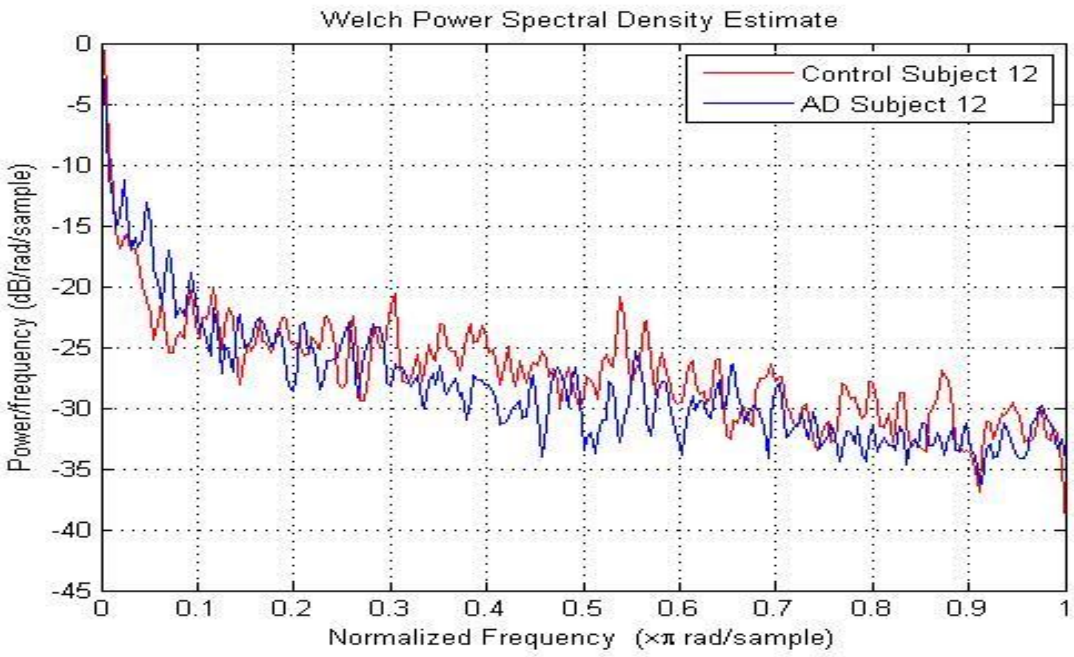

Figure A-11: Welch PSD estimate for AD subject 12 and control subject 12

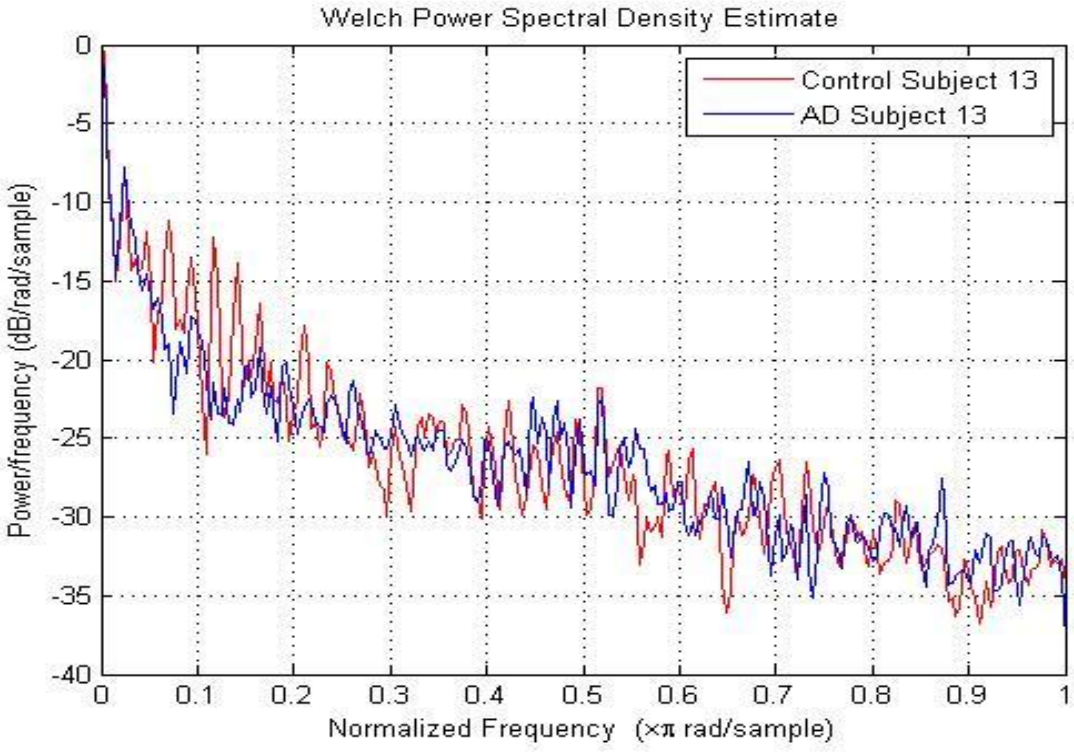

Figure A-12: Welch PSD estimate for AD subject 13 and control subject 13

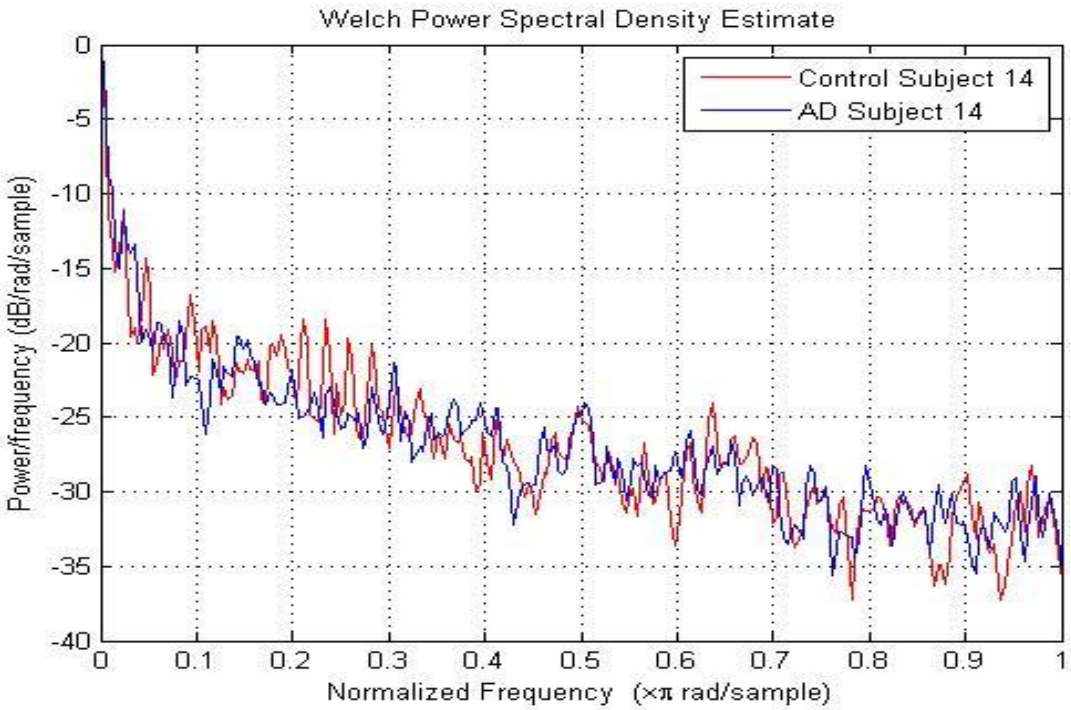

Figure A-13: Welch PSD estimate for AD subject 14 and control subject 14

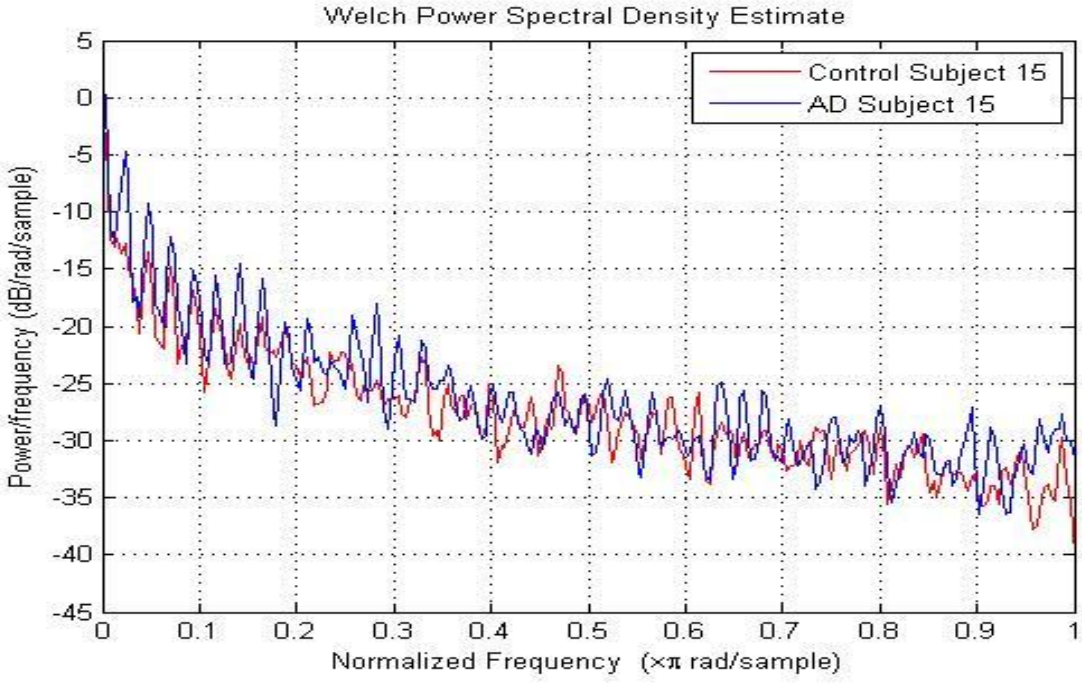

Figure A-14: Welch PSD estimate for AD subject 15 and control subject 15

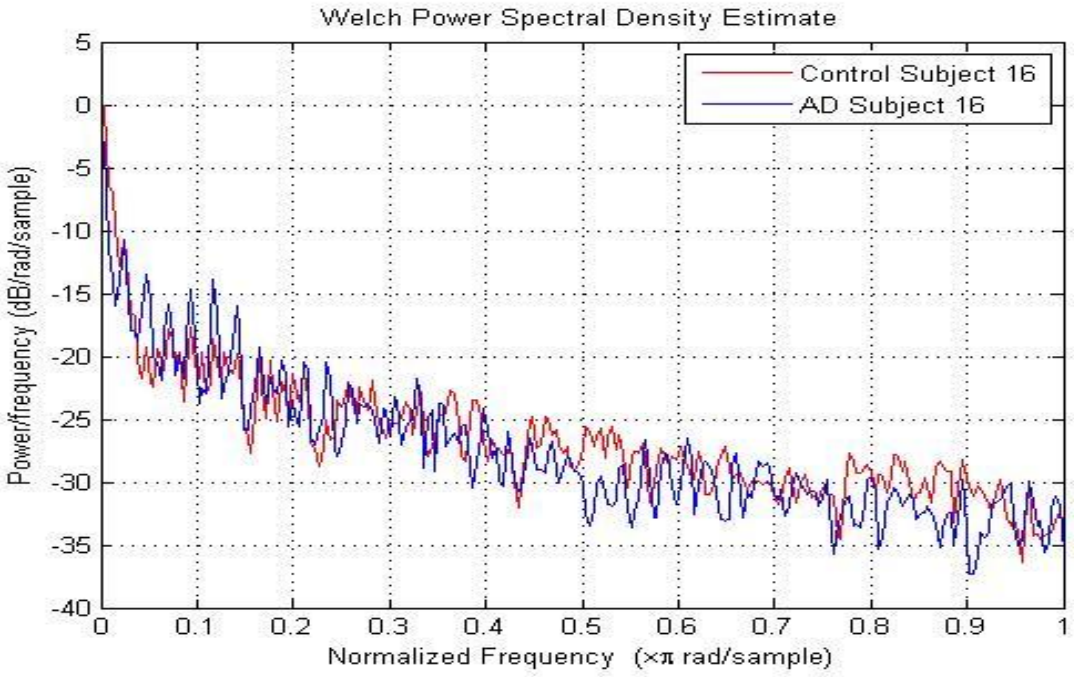

Figure A-15: Welch PSD estimate for AD subject 16 and control subject 16

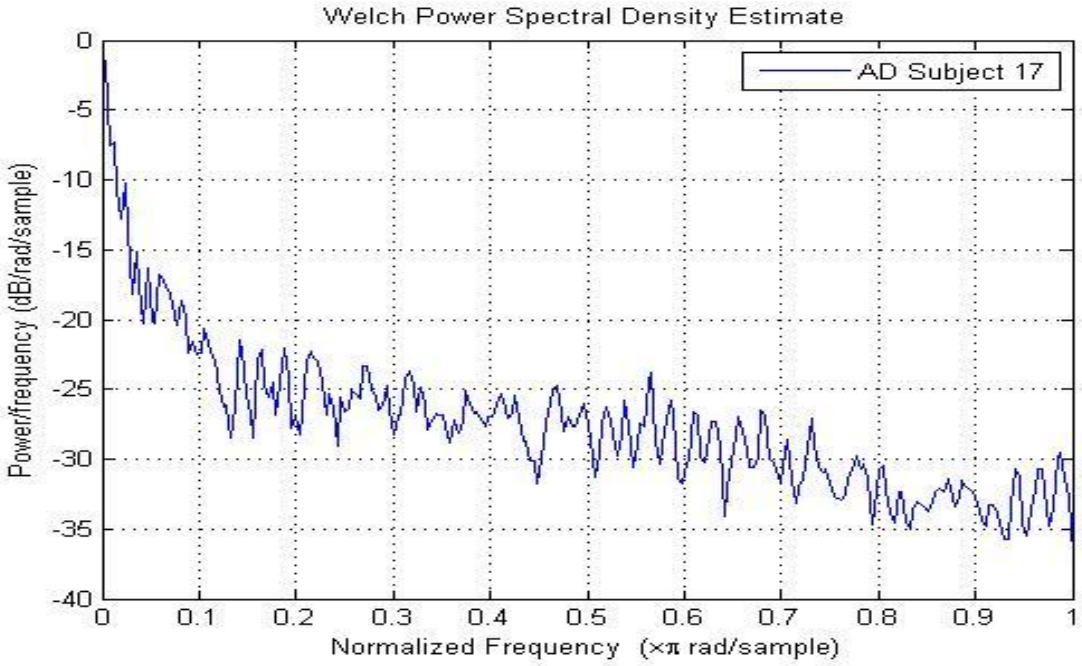

Figure A-16: Welch PSD estimate for AD subject 17

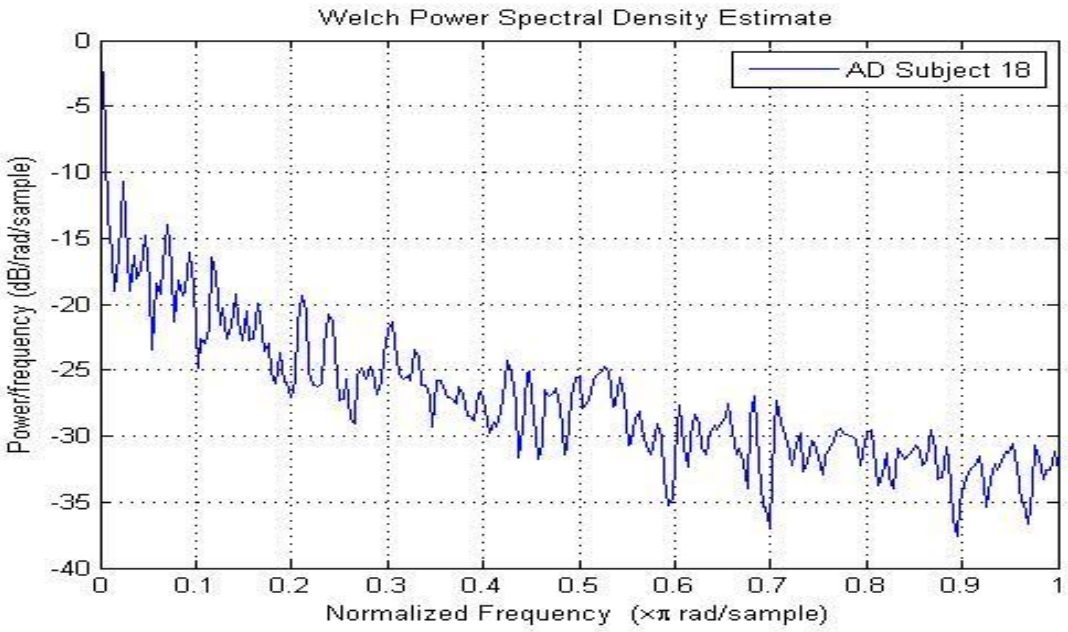

Figure A-17: Welch PSD estimate for AD subject 18

Appendix B

The Welch Power Spectrum with Moving Windows Plots for AD Subjects and Control Subjects

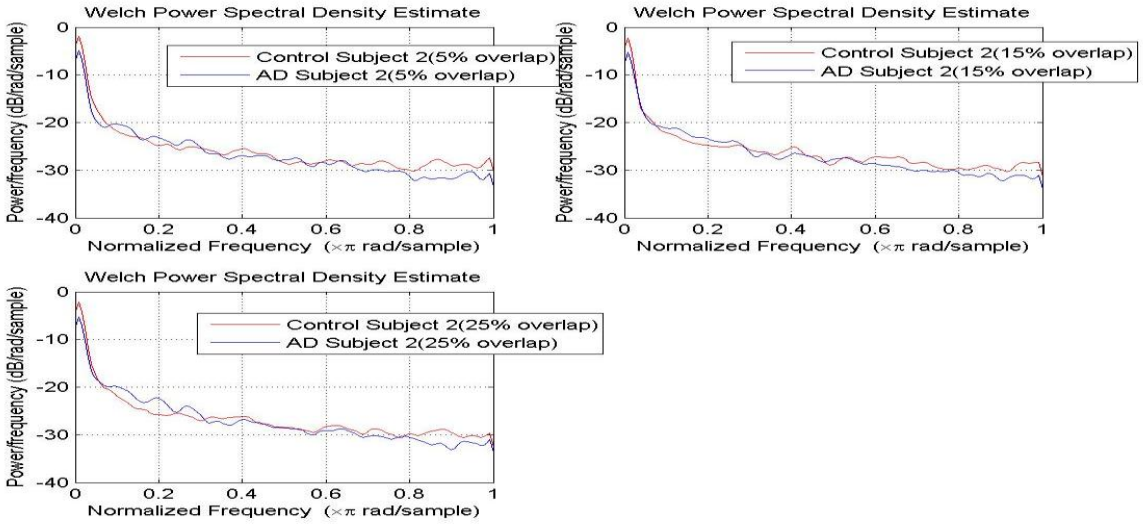

Figure B-1: Welch PSD estimate for AD subject 2 and control subject 2 with moving window analysis

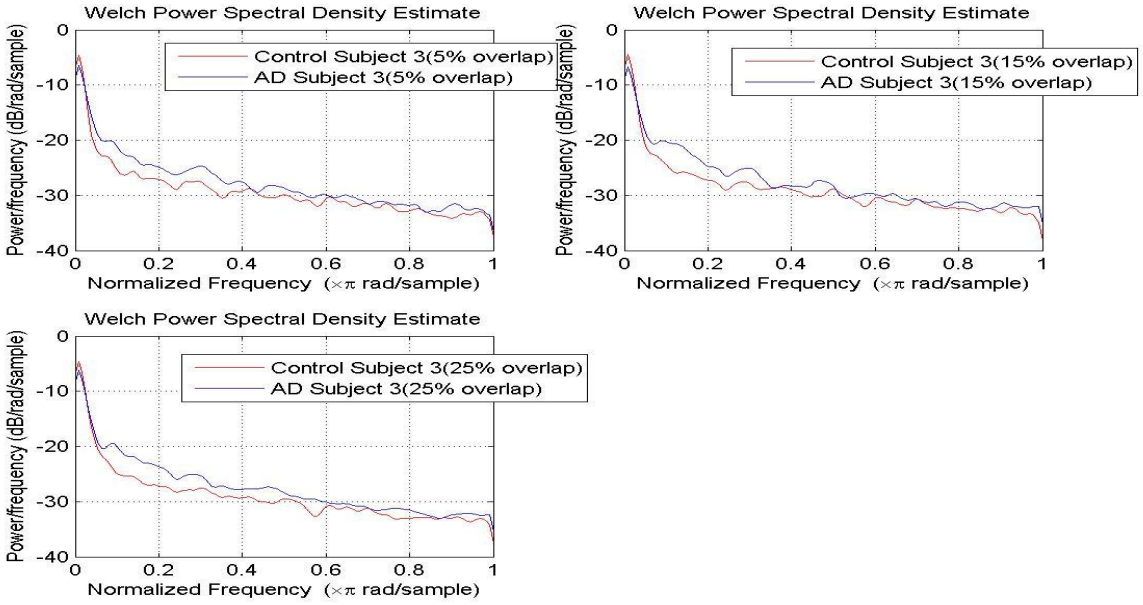

Figure B-2: Welch PSD estimate for AD subject 3 and control subject 3 with moving window analysis

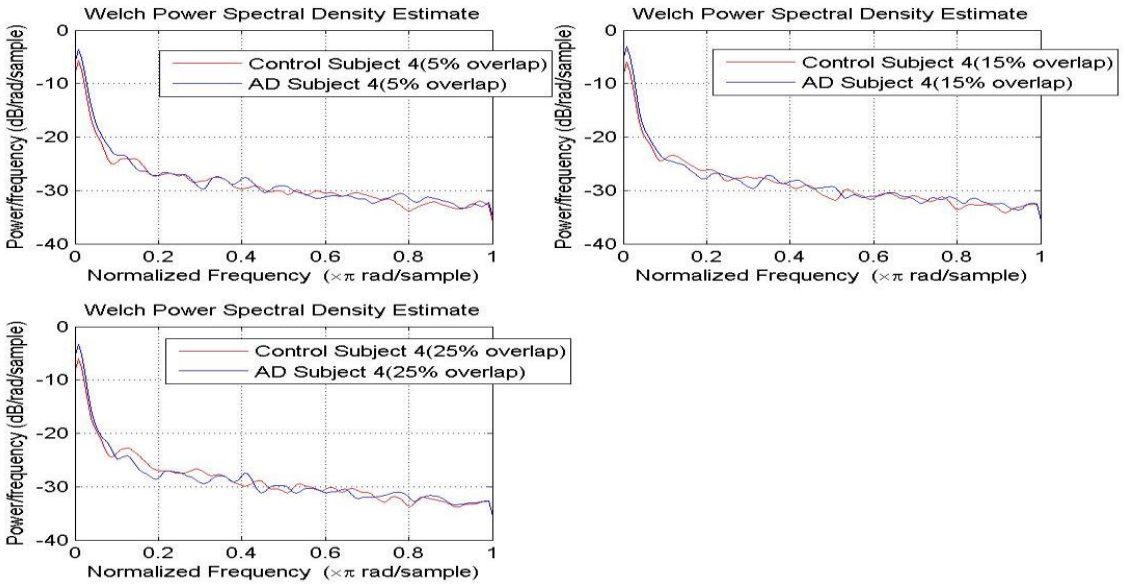

Figure B-3: Welch PSD estimate for AD subject 4 and control subject 4 with moving window analysis

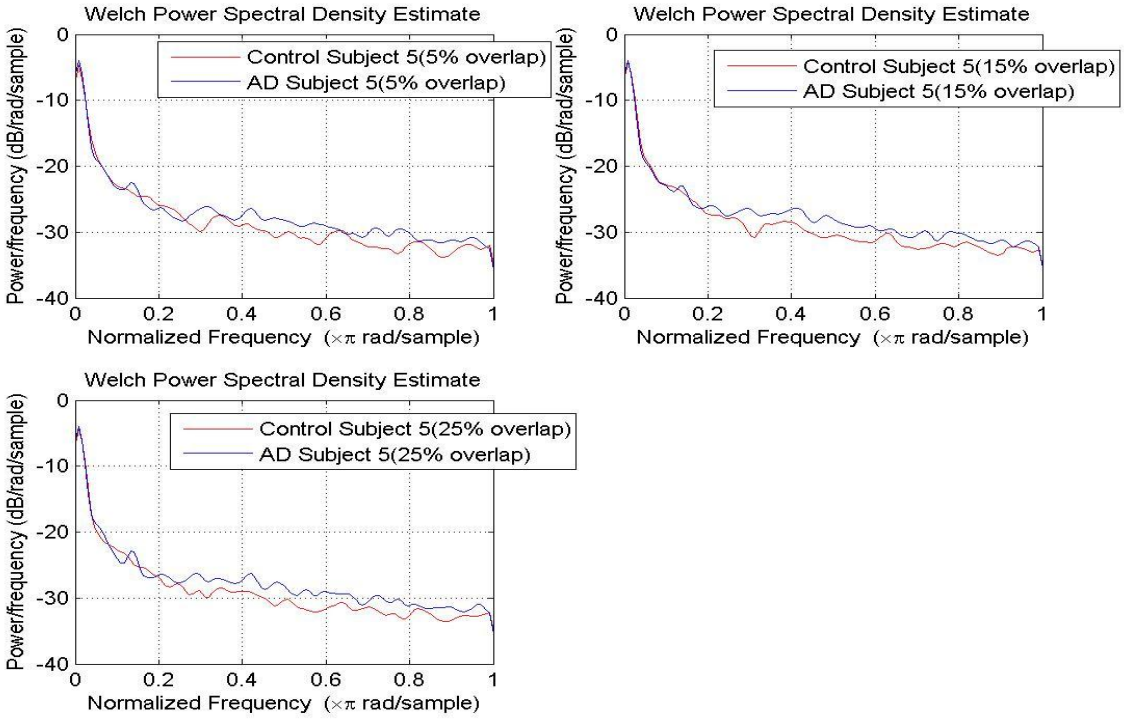

Figure B-4: Welch PSD estimate for AD subject 5 and control subject 5 with moving window analysis

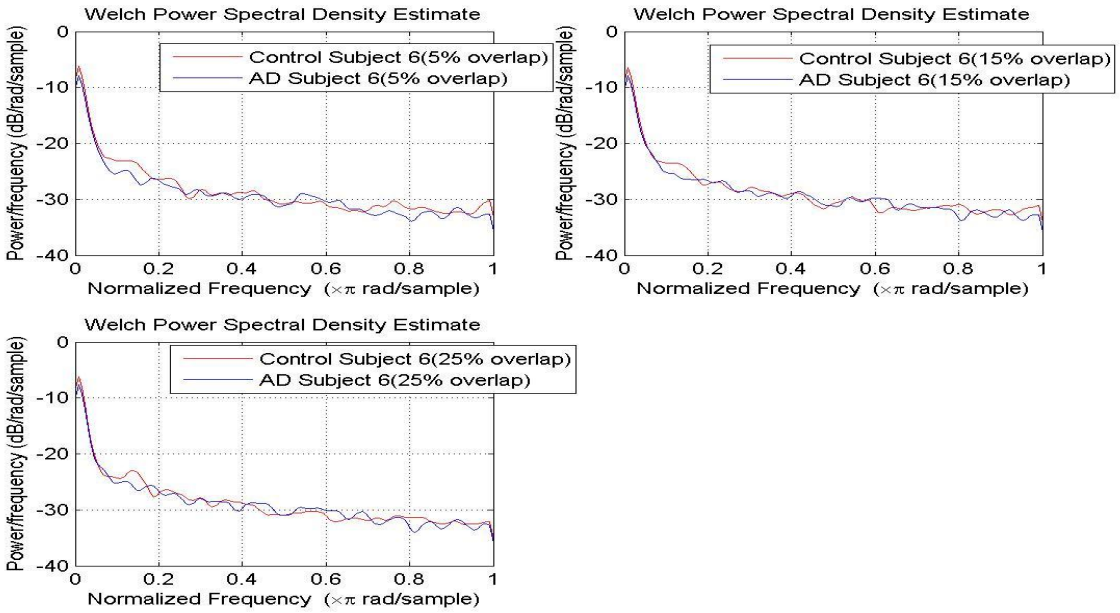

Figure B-5: Welch PSD estimate for AD subject 6 and control subject 6 with moving window analysis

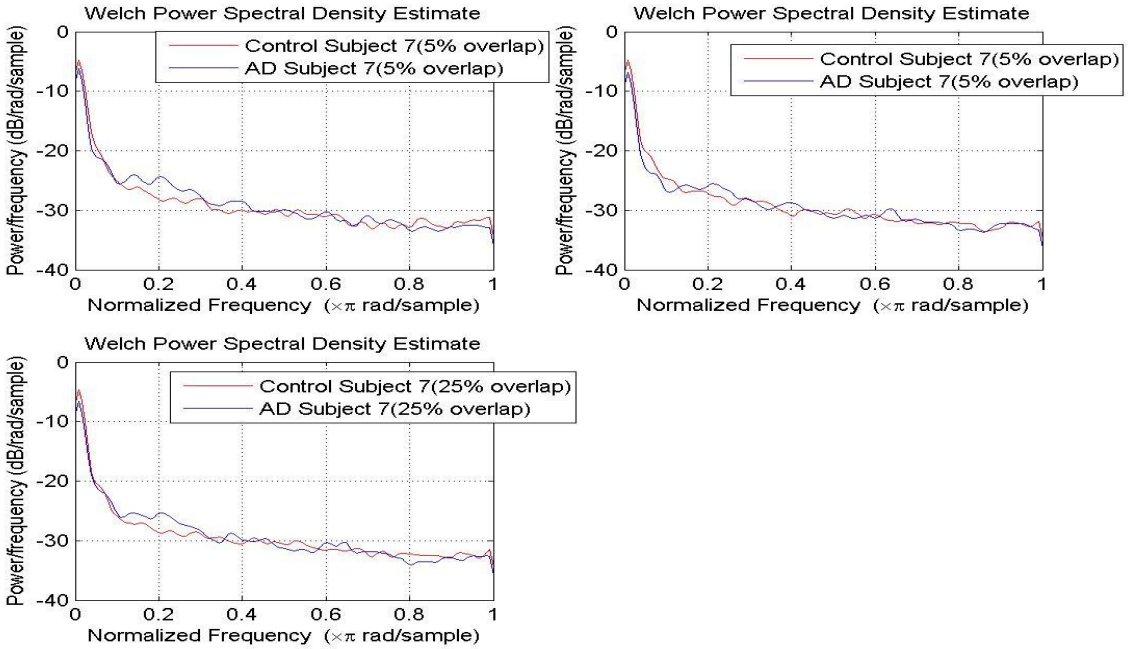

Figure B-6: Welch PSD estimate for AD subject 7 and control subject 7 with moving window analysis

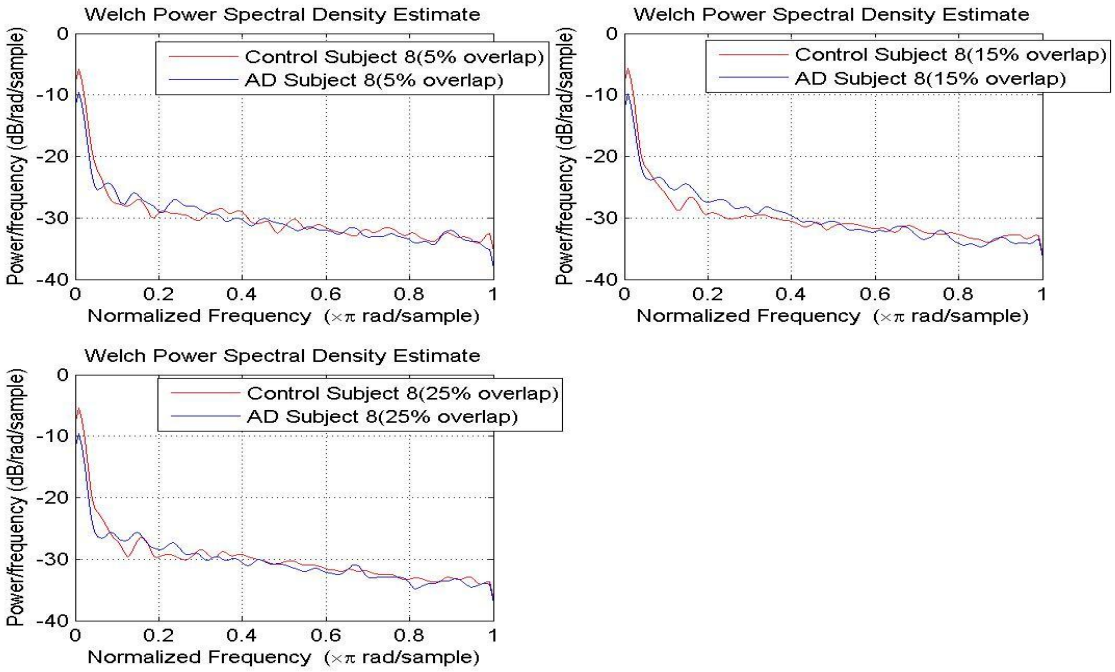

Figure B-7: Welch PSD estimate for AD subject 8 and control subject 8 with moving window analysis

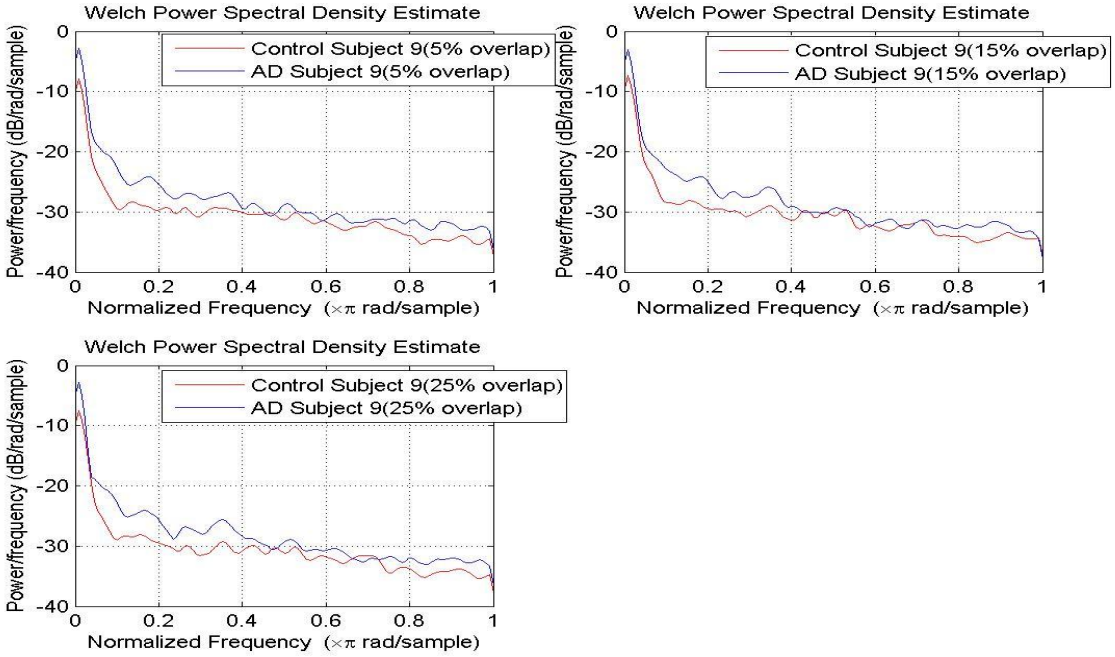

Figure B-8: Welch PSD estimate for AD subject 9 and control subject 9 with moving window analysis

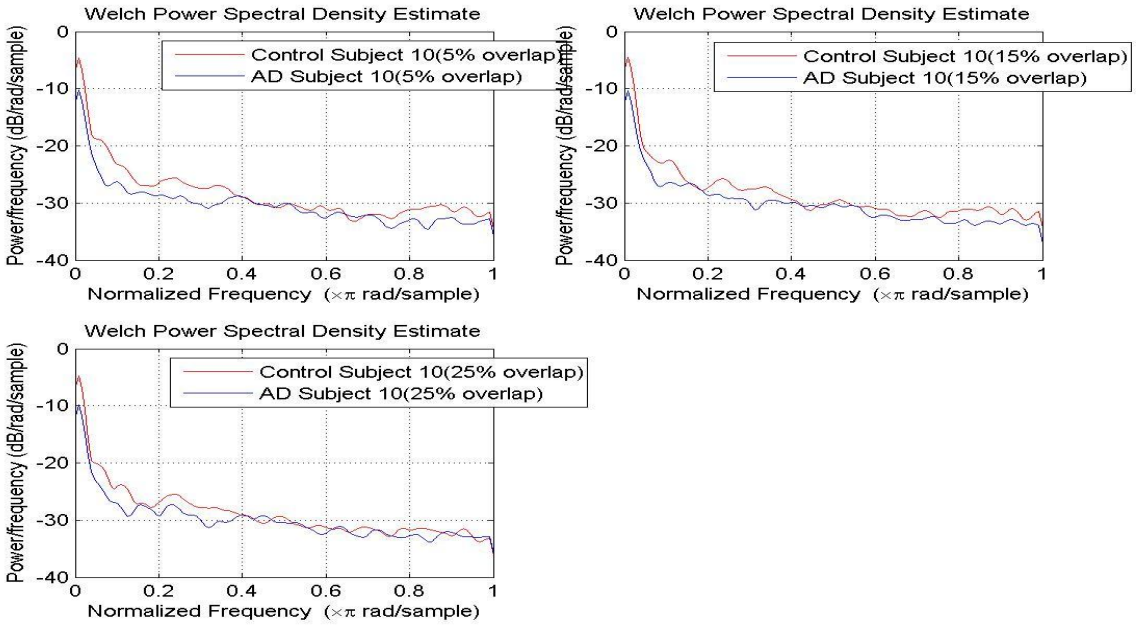

Figure B-9: Welch PSD estimate for AD subject 10 and control subject 10 with moving window analysis

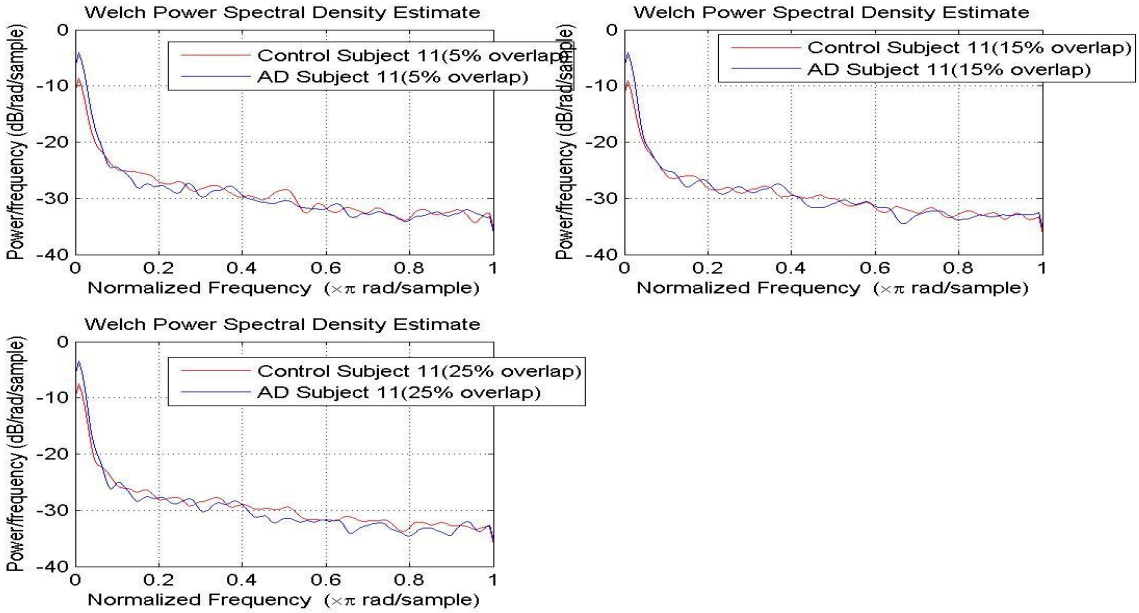

Figure B-10: Welch PSD estimate for AD subject 11 and control subject 11 with moving window analysis

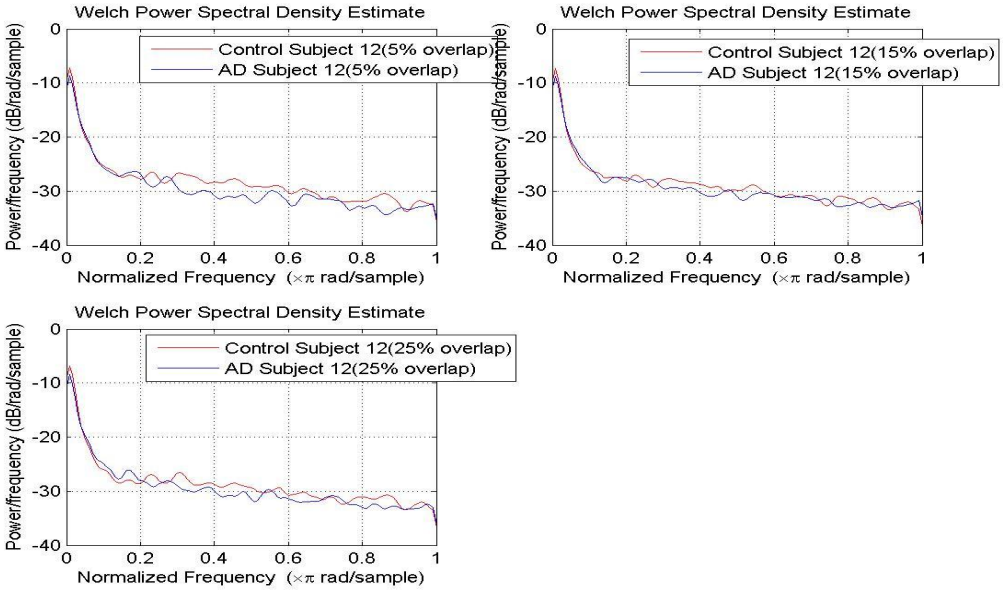

Figure B-11: Welch PSD estimate for AD subject 12 and control subject 12 with moving window analysis

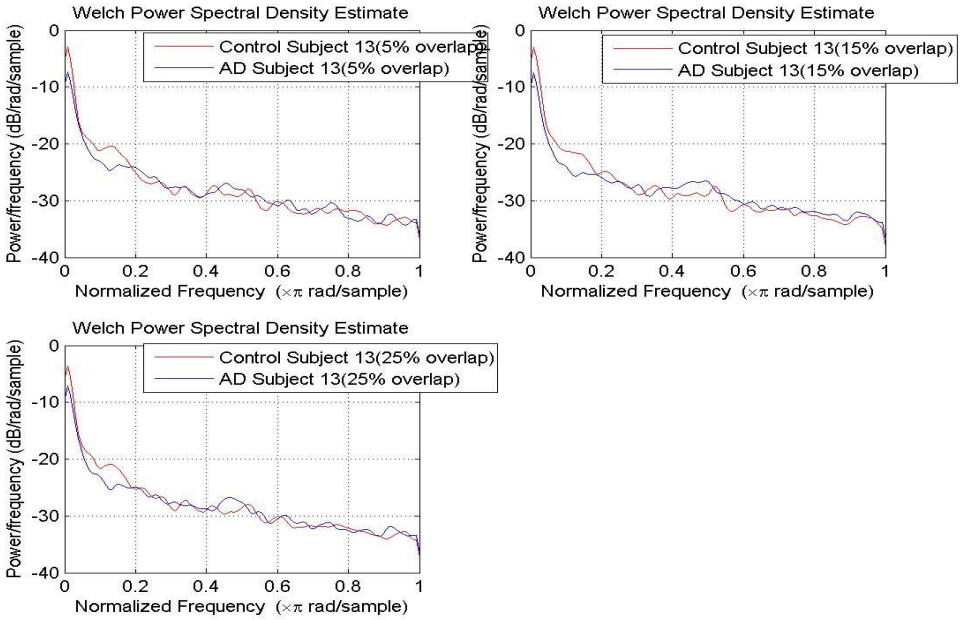

Figure B-12: Welch PSD estimate for AD subject 13 and control subject 13 with moving window analysis

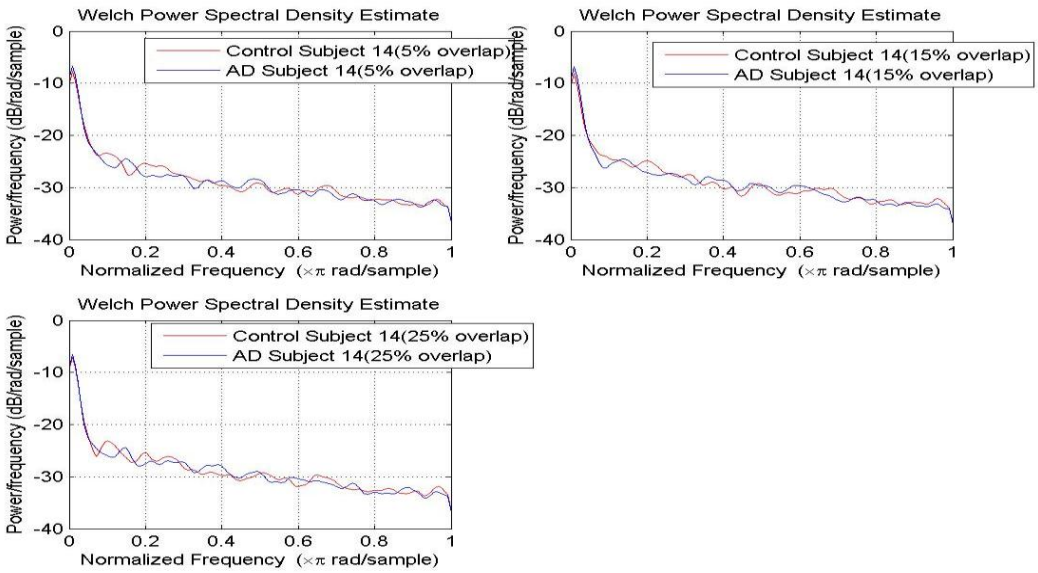

Figure B-13: Welch PSD estimate for AD subject 14 and control subject 14 with moving window analysis

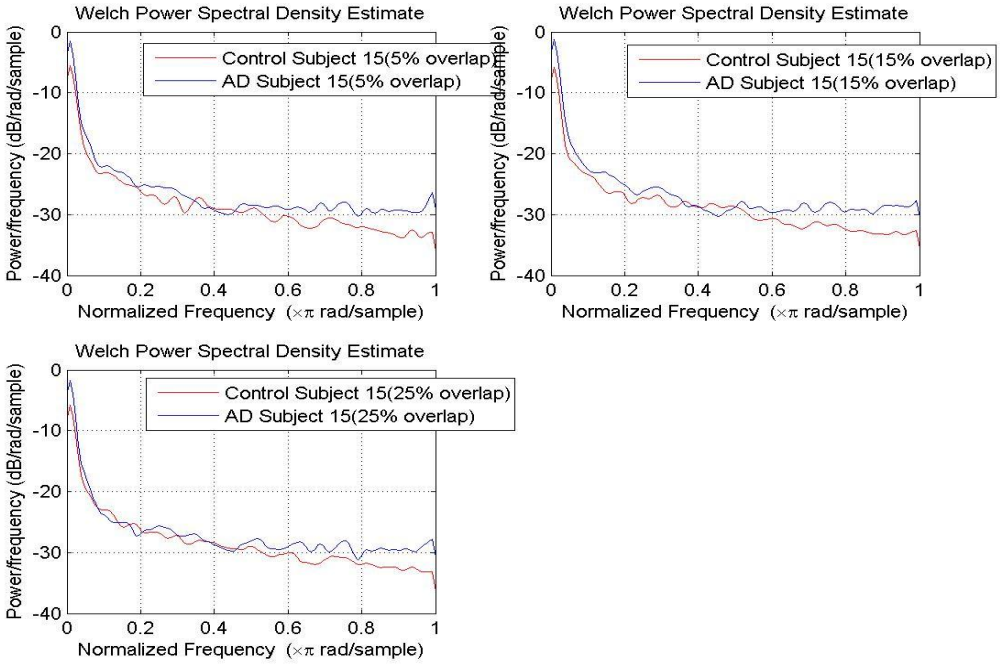

Figure B-14: Welch PSD estimate for AD subject 15 and control subject 15 with moving window analysis

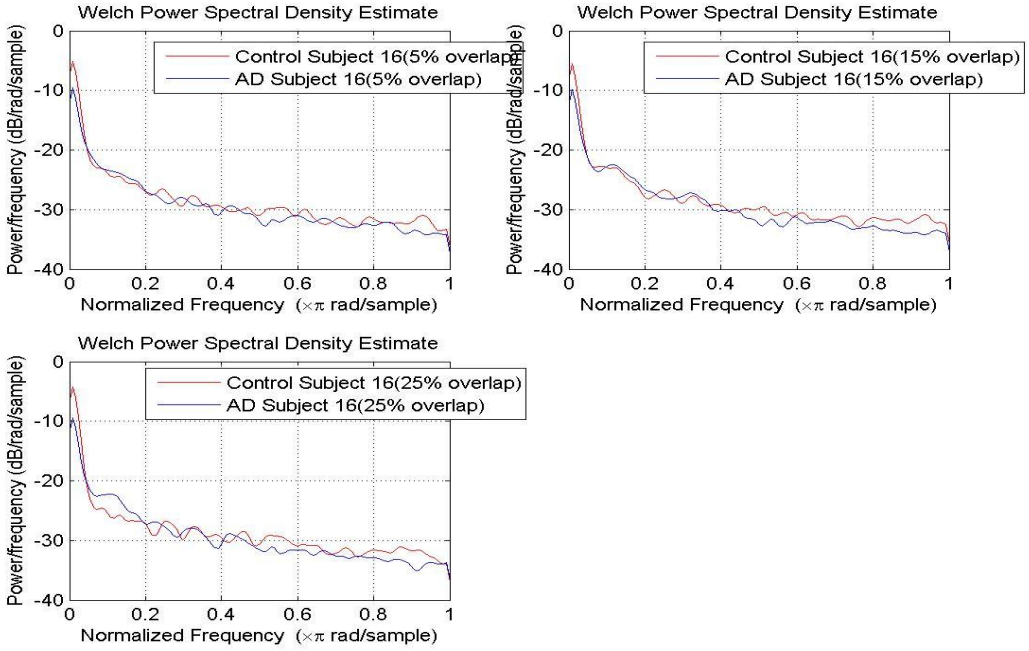

Figure B-15: Welch PSD estimate for AD subject 16 and control subject 16 with moving window analysis

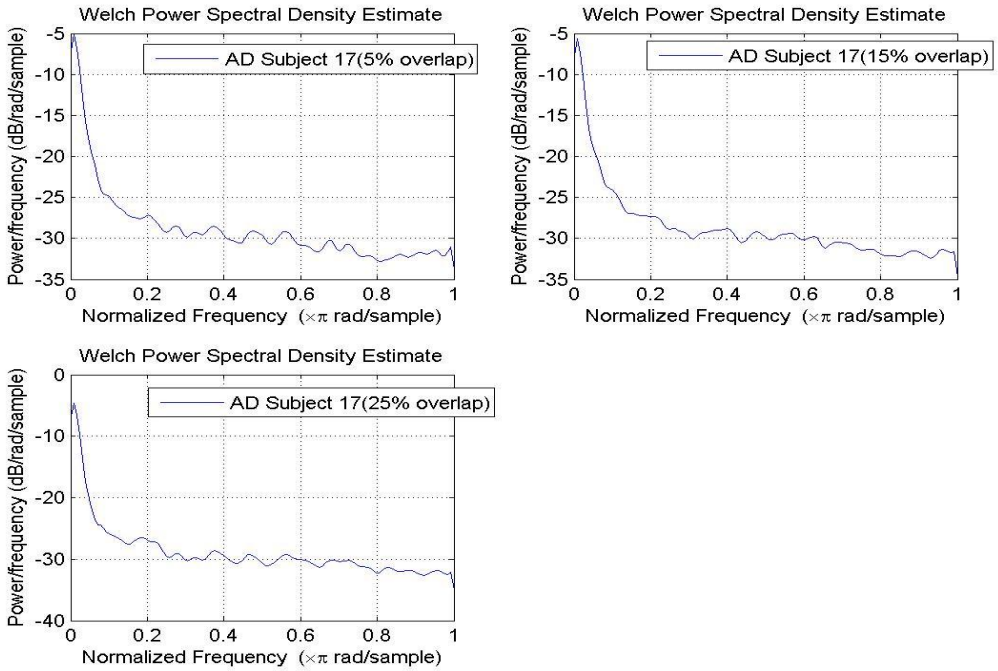

Figure B-16: Welch PSD estimate for AD subject 17 with moving window analysis

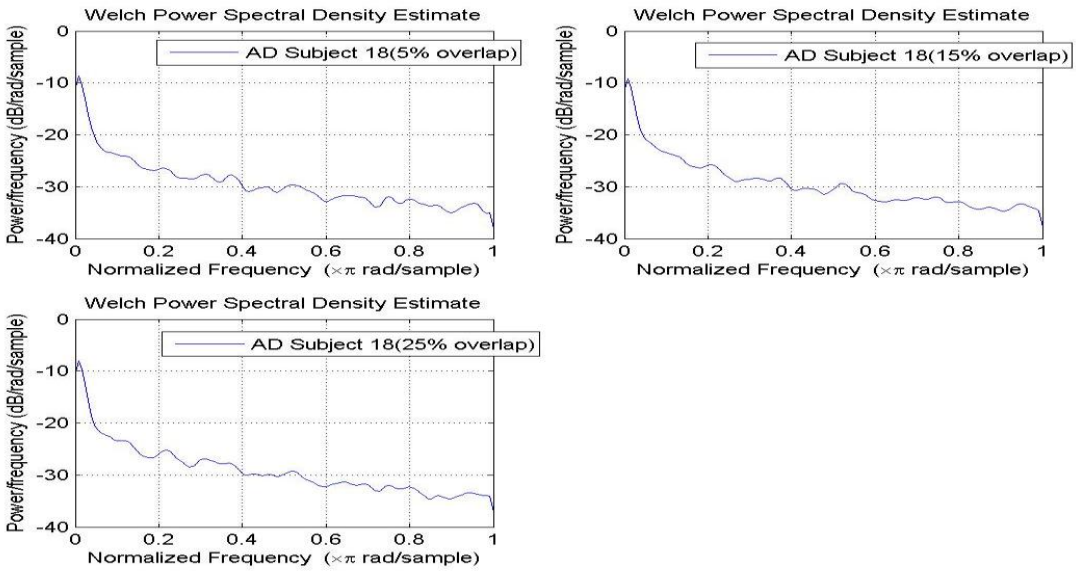

Figure B-17: Welch PSD estimate for AD subject 18 with moving window analysis

Appendix C

The DFT Plots for EEG Signals of AD Subjects and Control Subjects

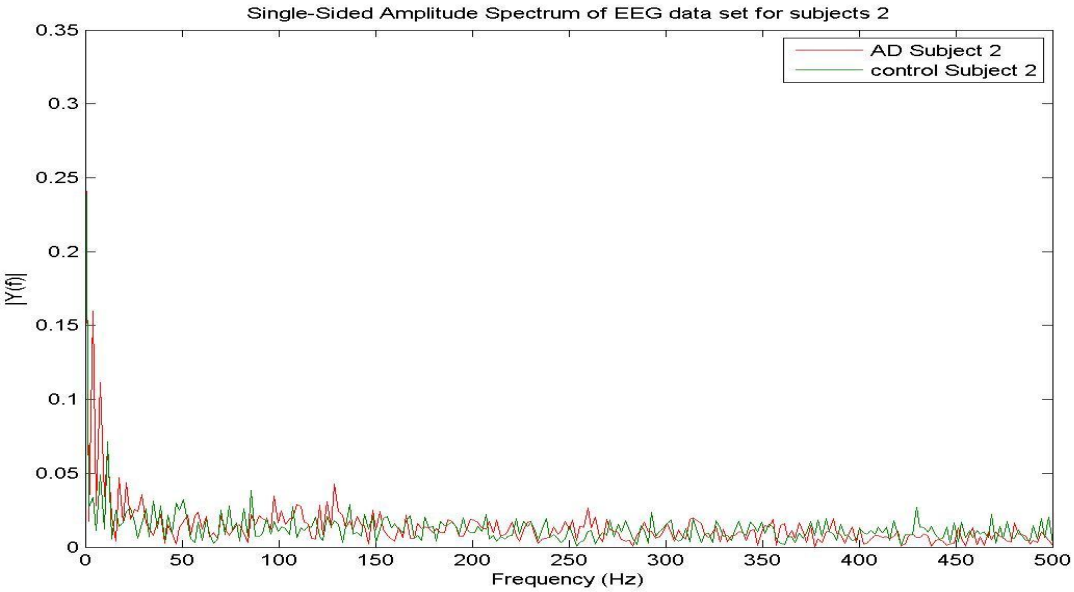

Figure C-1: The DFT of AD subject 2 and control subject 2

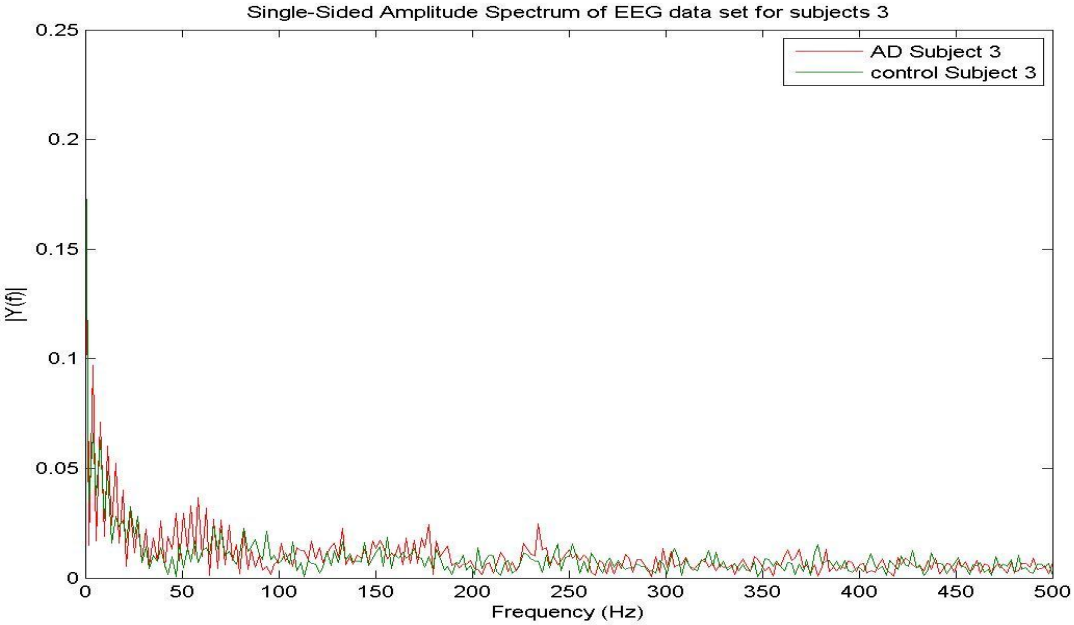

Figure C-2: The DFT of AD subject 3 and control subject 3

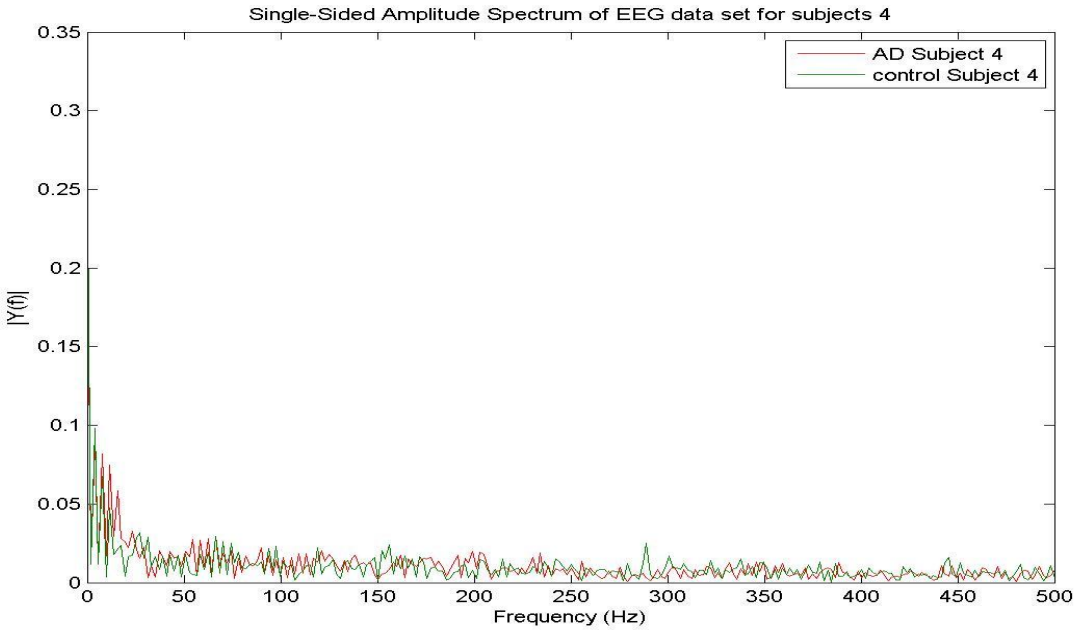

Figure C-3: The DFT of AD subject 4 and control subject 4

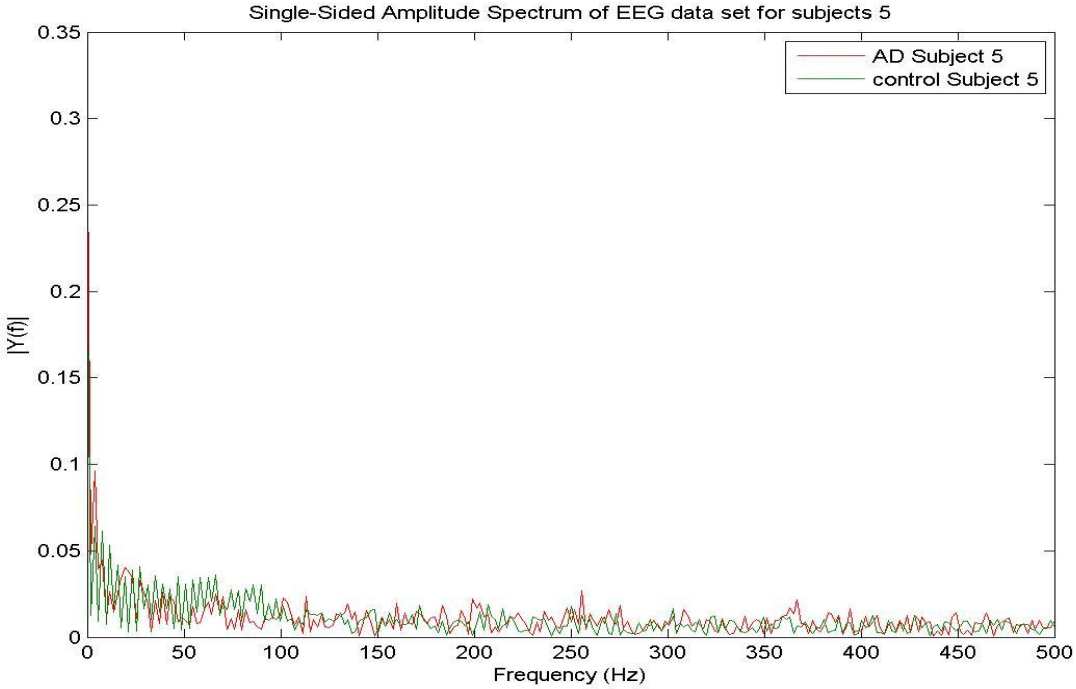

Figure C-4: The DFT of AD subject 5 and control subject 5

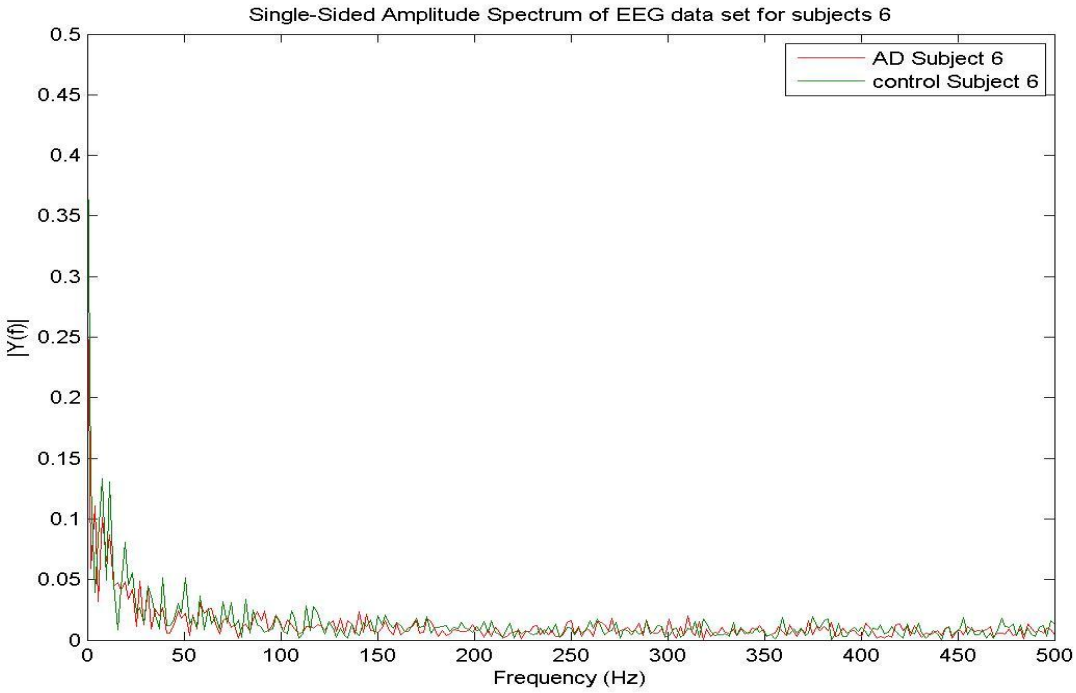

Figure C-5: The DFT of AD subject 6 and control subject 6

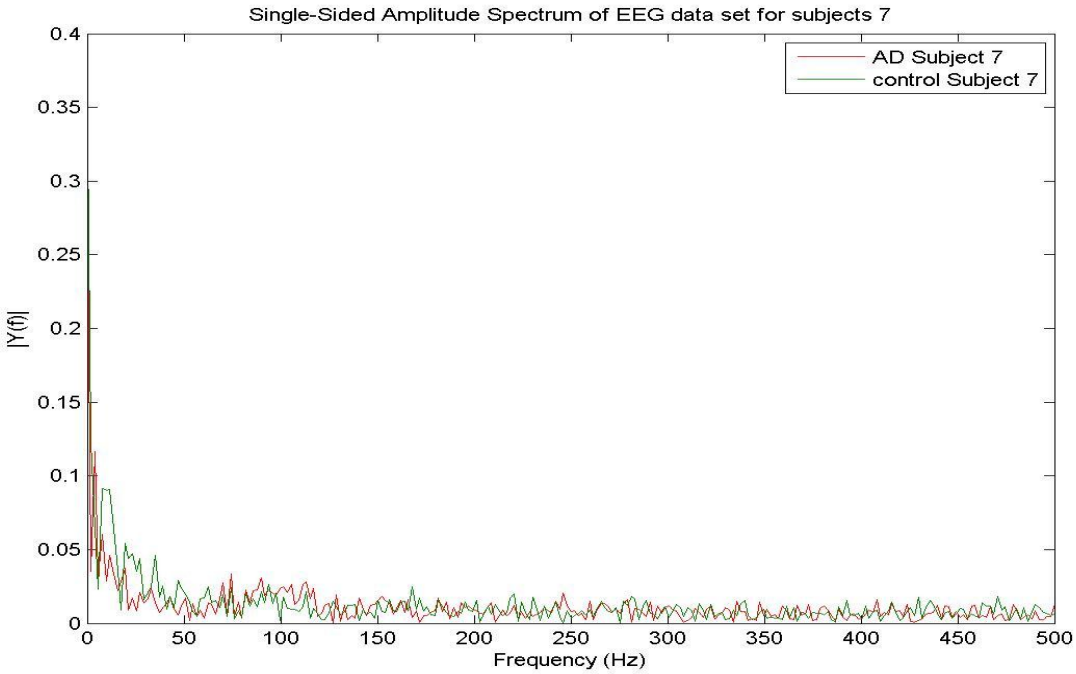

Figure C-6: The DFT of AD subject 7 and control subject 7

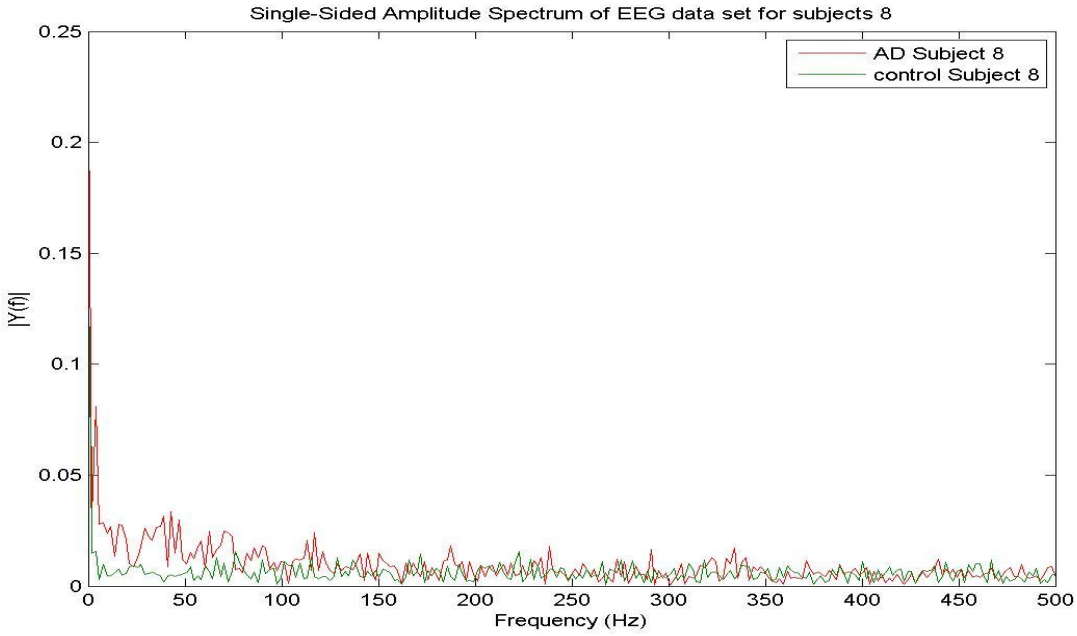

Figure C-7: The DFT of AD subject 8 and control subject 8

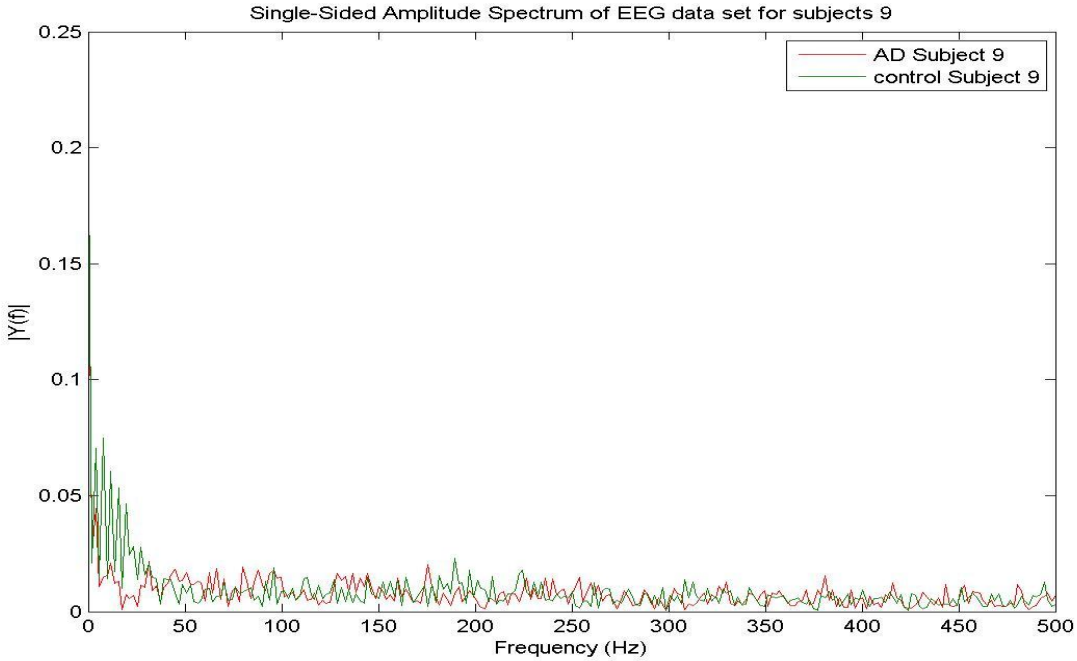

Figure C-8: The DFT of AD subject 9 and control subject 9

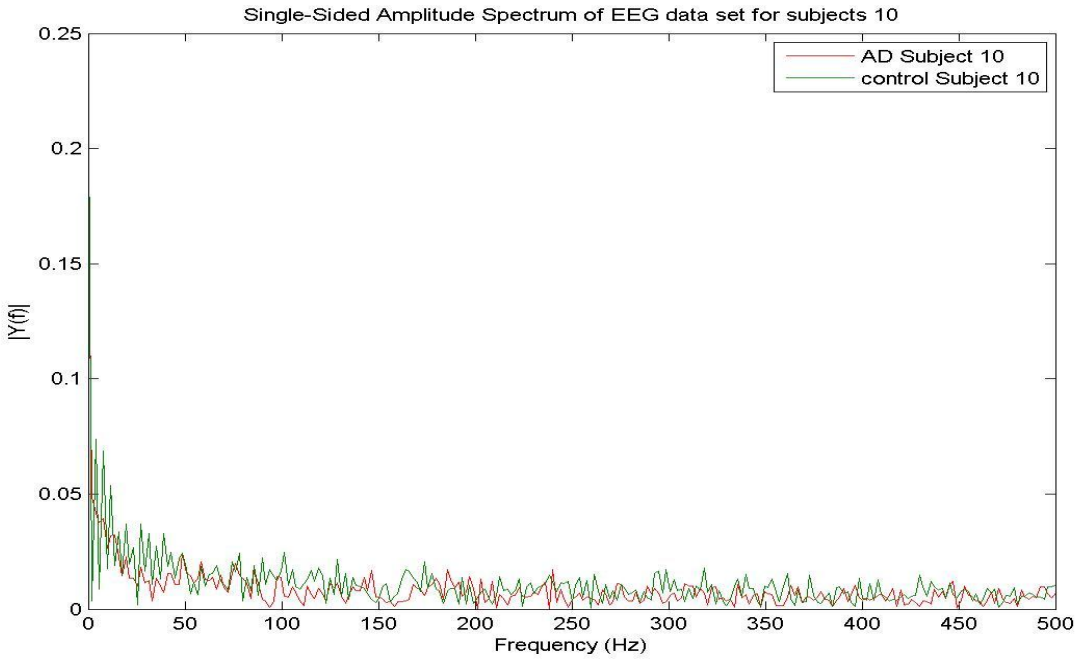

Figure C-9: The DFT of AD subject 10 and control subject 10

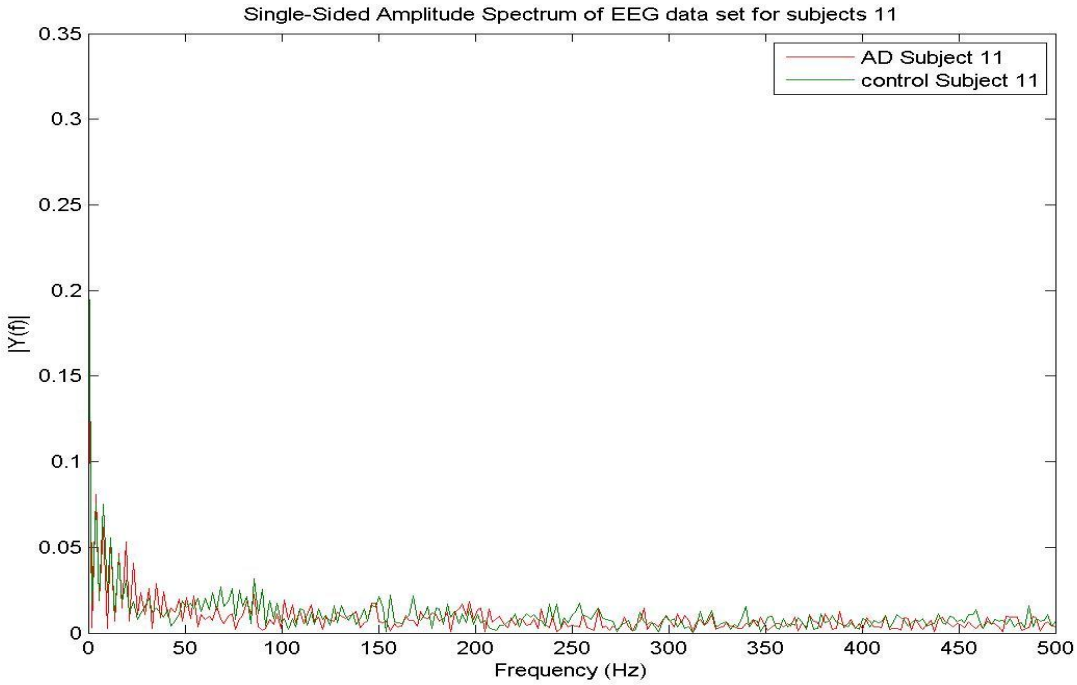

Figure C-10: The DFT of AD subject 11 and control subject 11

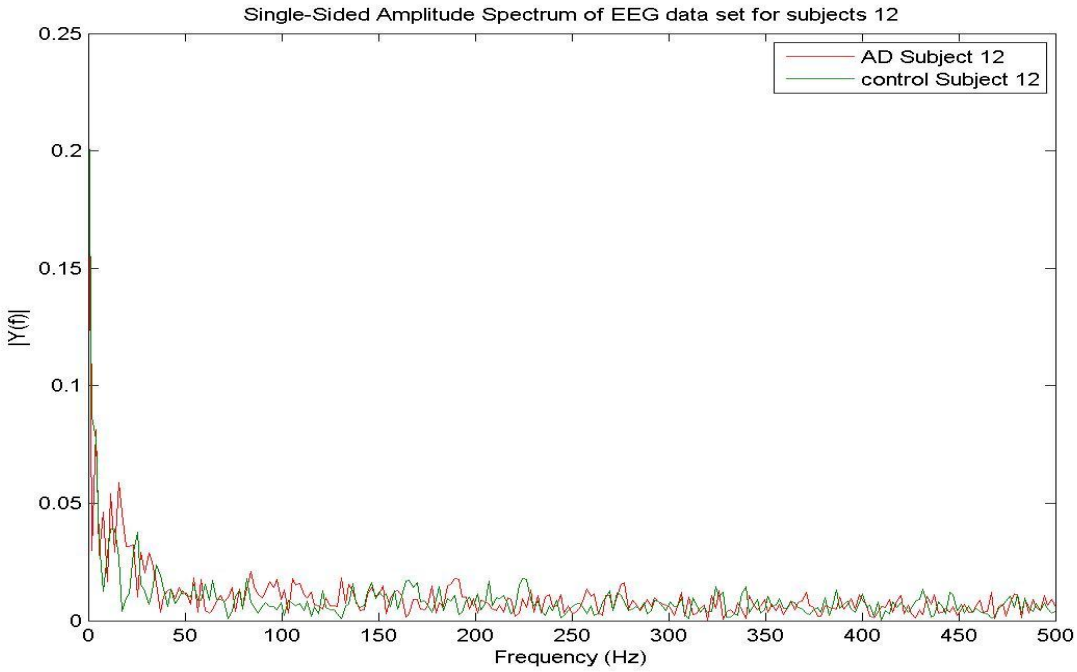

Figure C-11: The DFT of AD subject 12 and control subject 12

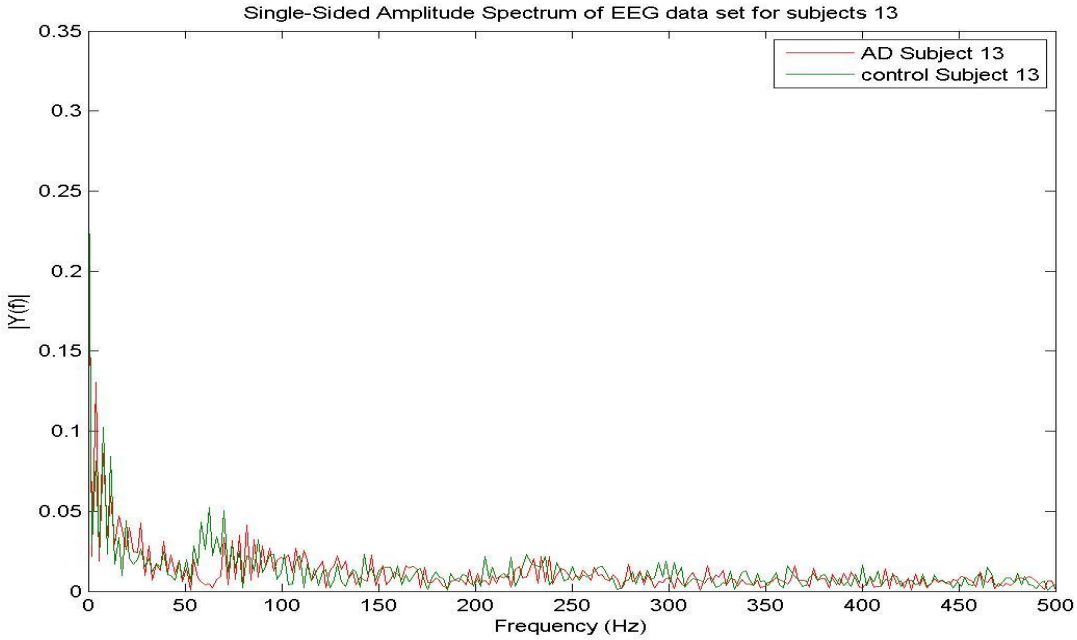

Figure C-12: The DFT of AD subject 13 and control subject 13

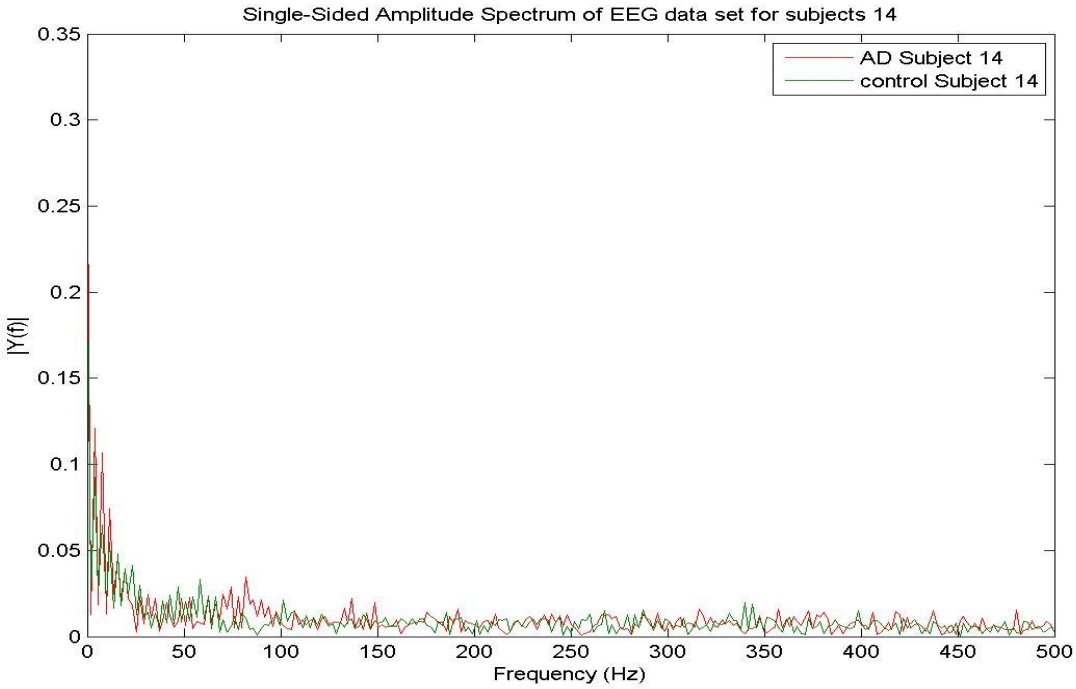

Figure C-13: The DFT of AD subject 14 and control subject 14

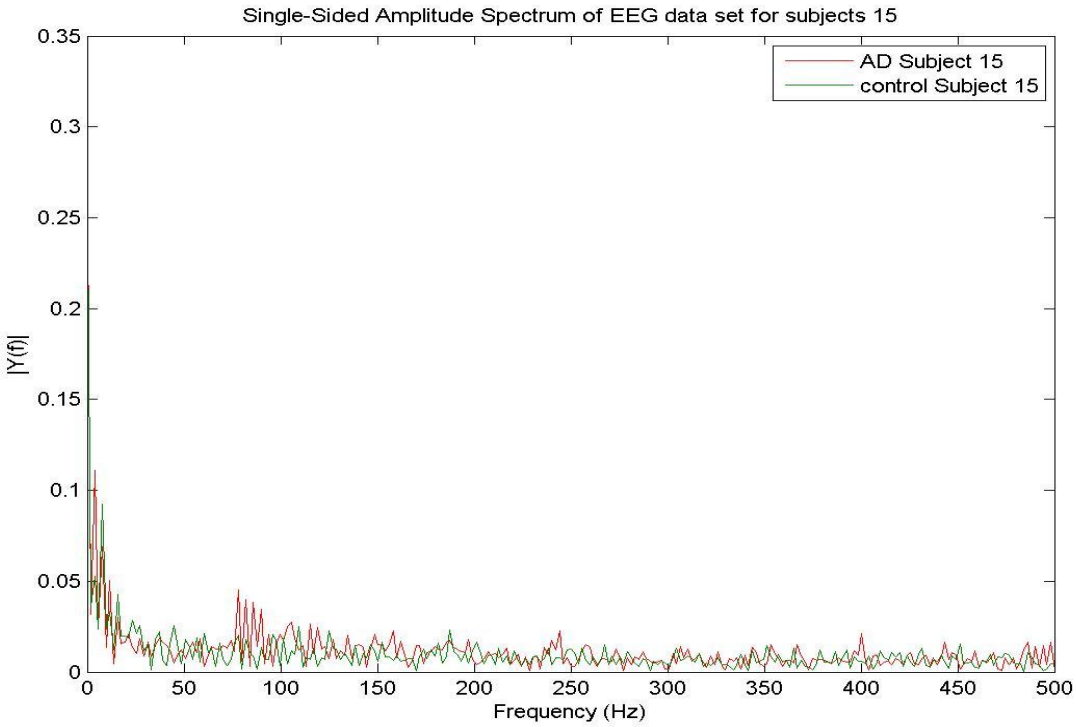

Figure C-14: The DFT of AD subject 15 and control subject 15

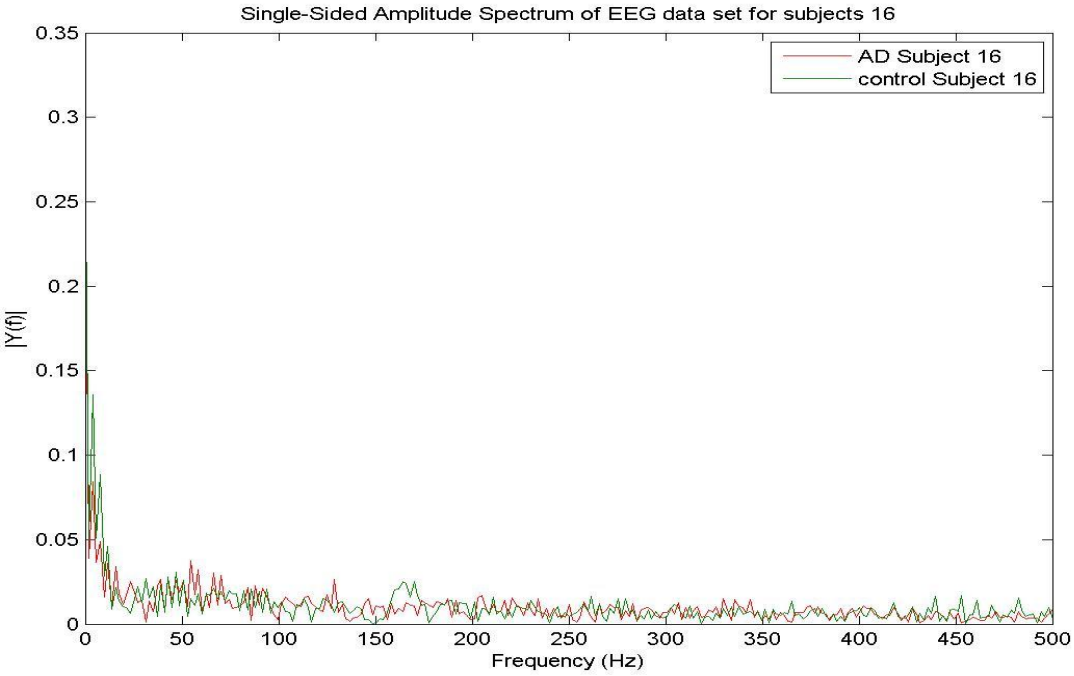

Figure C-15: The DFT of AD subject 16 and control subject 16

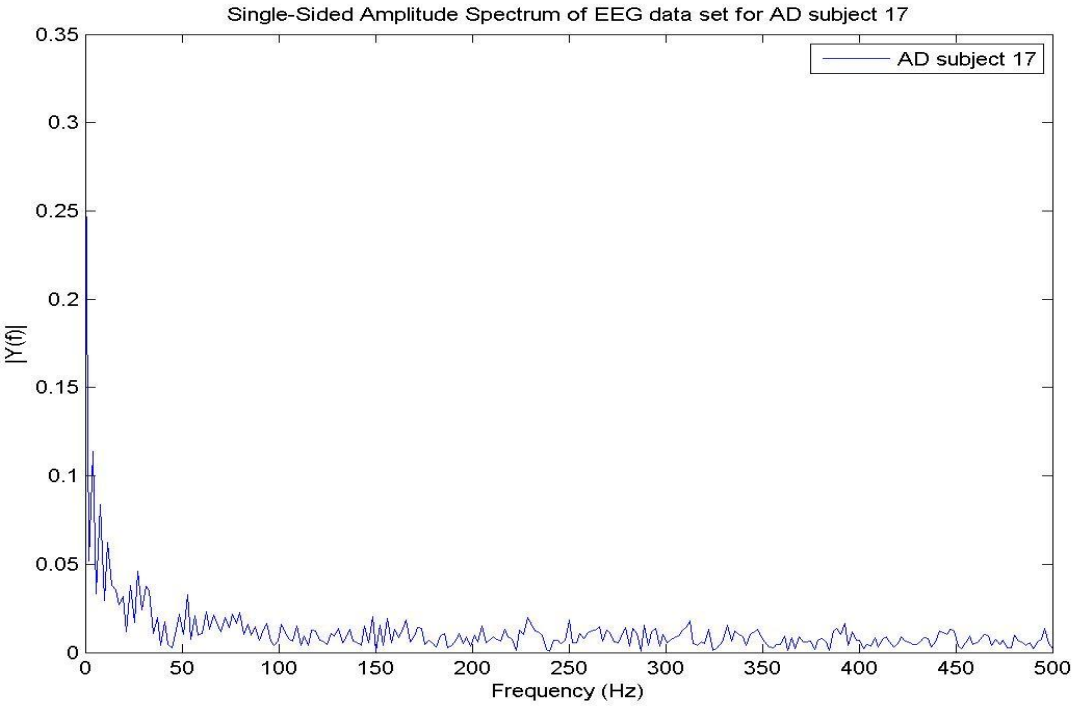

Figure C-16: The DFT of AD subject 17

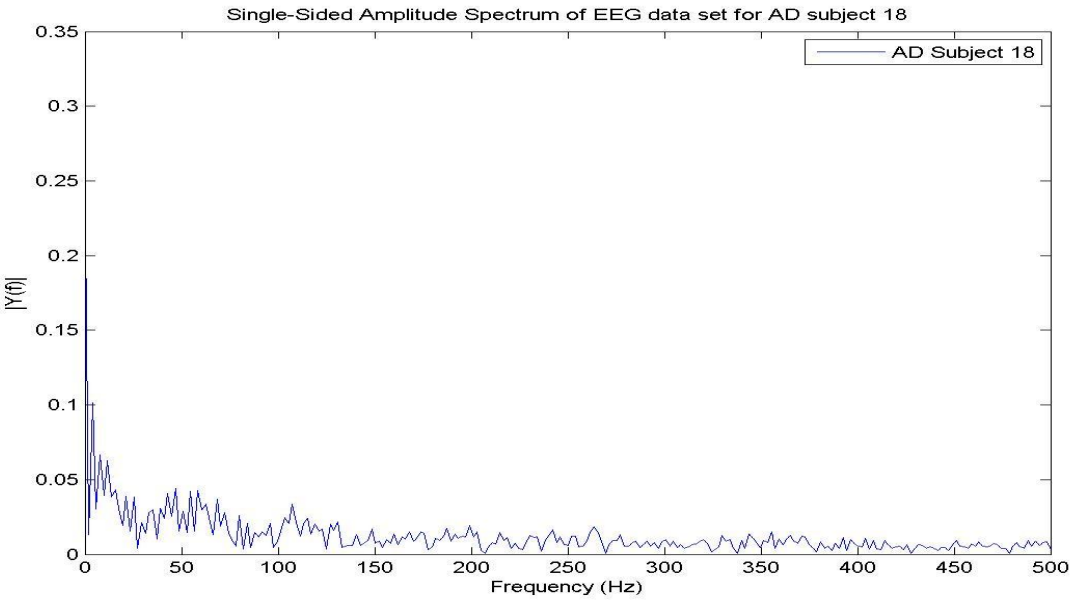

Figure C-17: The DFT of AD subject 18

Appendix D

The Welch Power Spectrum Plots with and without Moving Windows for Artifacts Removed EEG Signals

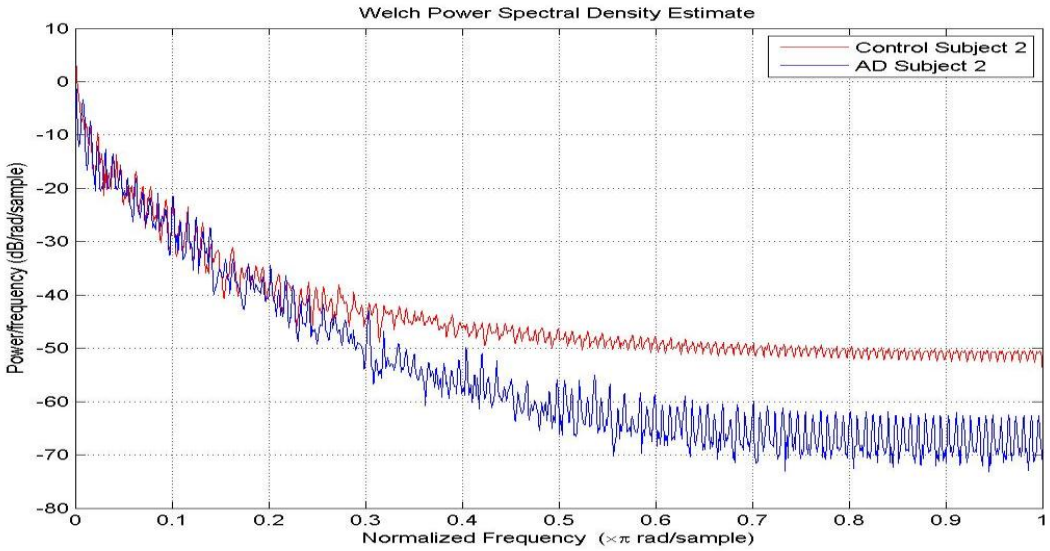

Figure D-1: Welch Power Spectrum for AD subject 2 and control subject 2 after artifact removal

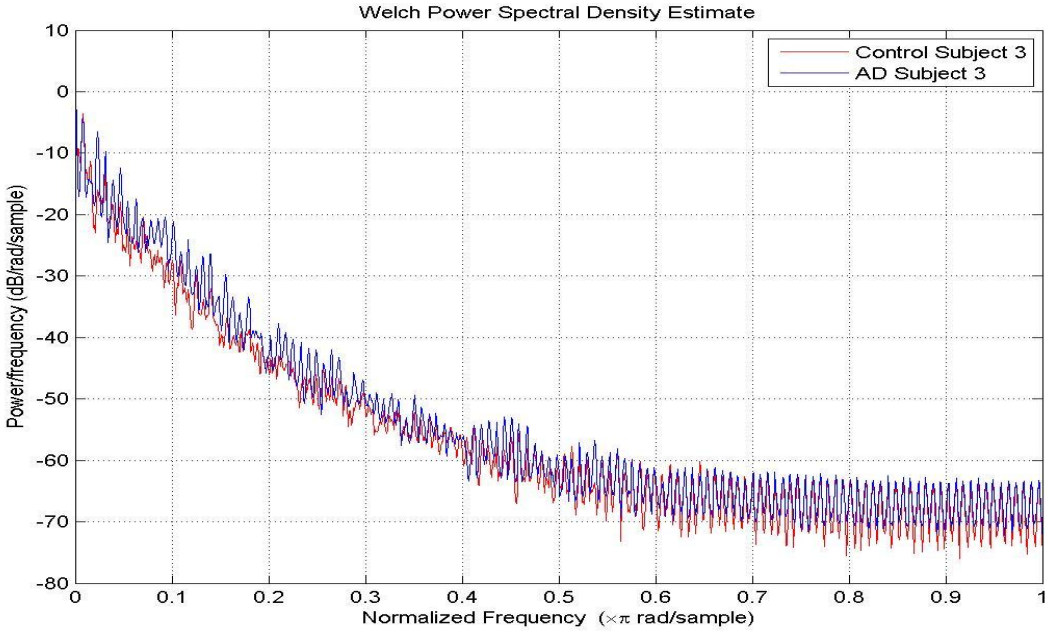

Figure D-2: Welch Power Spectrum for AD subject 3 and control subject 3 after artifact removal

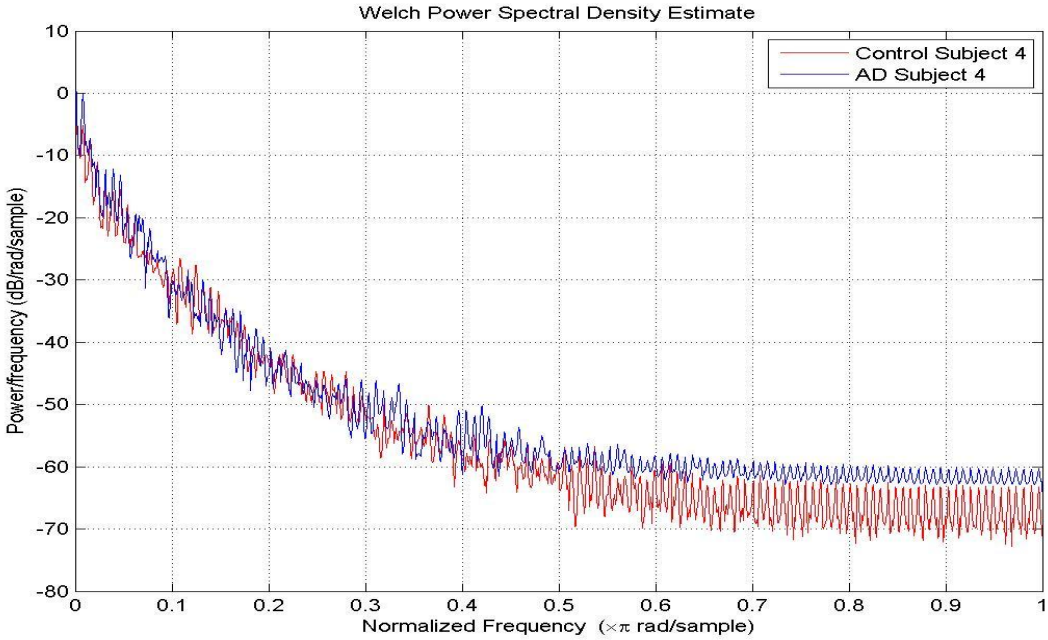

Figure D-3: Welch Power Spectrum for AD subject 4 and control subject 4 after artifact removal

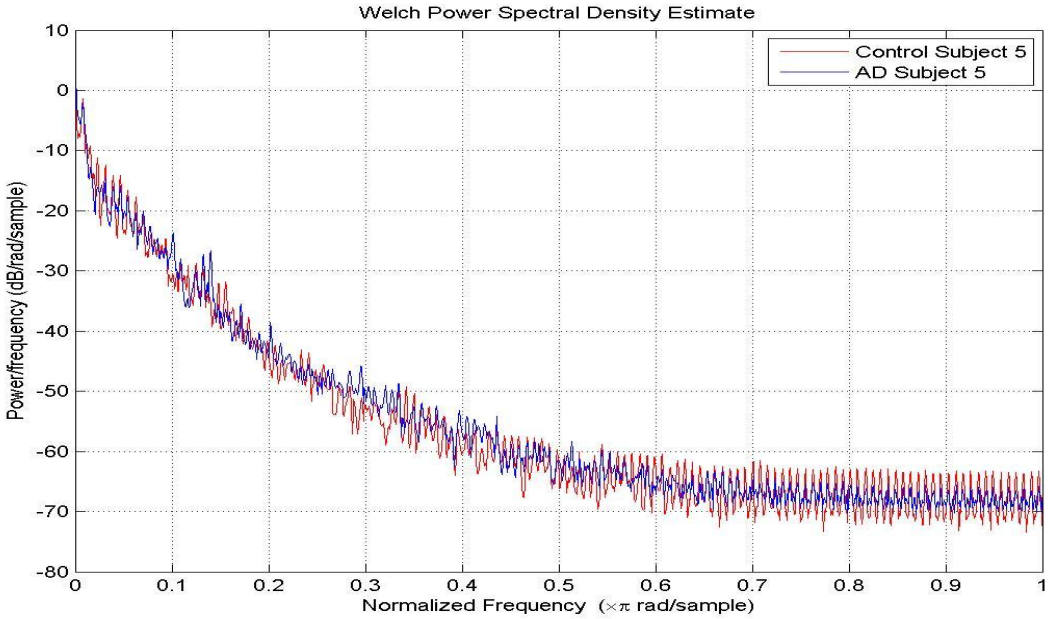

Figure D-4: Welch Power Spectrum for AD subject 5 and control subject 5 after artifact removal

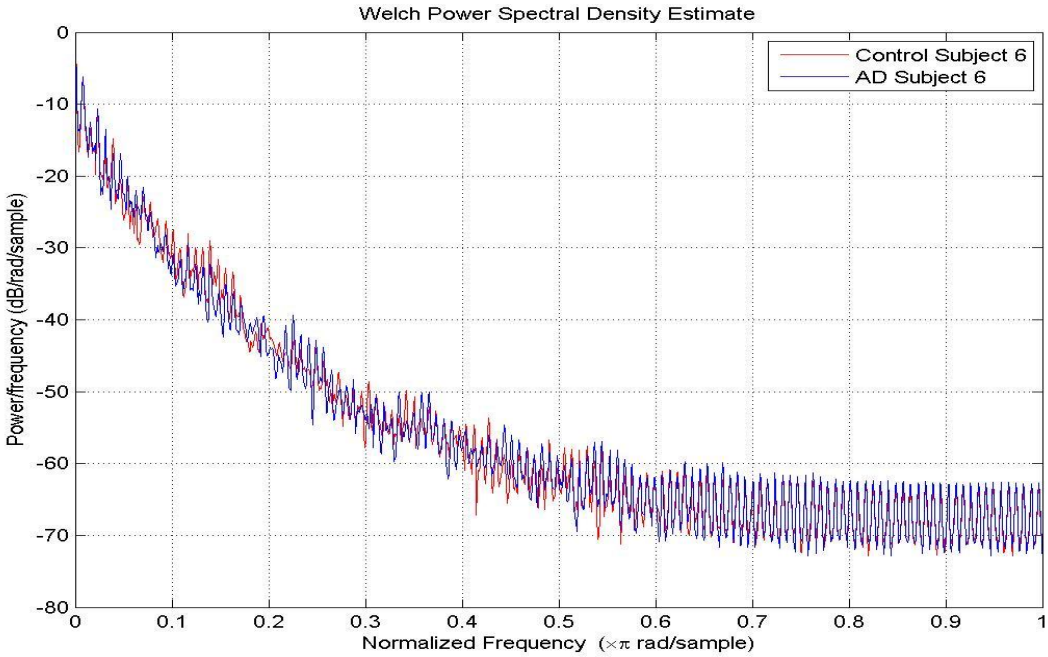

Figure D-5: Welch Power Spectrum for AD subject 6 and control subject 6 after artifact removal

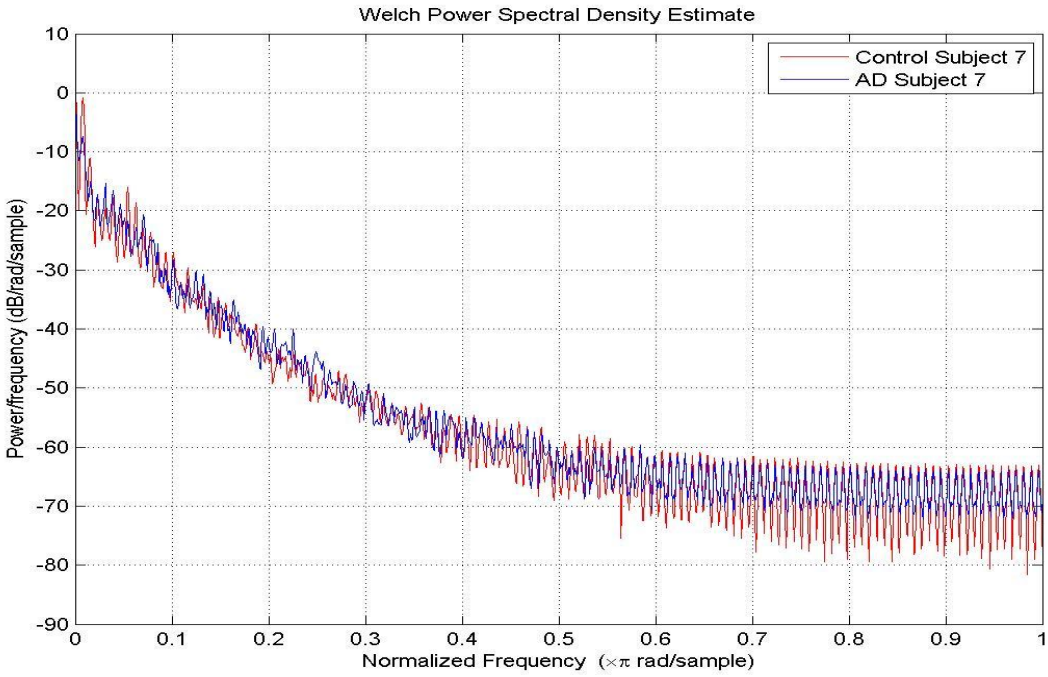

Figure D-6: Welch Power Spectrum for AD subject 7 and control subject 7 after artifact removal

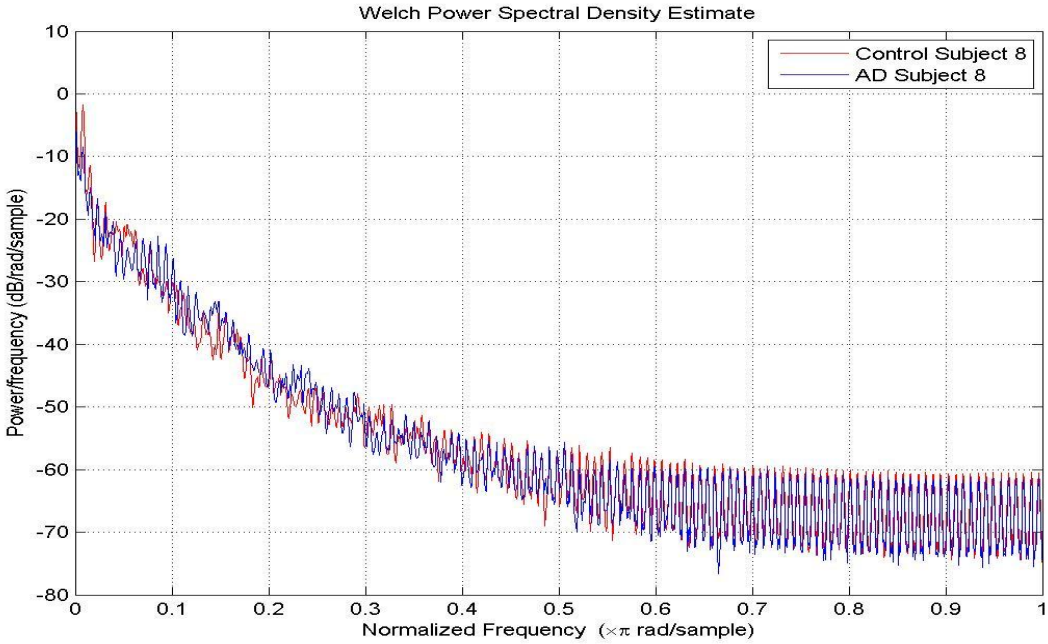

Figure D-7: Welch Power Spectrum for AD subject 8 and control subject 8 after artifact removal

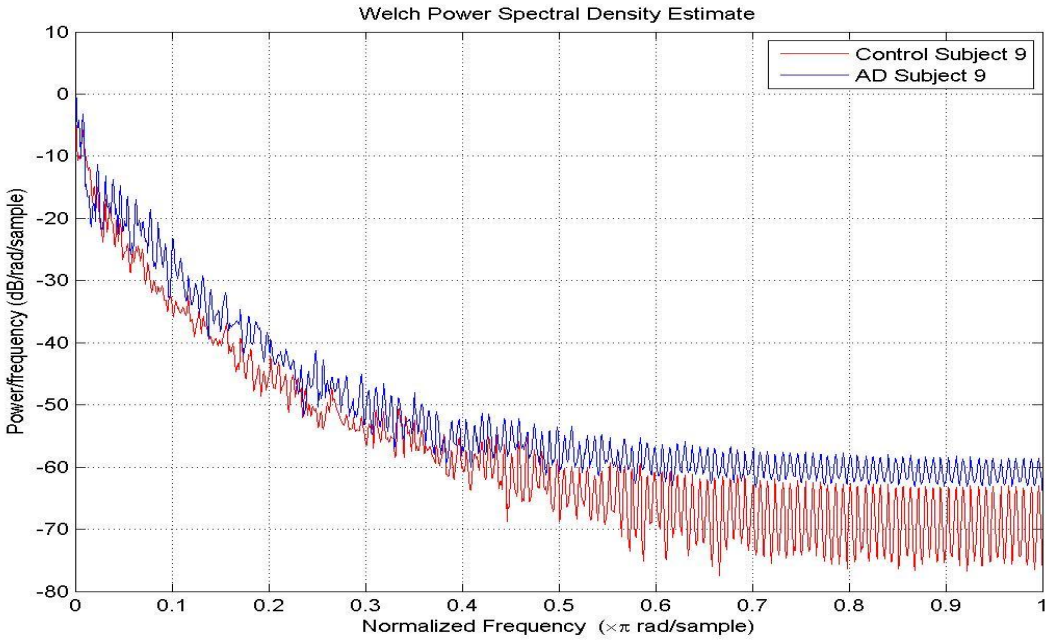

Figure D-8: Welch Power Spectrum for AD subject 9 and control subject 9 after artifact removal

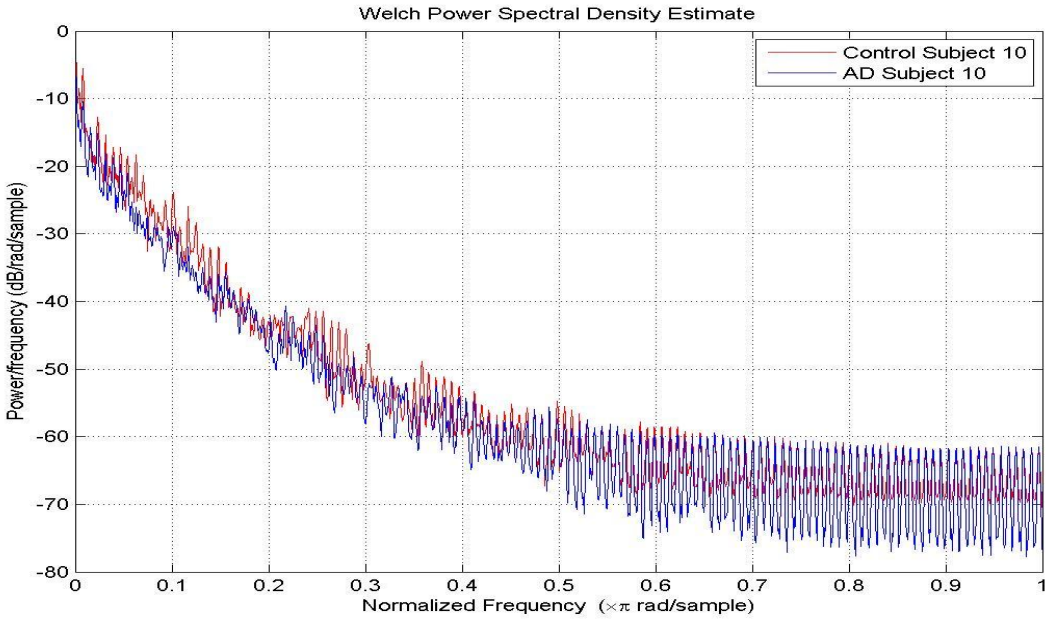

Figure D-9: Welch Power Spectrum for AD subject 10 and control subject 10 after artifact removal

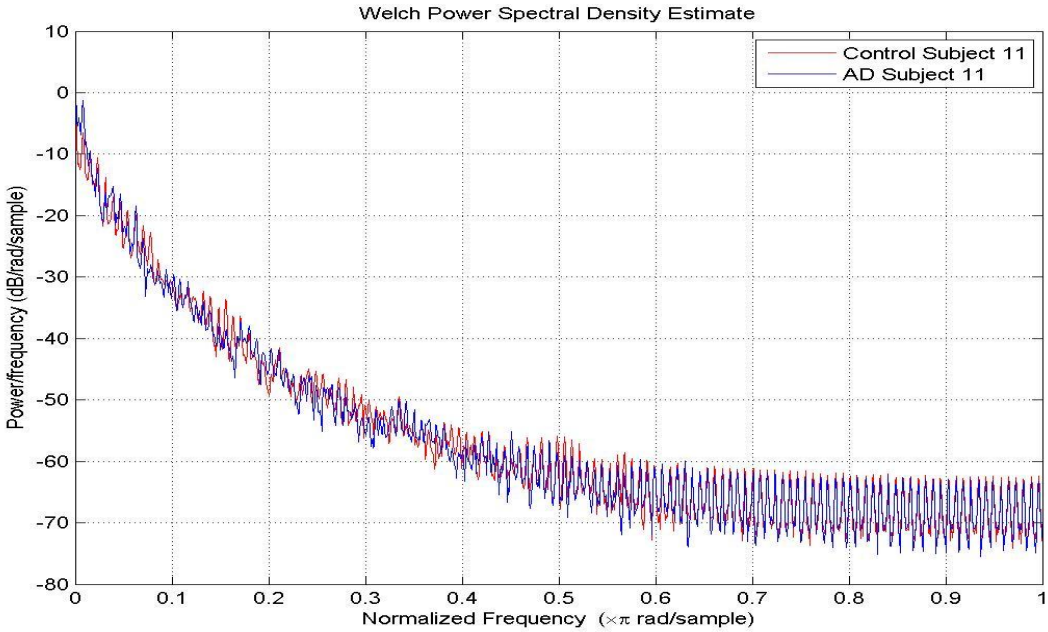

Figure D-10: Welch Power Spectrum for AD subject 11 and control subject 11 after artifact removal

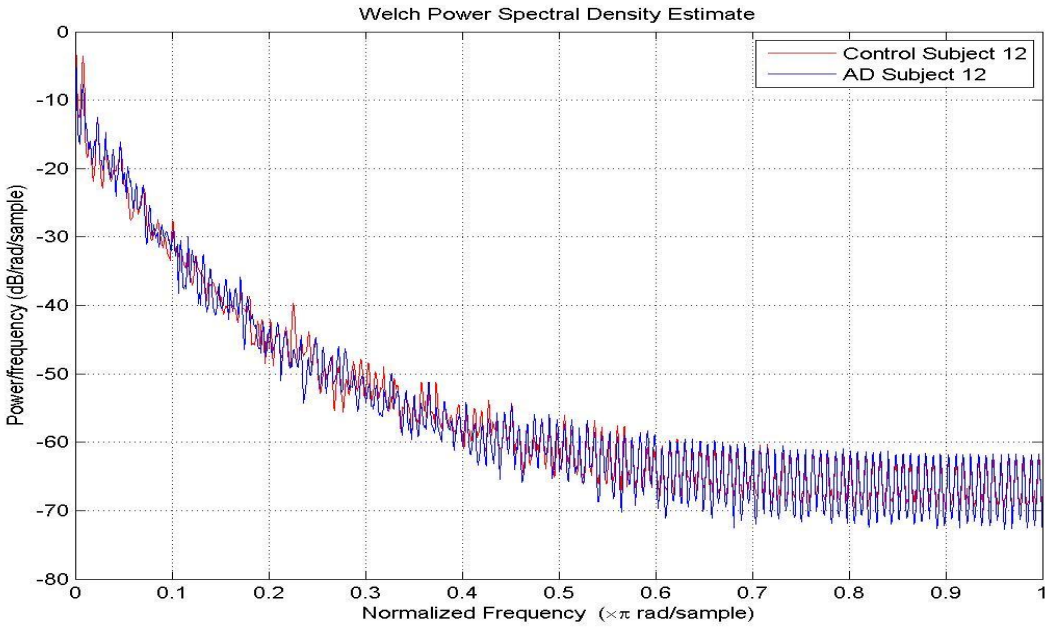

Figure D-11: Welch Power Spectrum for AD subject 12 and control subject 12 after artifact removal

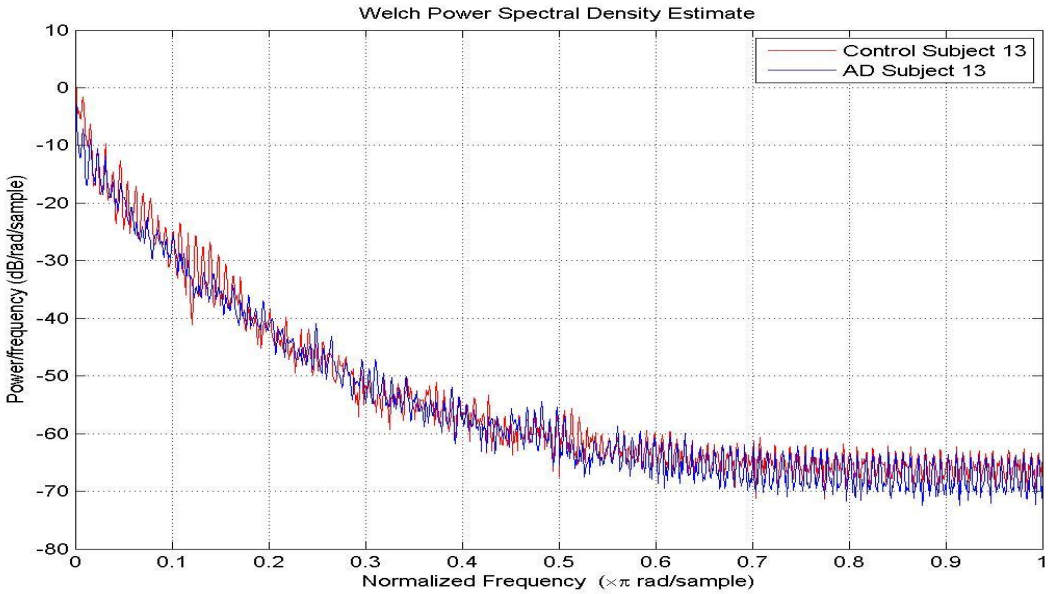

Figure D-12: Welch Power Spectrum for AD subject 13 and control subject 13 after artifact removal

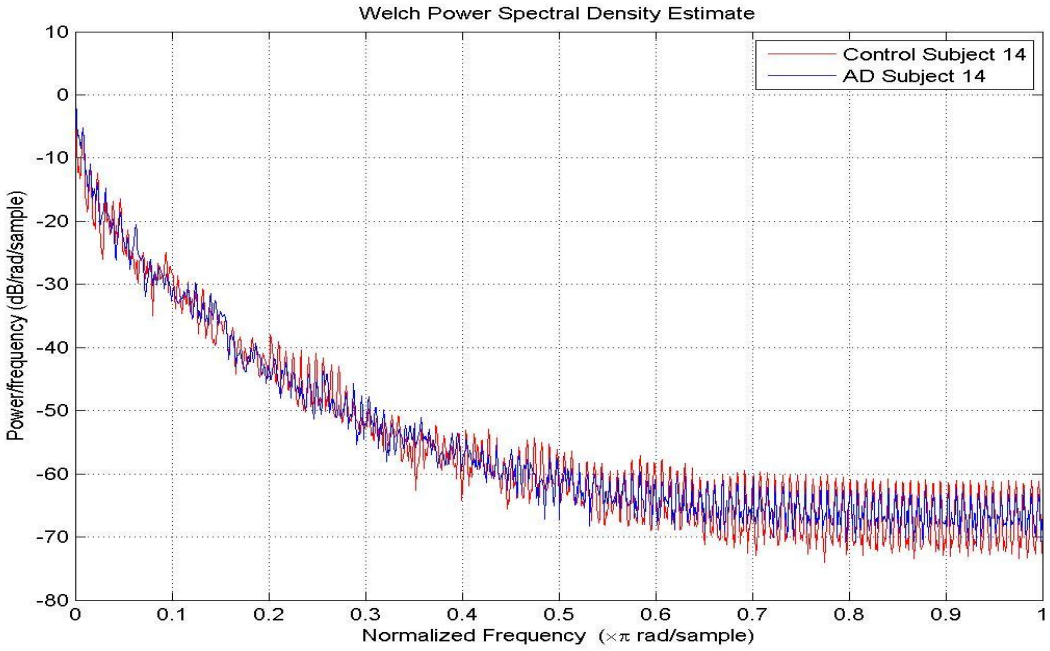

Figure D-13: Welch Power Spectrum for AD subject 14 and control subject 14 after artifact removal

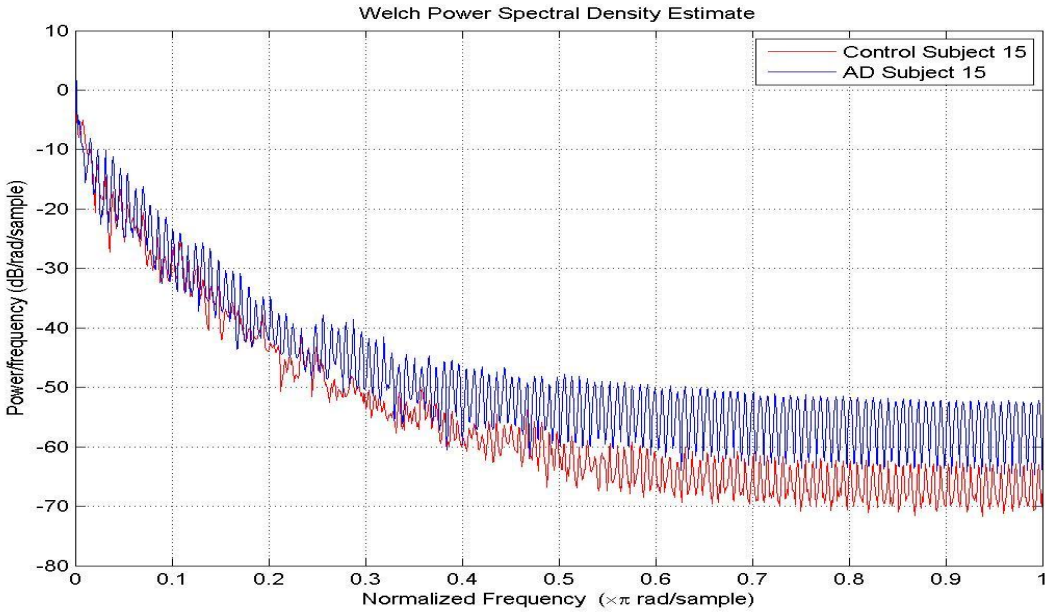

Figure D-14: Welch Power Spectrum for AD subject 15 and control subject 15 after artifact removal

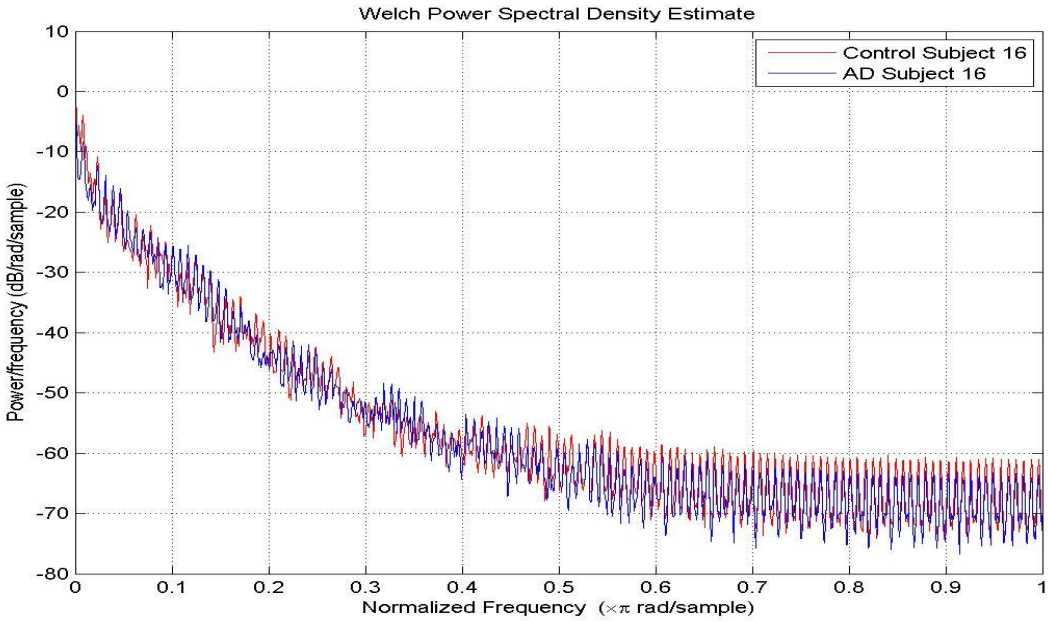

Figure D-15: Welch Power Spectrum for AD subject 16 and control subject 16 after artifact removal

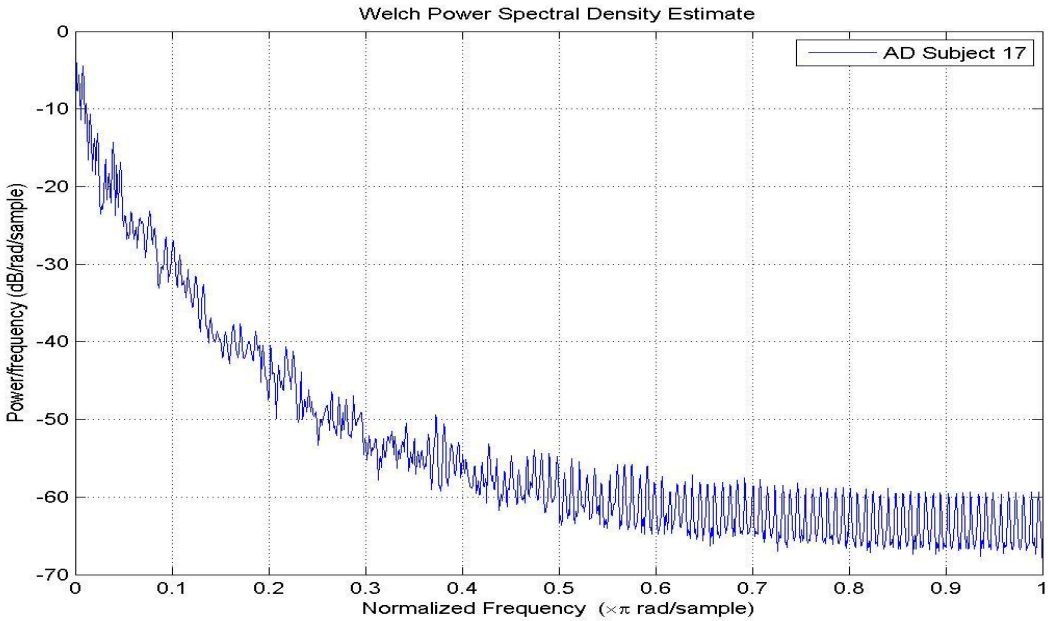

Figure D-16: Welch Power Spectrum for AD subject 17 after artifact removal

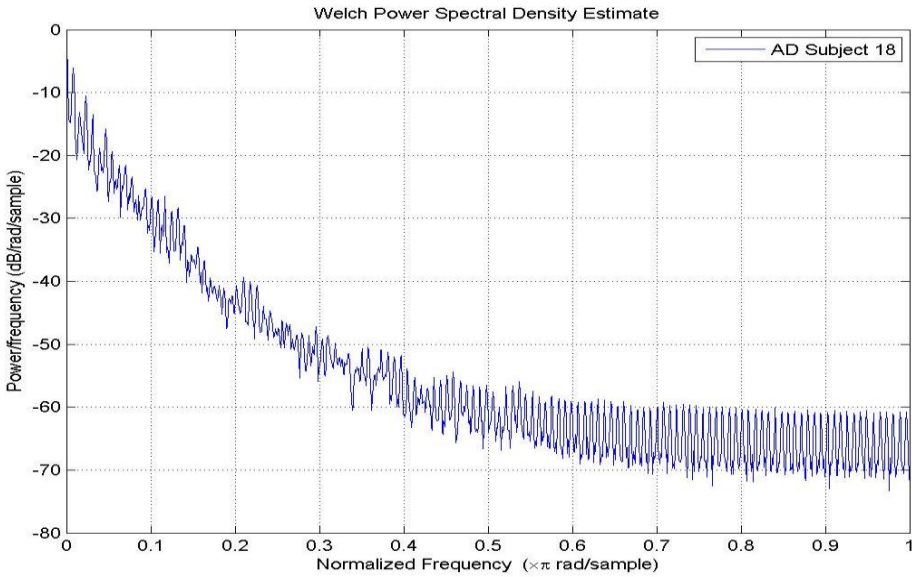

Figure D-17: Welch Power Spectrum for AD subject 18 and after artifact removal

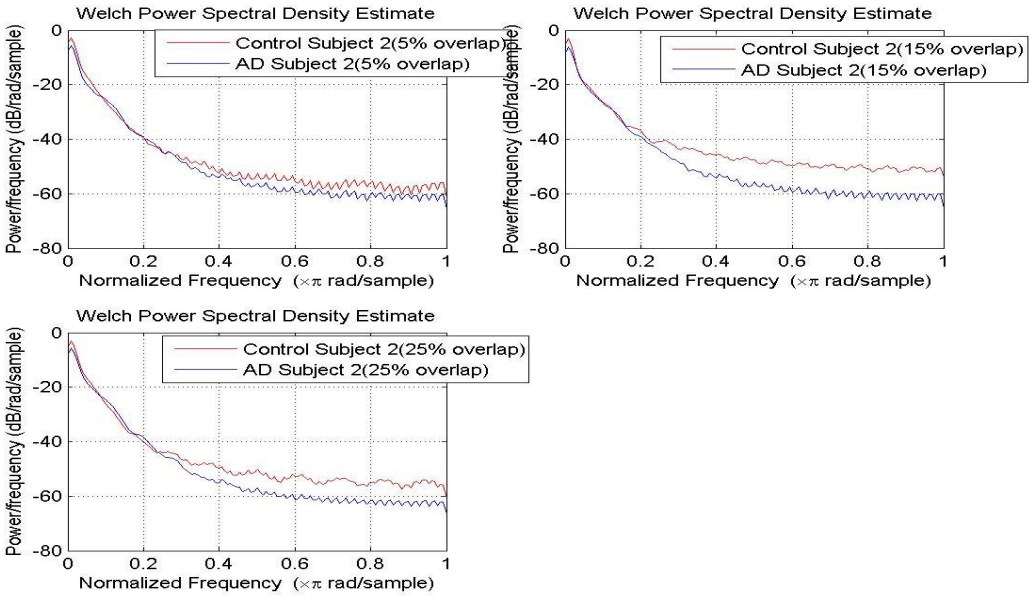

Figure D-18: Welch Power Spectrum for AD subject 2 and control subject 2 with moving window analysis after artifact removal

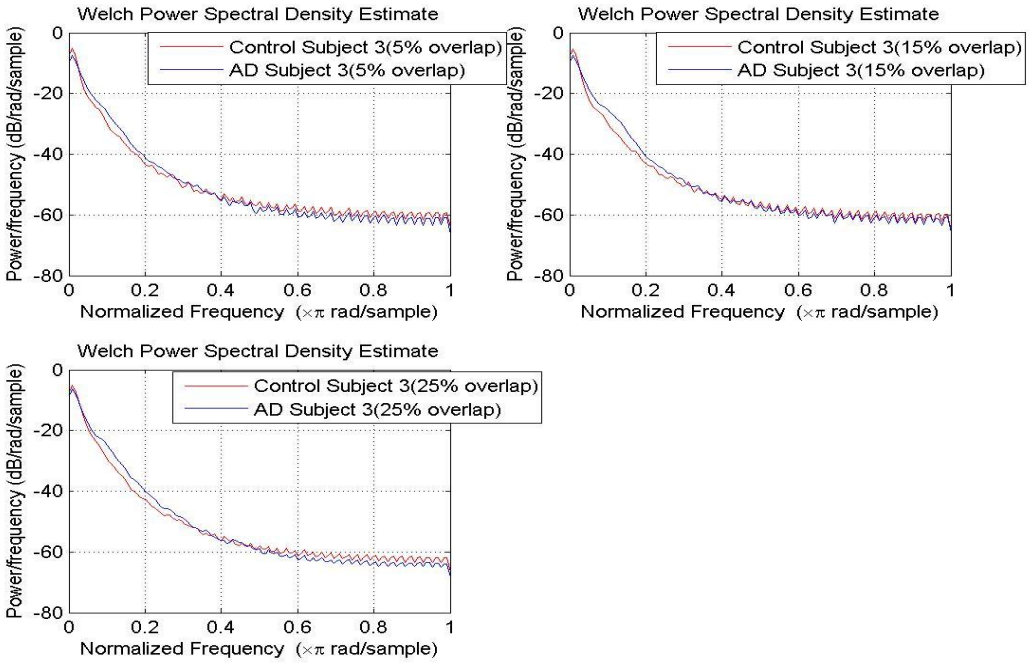

Figure D-19: Welch Power Spectrum for AD subject 3 and control subject 3 with moving window analysis after artifact removal

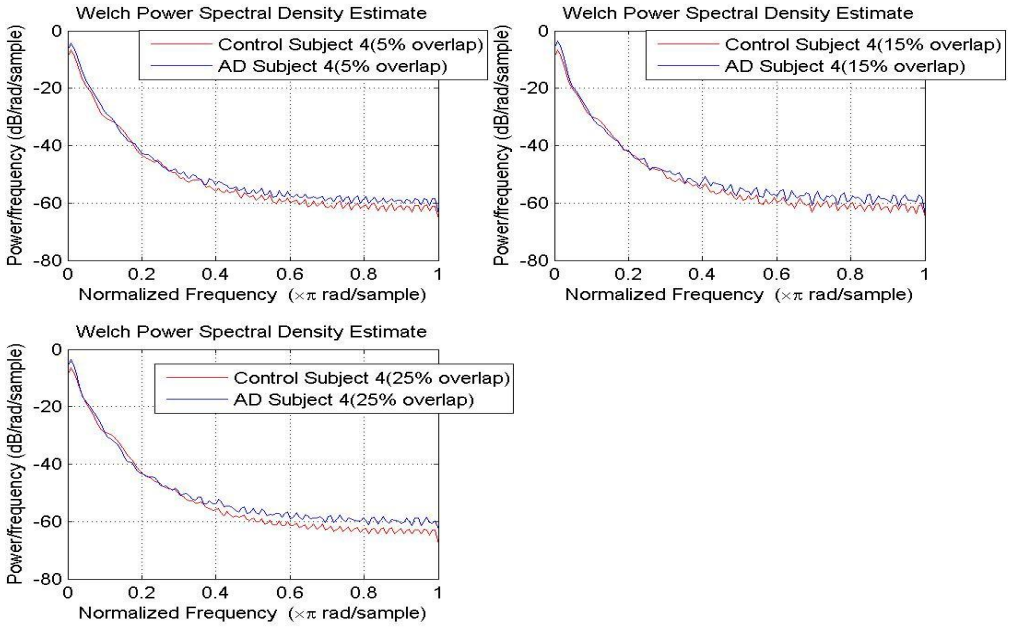

Figure D-20: Welch Power Spectrum for AD subject 4 and control subject 4 with moving window analysis after artifact removal

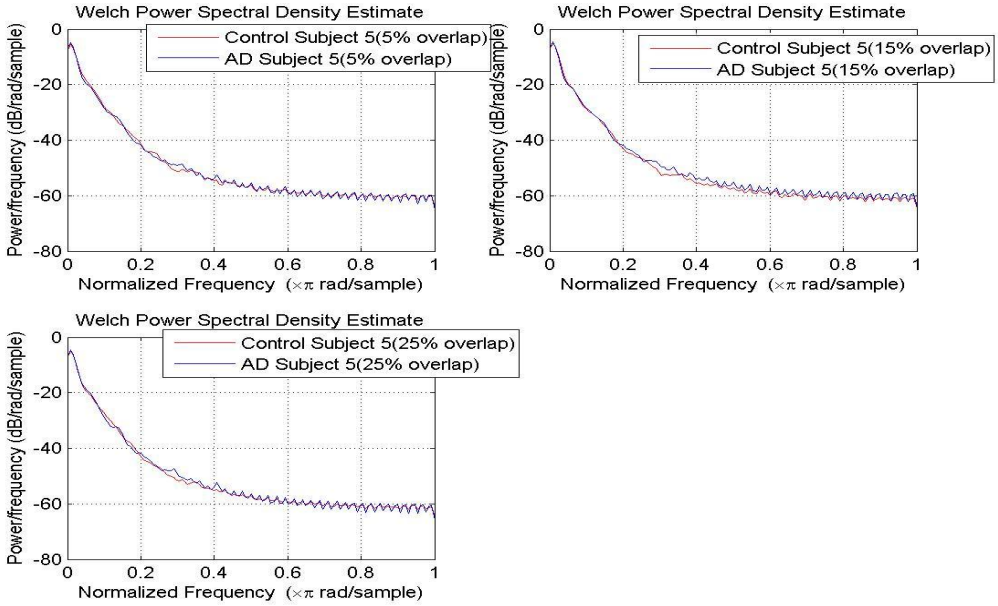

Figure D-21: Welch Power Spectrum for AD subject 5 and control subject 5 with moving window analysis after artifact removal

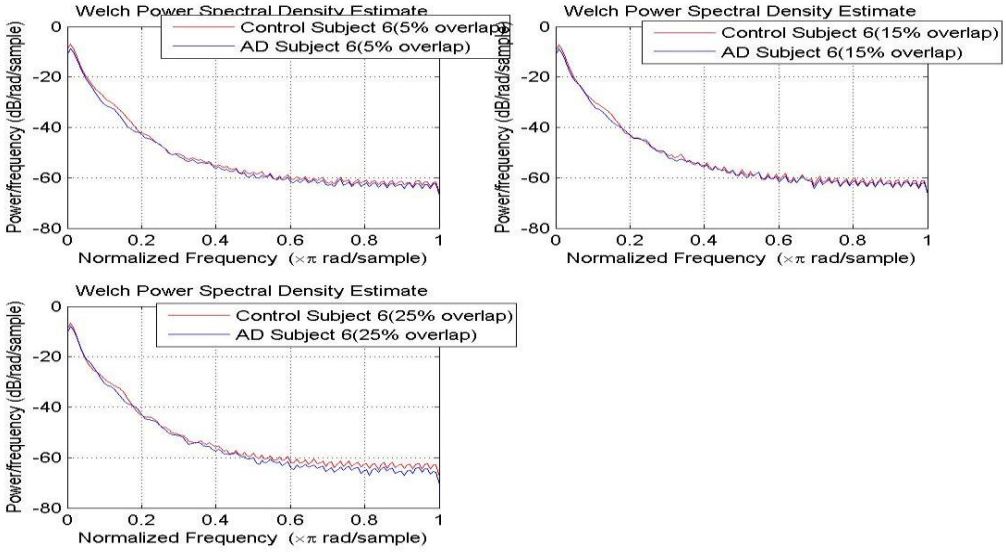

Figure D-22: Welch Power Spectrum for AD subject 6 and control subject 6 with moving window analysis after artifact removal

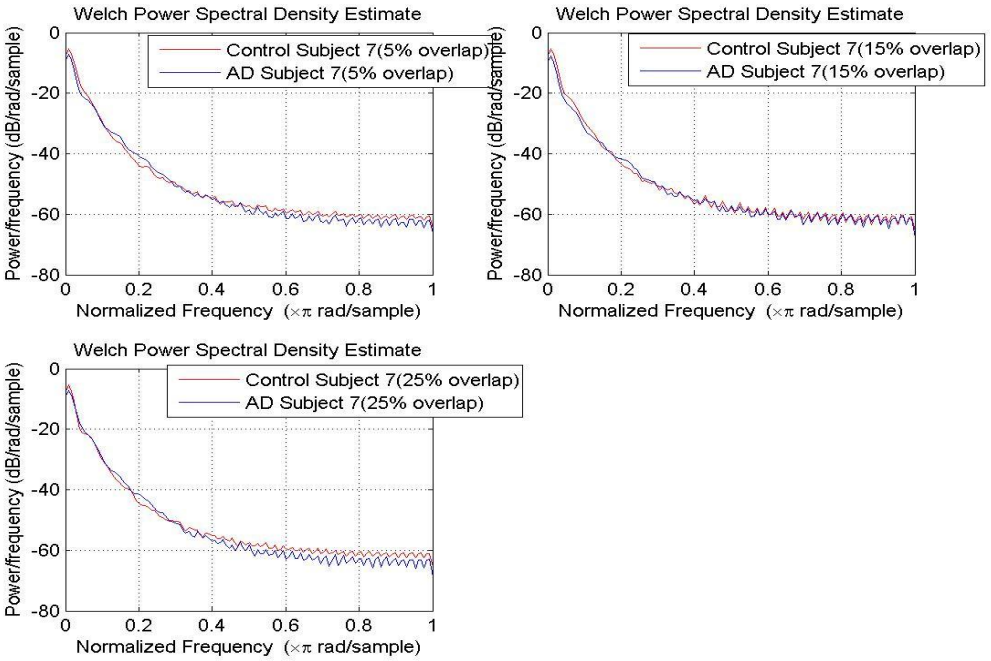

Figure D-23: Welch Power Spectrum for AD subject 7 and control subject 7 with moving window analysis after artifact removal

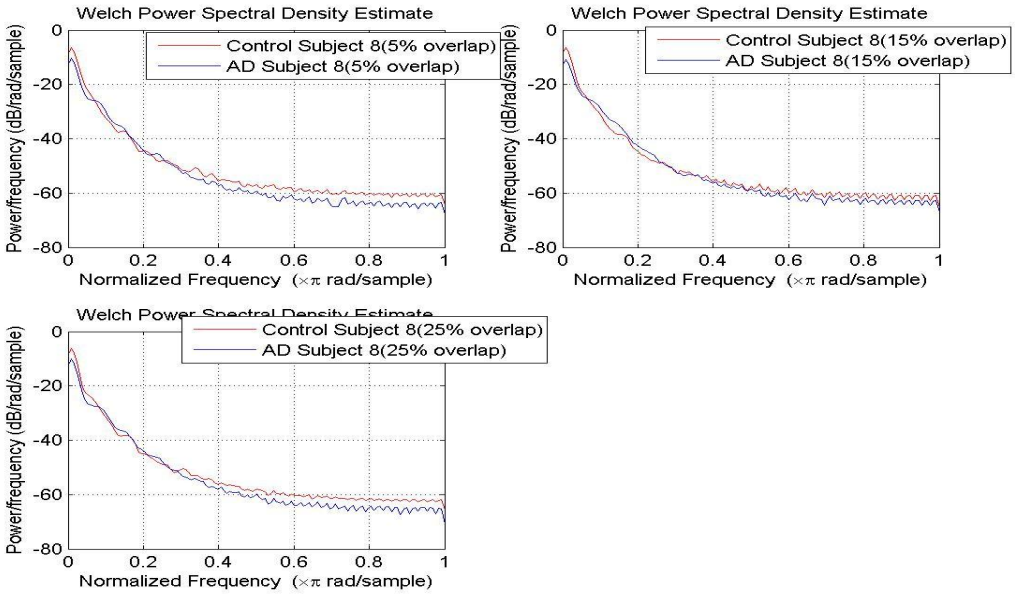

Figure D-24: Welch Power Spectrum for AD subject 8 and control subject 8 with moving window analysis after artifact removal

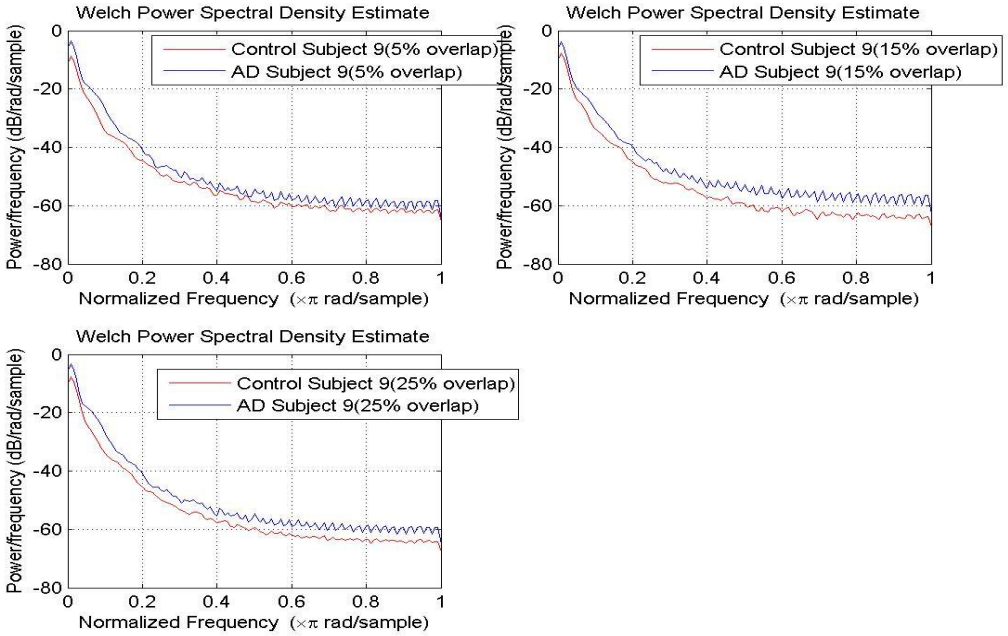

Figure D-25: Welch Power Spectrum for AD subject 9 and control subject 9 with moving window analysis after artifact removal

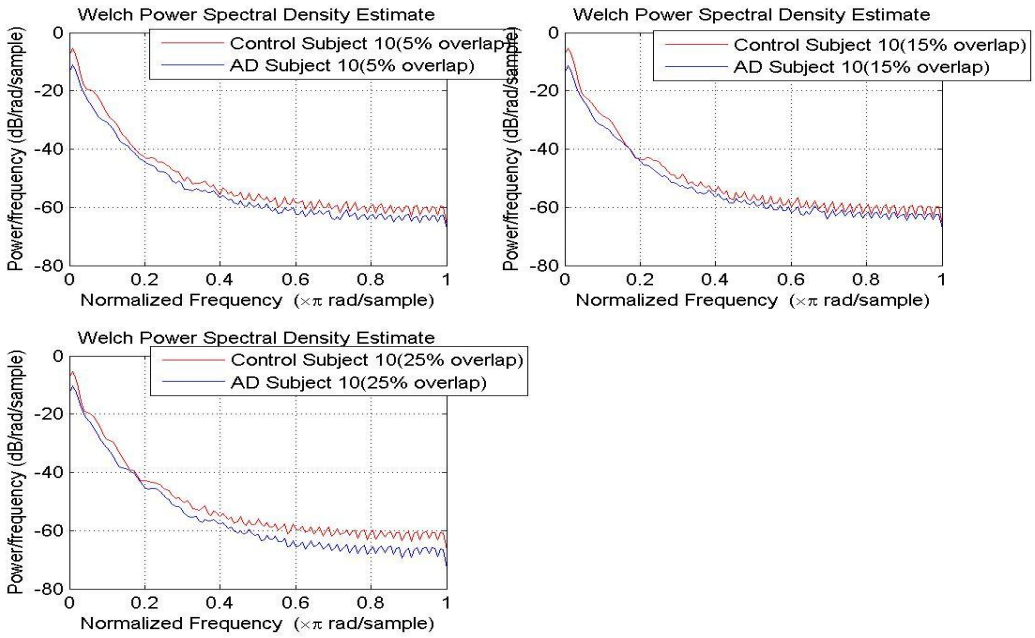

Figure D-26: Welch Power Spectrum for AD subject 10 and control subject 10 with moving window analysis after artifact removal

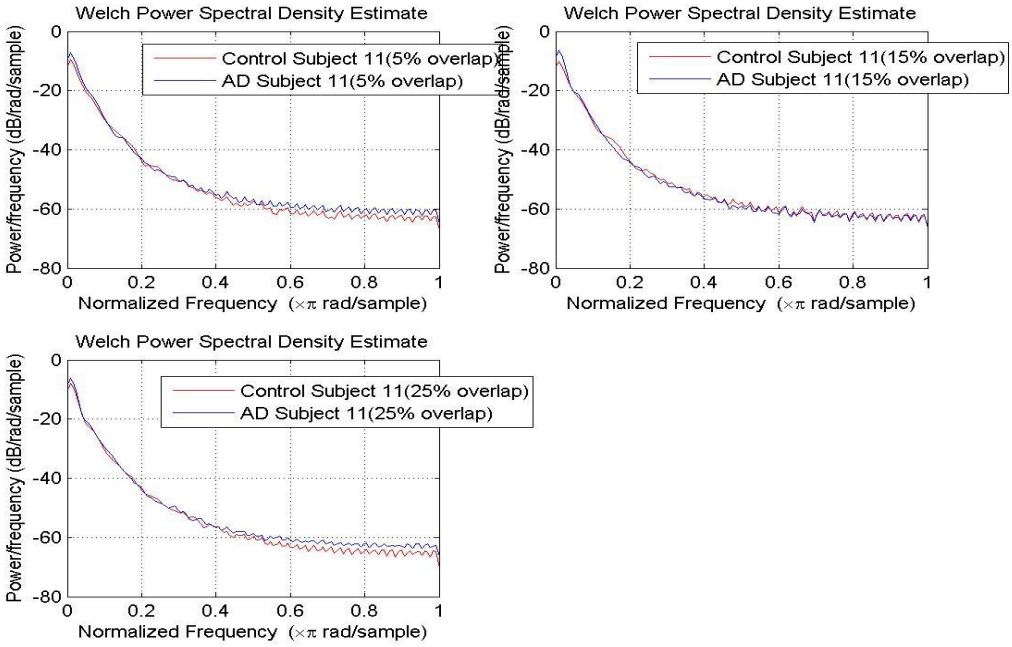

Figure D-27: Welch Power Spectrum for AD subject 11 and control subject 11 with moving window analysis after artifact removal

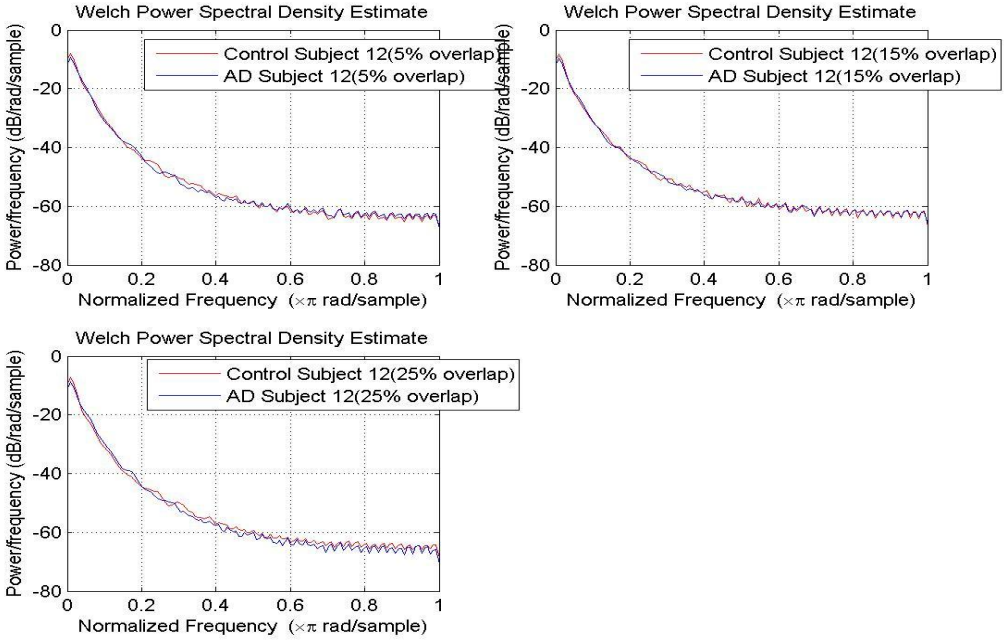

Figure D-28: Welch Power Spectrum for AD subject 12 and control subject 12 with moving window analysis after artifact removal

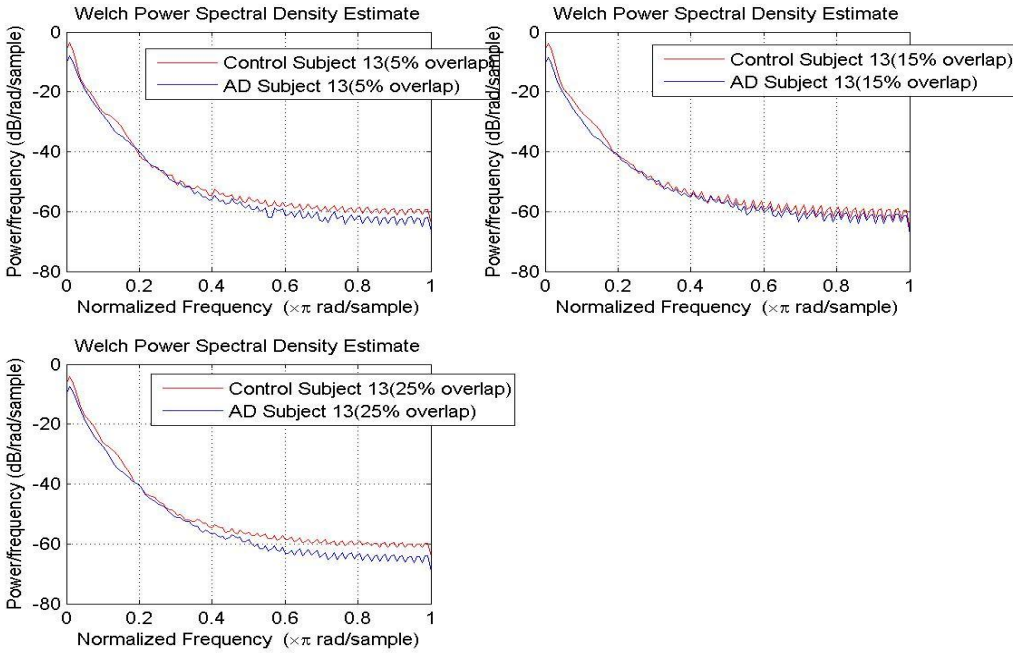

Figure D-29: Welch Power Spectrum for AD subject 13 and control subject 13 with moving window analysis after artifact removal

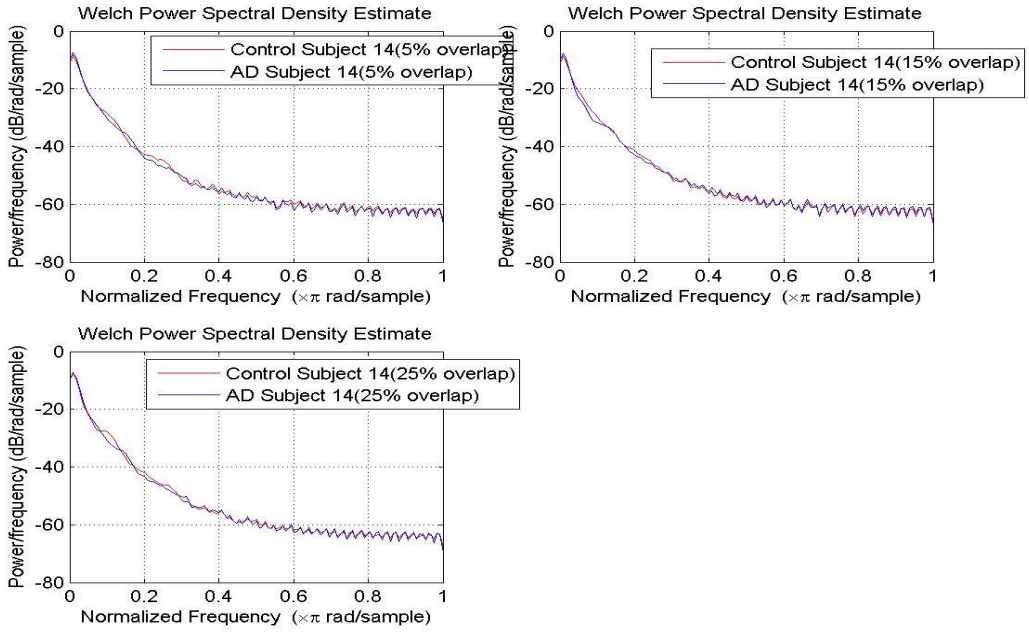

Figure D-30: Welch Power Spectrum for AD subject 14 and control subject 14 with moving window analysis after artifact removal

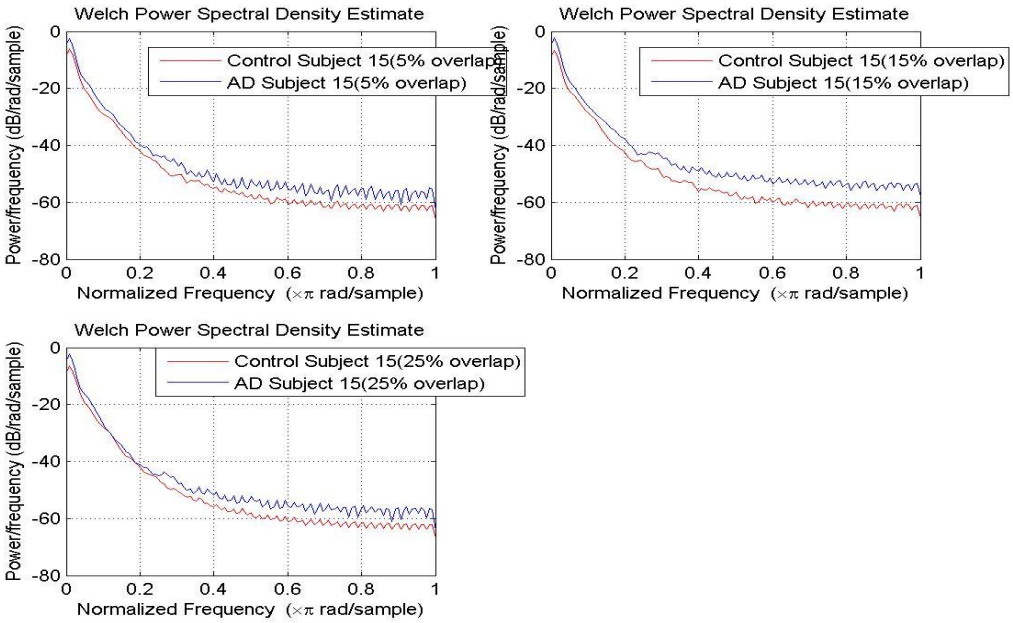

Figure D-31: Welch Power Spectrum for AD subject 15 and control subject 15 with moving window analysis after artifact removal

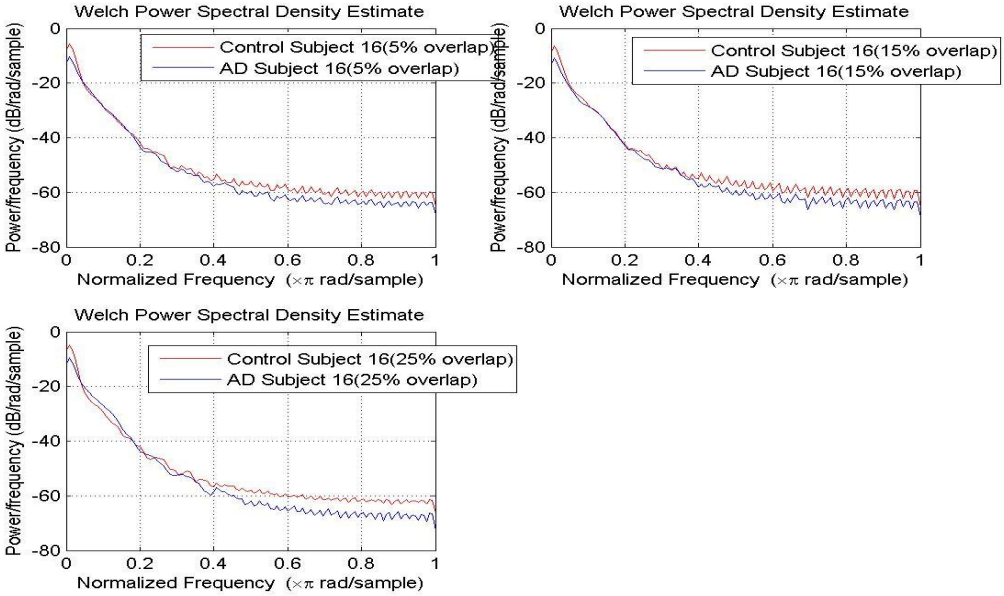

Figure D-32: Welch Power Spectrum for AD subject 16 and control subject 16 with moving window analysis after artifact removal

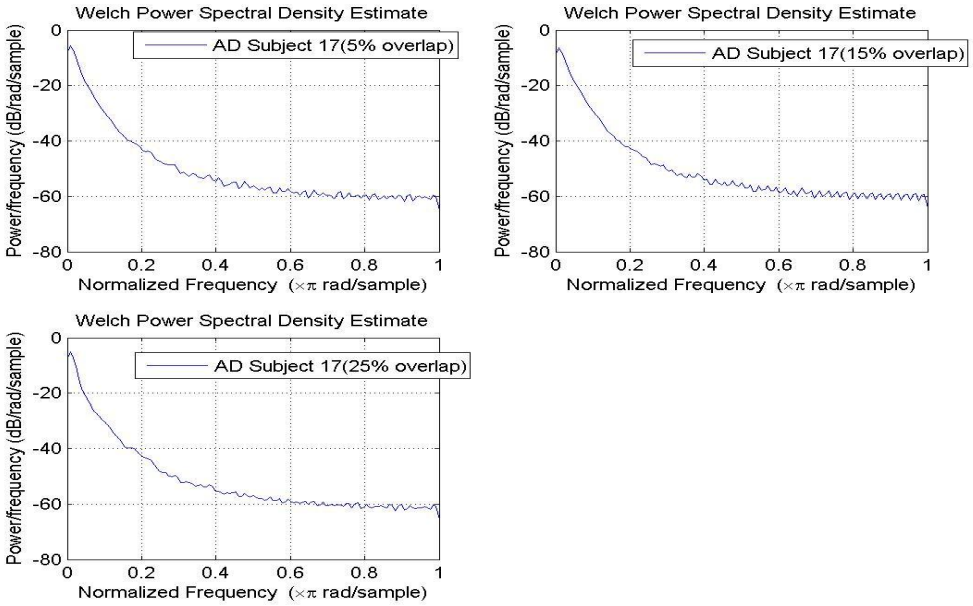

Figure D-33: Welch Power Spectrum for AD subject 17 with moving window analysis after artifact removal

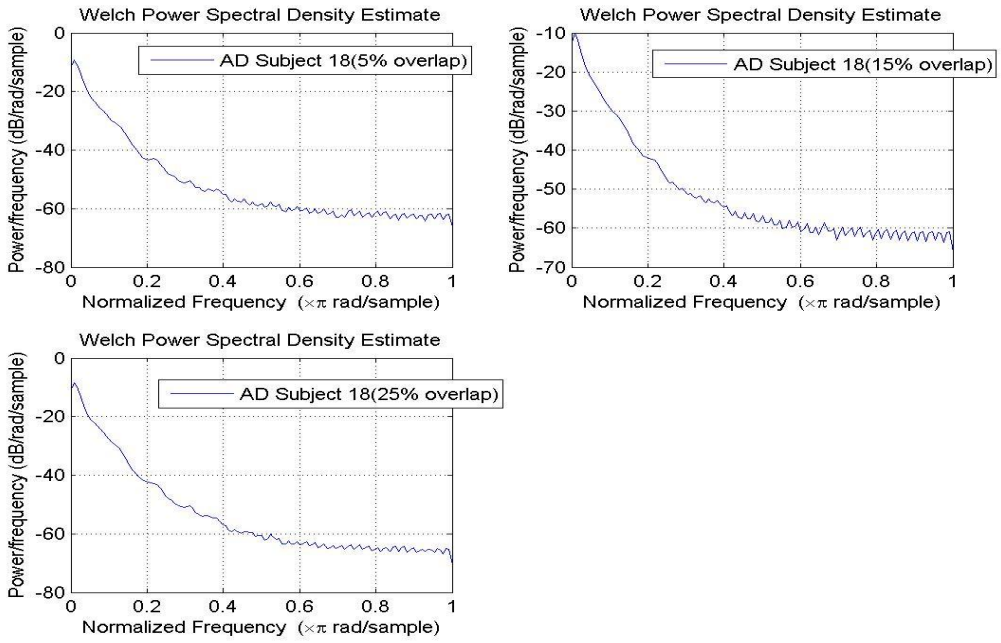

Figure D-34: Welch Power Spectrum for AD subject 18 with moving window analysis after artifact removal

Appendix E

The DFT Plots for Artifacts Removed EEG Signals

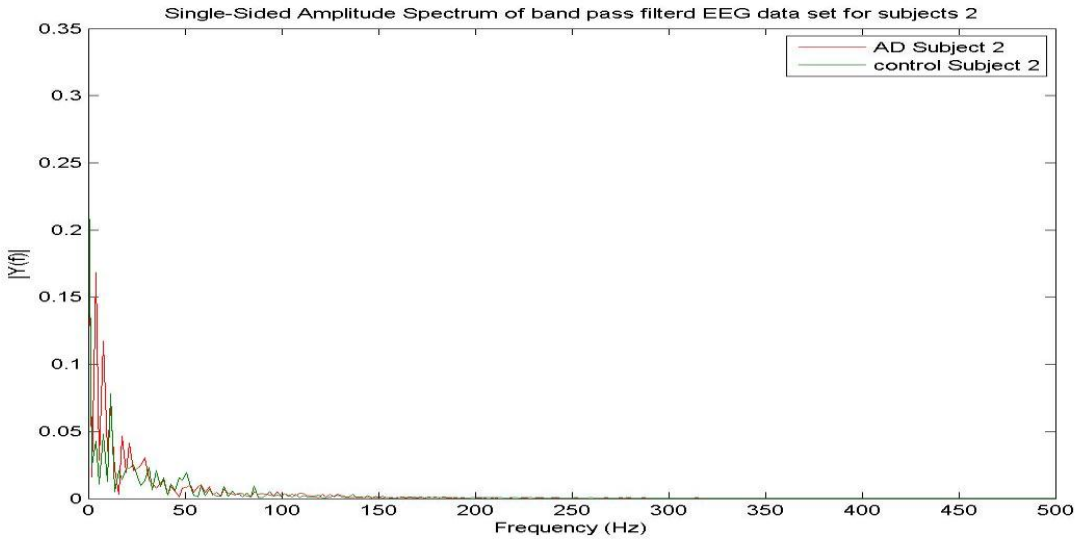

Figure E-1: The DFT for AD subject 2 and control subject 2 after artifact removal

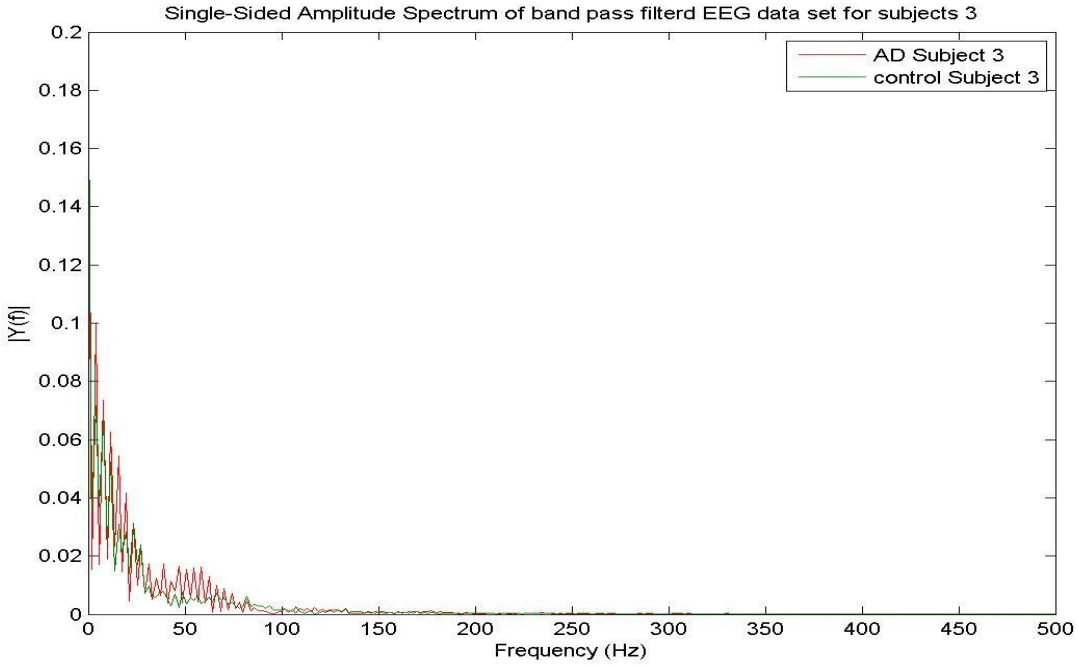

Figure E-2: The DFT for AD subject 3 and control subject 3 after artifact removal

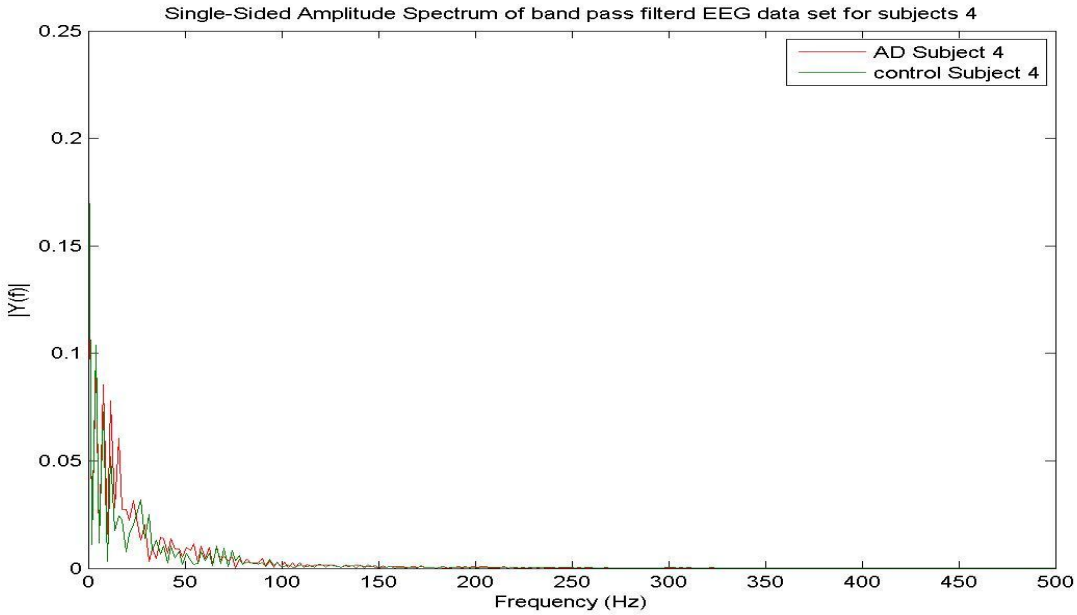

Figure E-3: The DFT for AD subject 4 and control subject 4 after artifact removal

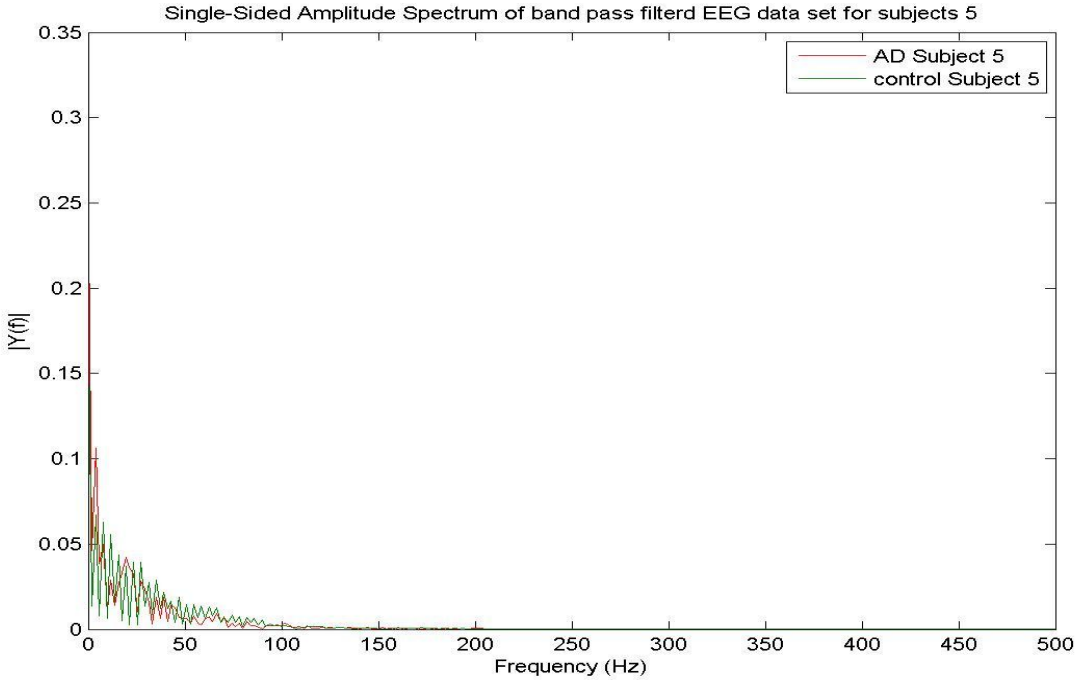

Figure E-4: The DFT for AD subject 5 and control subject 5 after artifact removal

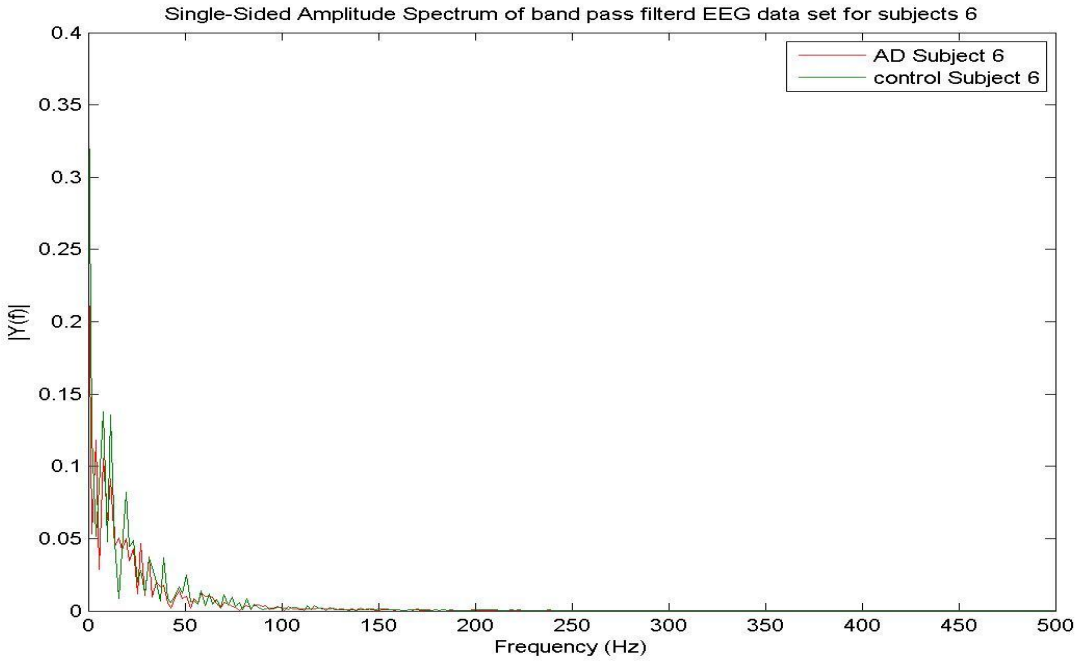

Figure E-5: The DFT for AD subject 6 and control subject 6 after artifact removal

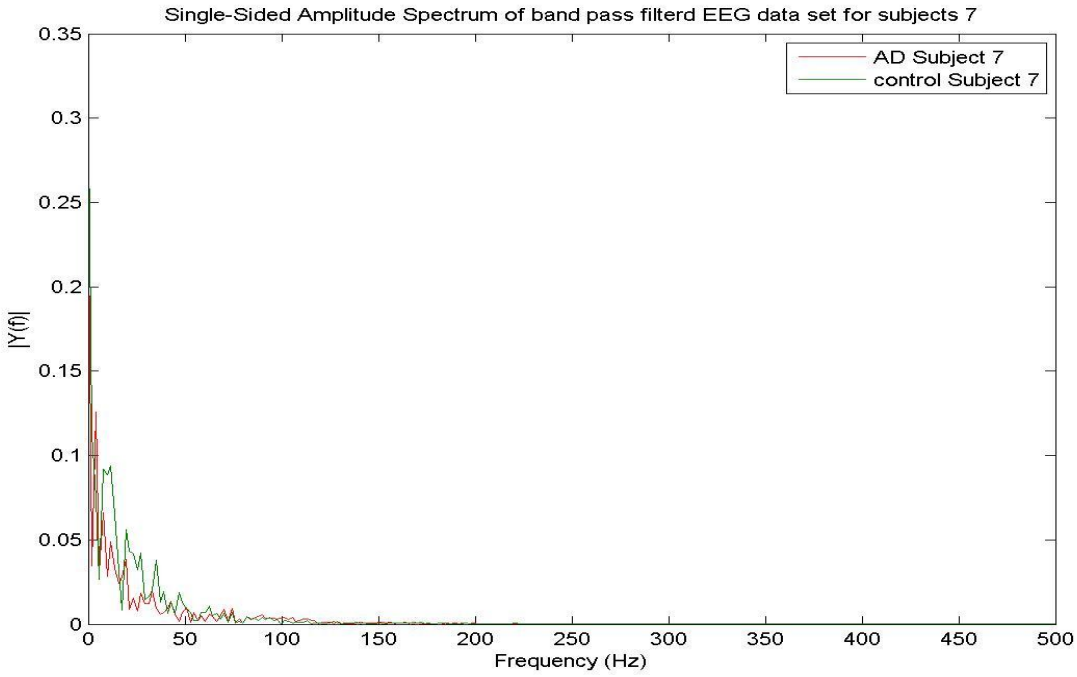

Figure E-6: The DFT for AD subject 7 and control subject 7 after artifact removal

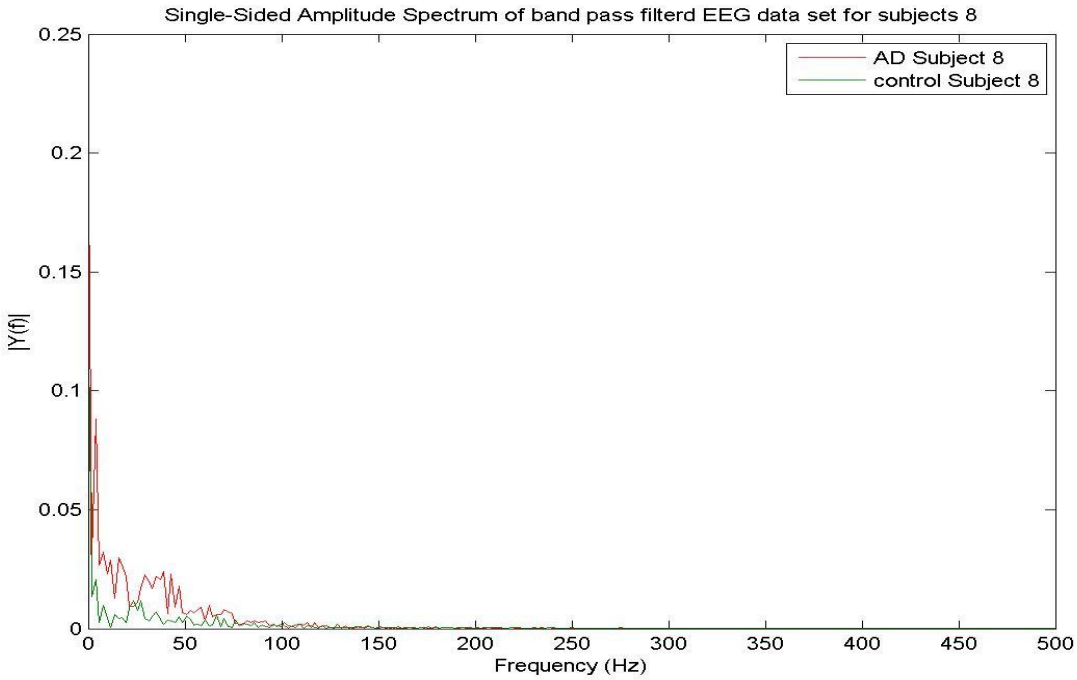

Figure E-7: The DFT for AD subject 8 and control subject 8 after artifact removal

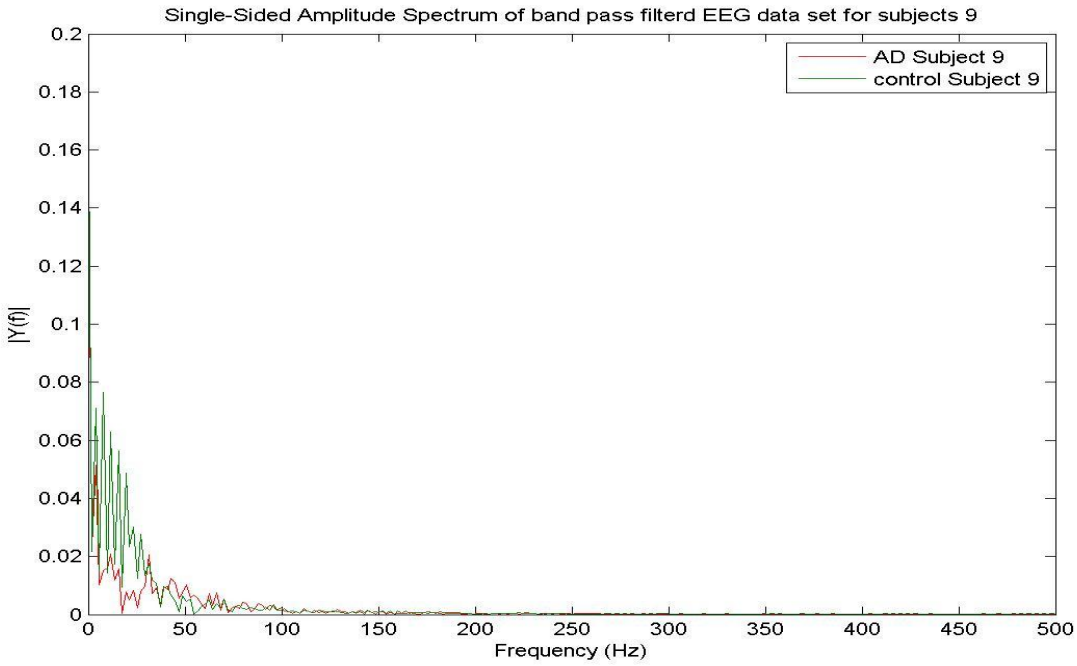

Figure E-8: The DFT for AD subject 9 and control subject 9 after artifact removal

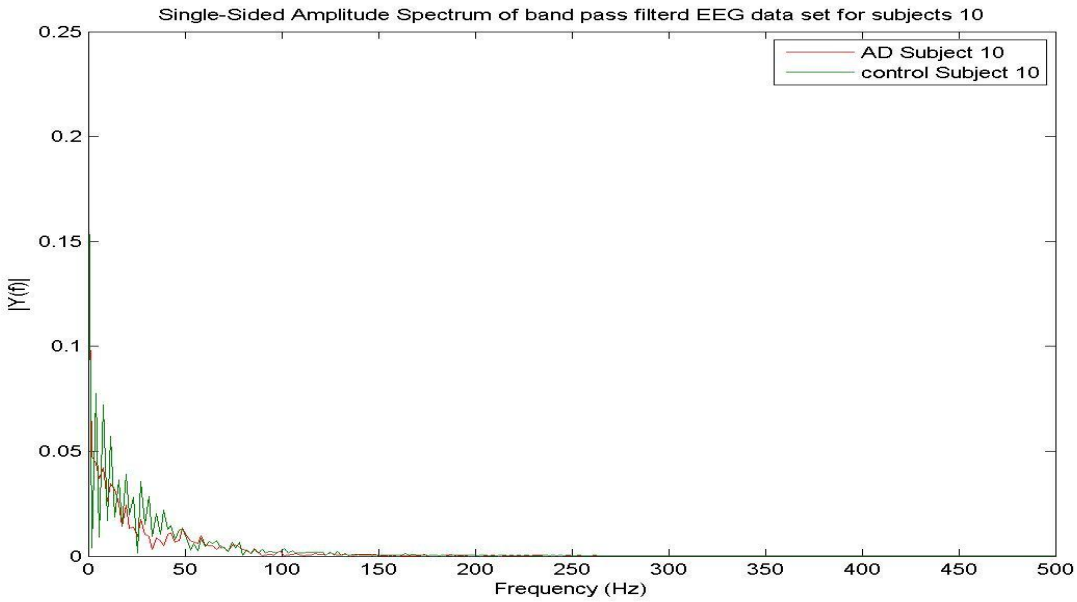

Figure E-9: The DFT for AD subject 10 and control subject 10 after artifact removal

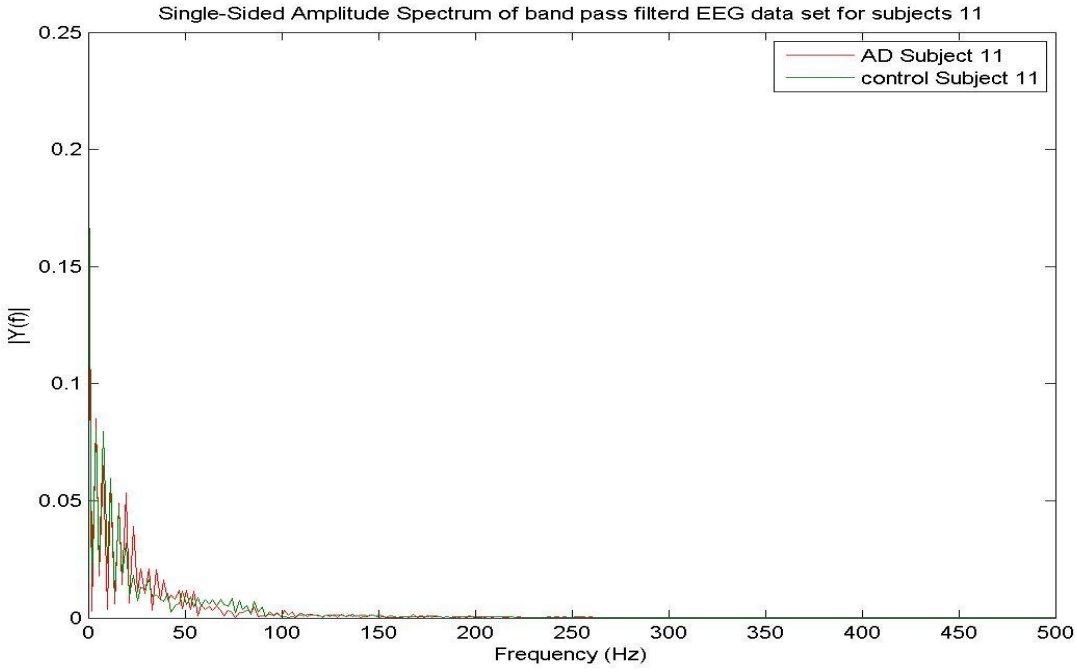

Figure E-10: The DFT for AD subject 11 and control subject 11 after artifact removal

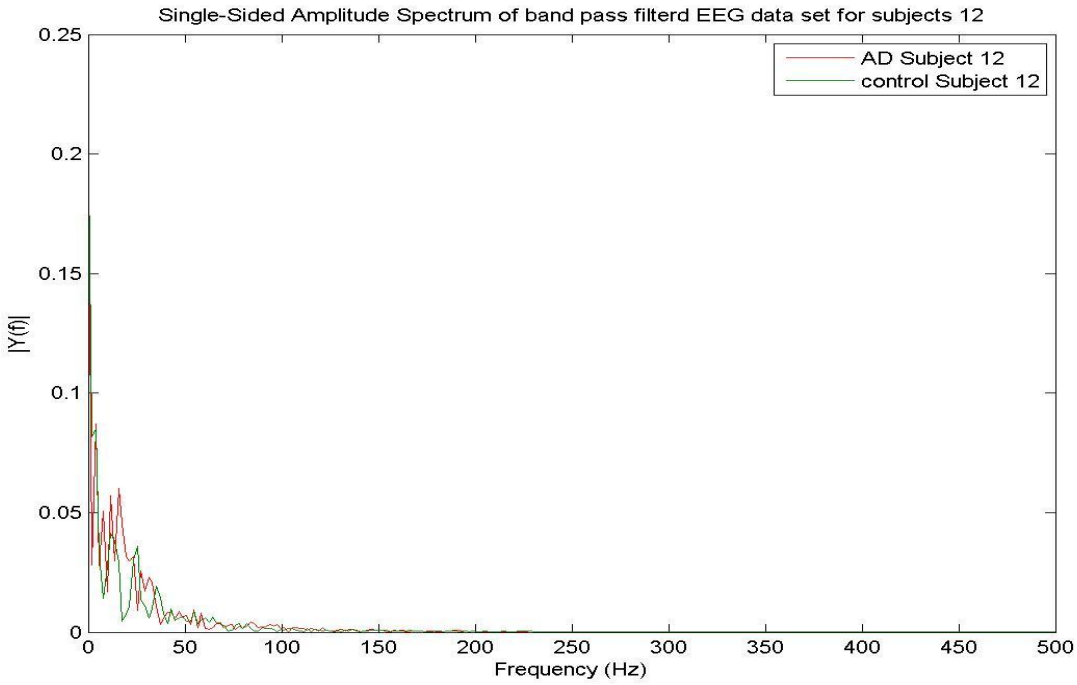

Figure E-11: The DFT for AD subject 12 and control subject 12 after artifact removal

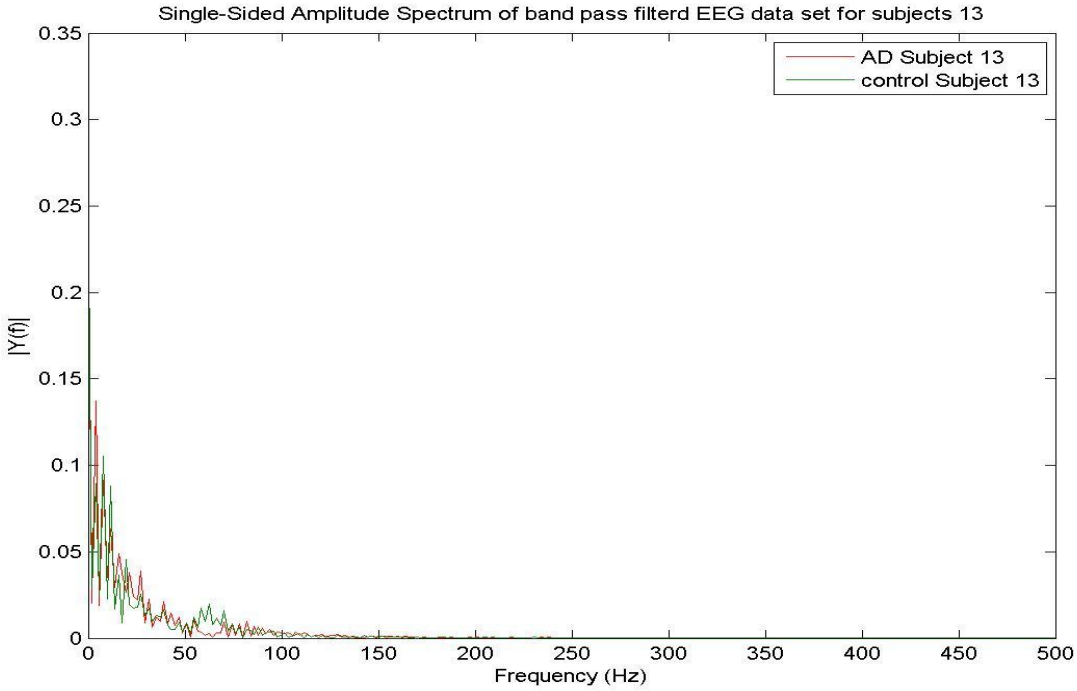

Figure E-12: The DFT for AD subject 13 and control subject 13 after artifact removal

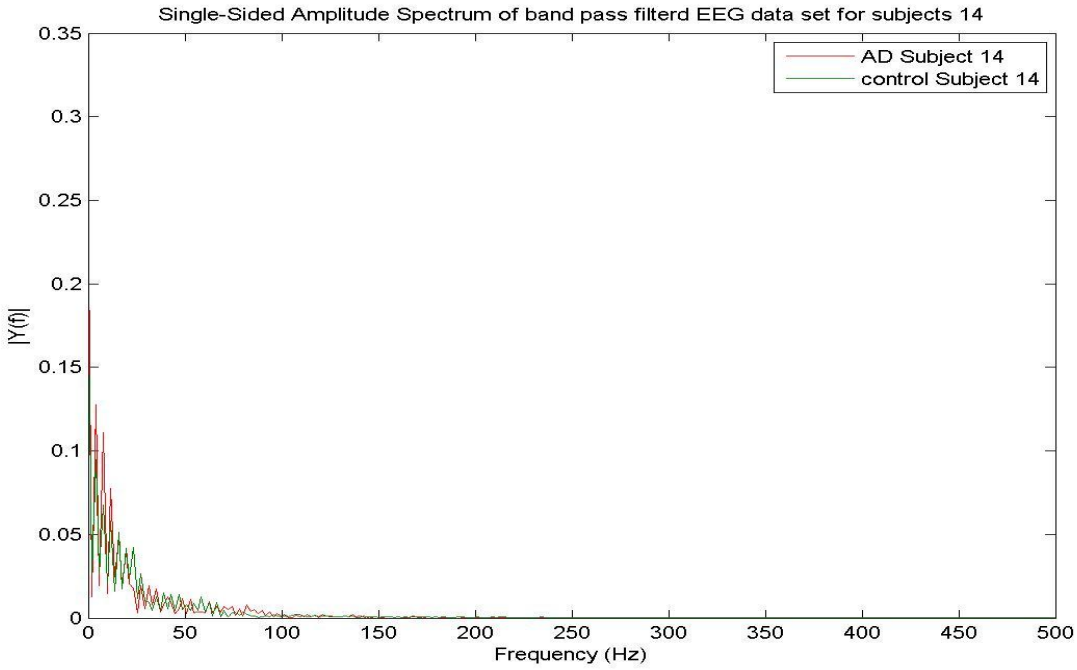

Figure E-13: The DFT for AD subject 14 and control subject 14 after artifact removal

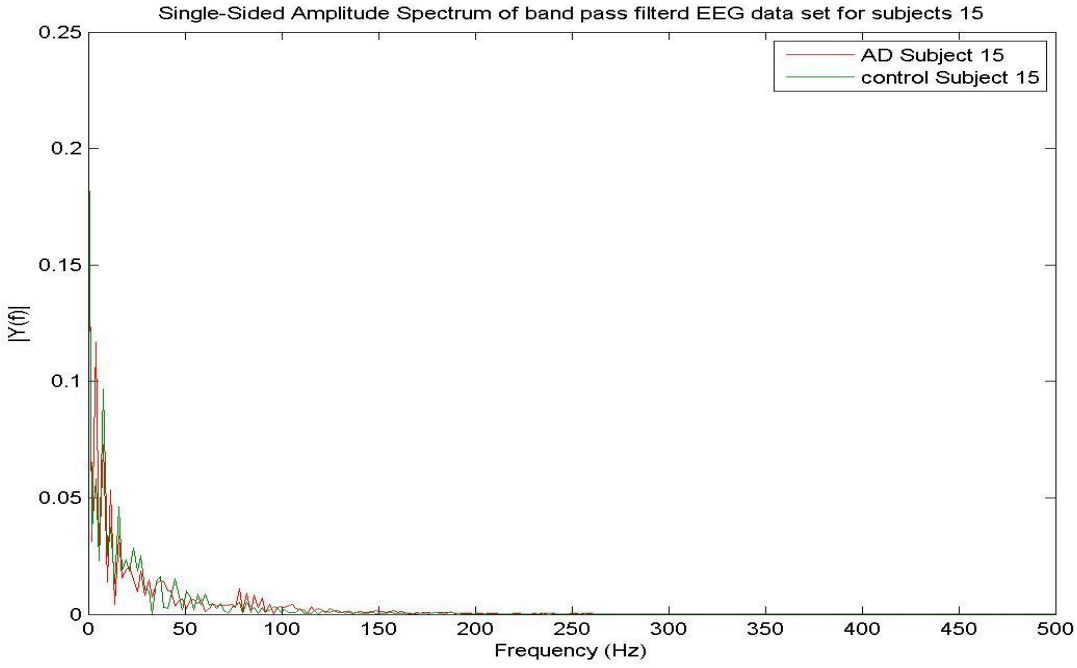

Figure E-14: The DFT for AD subject 15 and control subject 15 after artifact removal

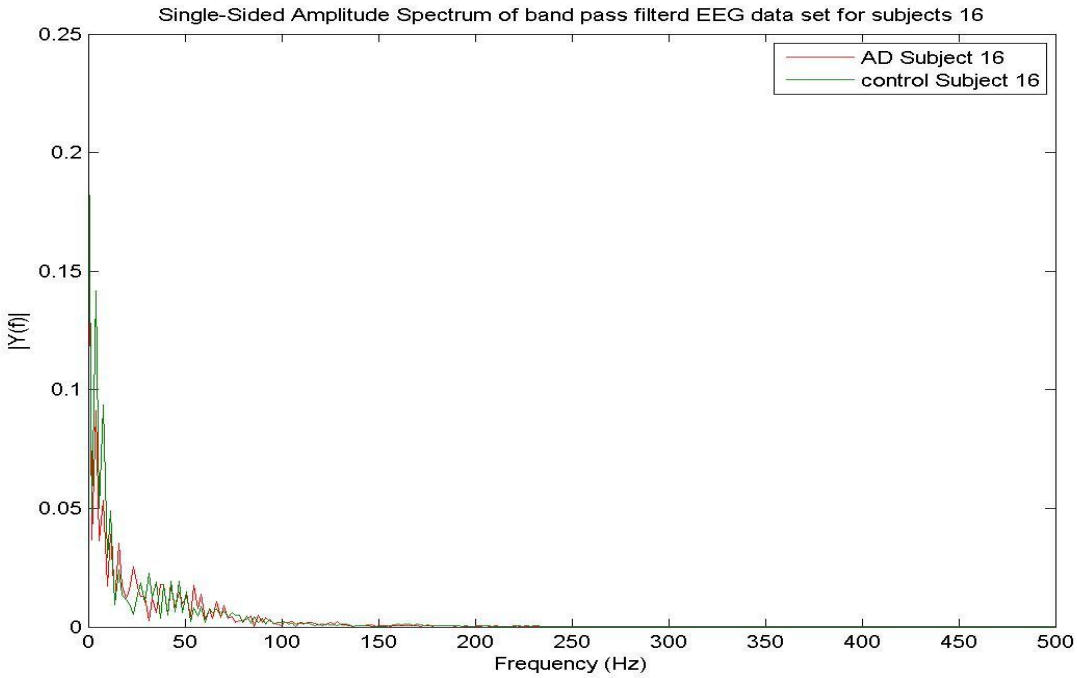

Figure E-15: The DFT for AD subject 16 and control subject 16 after artifact removal

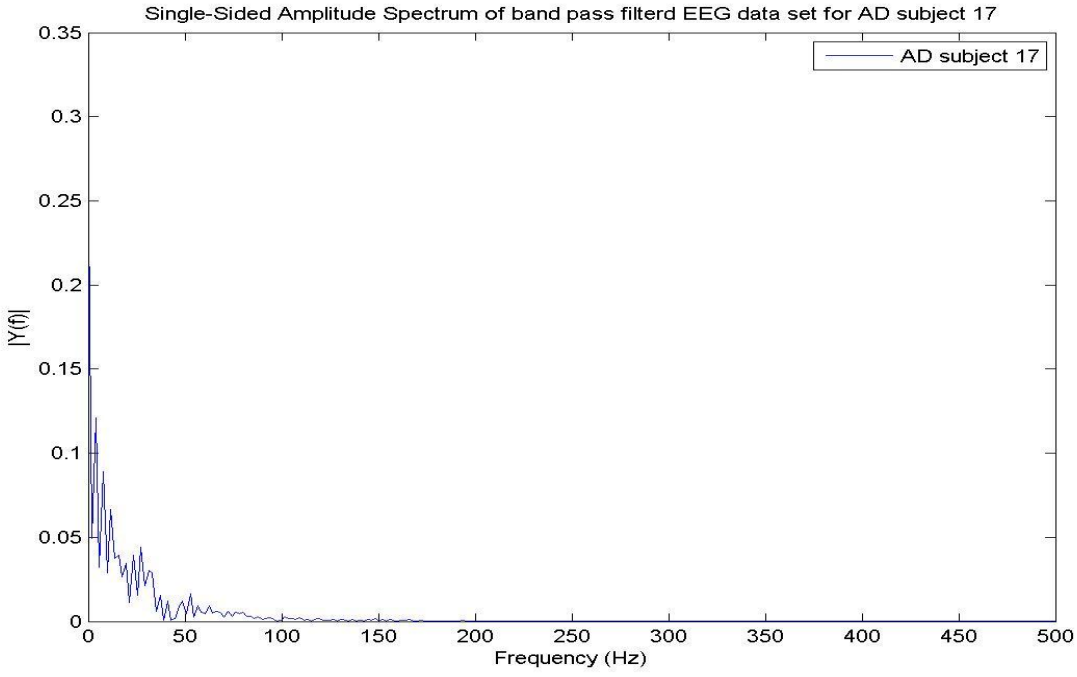

Figure E-16: The DFT for AD subject 17 after artifact removal

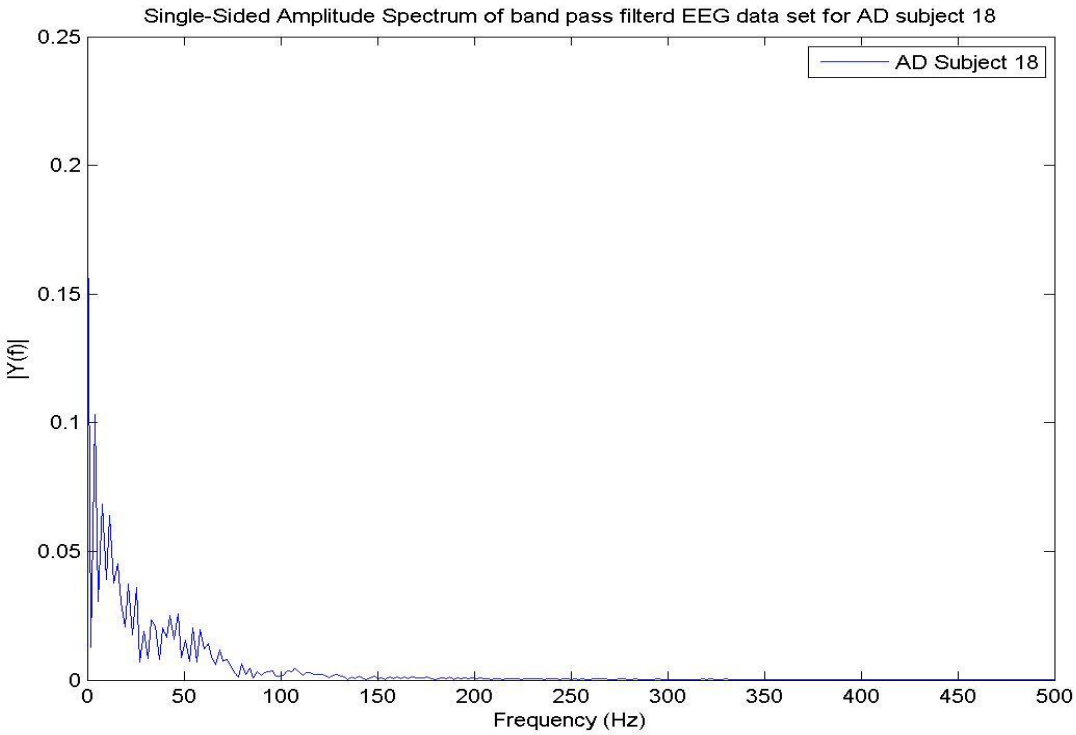

Figure E-17: The DFT for AD subject 18 after artifact removal